

UNIVERSITY OF NIŠ



ISSN 0354-4605 (Print)
ISSN 2406-0860 (Online)
COBISS.SR-ID 98807559
UDC 71/72+62

FACTA UNIVERSITATIS

Series

ARCHITECTURE AND CIVIL ENGINEERING

Vol. 22, N° 2, 2024

The background of the cover features a complex, abstract architectural drawing. It consists of a grid of thin white lines and thicker yellow lines that form various rectangular and stepped shapes, resembling a technical drawing or a floor plan. The overall color palette is a mix of grey, white, and yellow.

22 | 2

Scientific Journal FACTA UNIVERSITATIS

UNIVERSITY OF NIŠ

Univerzitetski trg 2, 18000 Niš, Serbia

Phone: +381 18 257 095 Telefax: +381 18 257 950

e-mail: facta@ni.ac.rs <http://casopisi.junis.ni.ac.rs/>

Scientific Journal FACTA UNIVERSITATIS publishes original high scientific level works in the fields classified accordingly into the following periodical and independent series:

<i>Architecture and Civil Engineering</i>	<i>Linguistics and Literature</i>	<i>Physical Education and Sport</i>
<i>Automatic Control and Robotics</i>	<i>Mathematics and Informatics</i>	<i>Physics, Chemistry and Technology</i>
<i>Economics and Organization</i>	<i>Mechanical Engineering</i>	<i>Teaching, Learning and Teacher Education</i>
<i>Electronics and Energetics</i>	<i>Medicine and Biology</i>	<i>Visual Arts and Music</i>
<i>Law and Politics</i>	<i>Philosophy, Sociology, Psychology and History</i>	<i>Working and Living Environmental Protection</i>

SERIES

ARCHITECTURE AND CIVIL ENGINEERING

Editor-in-Chief: **Zoran Bonić**, e-mail: zoran.bonic@gaf.ni.ac.rs

Section Editors: **Milena Dinić Branković**, e-mail: milena.dinic@gaf.ni.ac.rs

Žarko Petrović, e-mail: zarko.petrovic@gaf.ni.ac.rs

Vuk Milošević, e-mail: vuk.milosevic@gaf.ni.ac.rs

University of Niš, Serbia, Faculty of Civil Engineering and Architecture

18000 Niš, Aleksandra Medvedeva 14, 18000 Niš

Phone: +381 18 588 181, Fax: +381 18 588 181

Technical Assistance: **Vladan Nikolić, Vojislav Nikolić**, e-mail: fuacets@junis.ni.ac.rs

University of Niš, Serbia, Faculty of Civil Engineering and Architecture

EDITORIAL BOARD:

Branislav Mitrović,

Serbian Academy of Sciences and Arts, Belgrade, Serbia

Slaviša Trajković,

Faculty of Civil Engineering and Architecture,
University of Niš, Serbia

Günther Meschke,

Faculty of Civil and Environmental Engineering,
Ruhr University Bochum, Germany

Hartmut Pasternak,

Faculty of Architecture, Civil Engineering and Urban
Planning, Brandenburg University of Technology,
Cottbus, Germany

Harsha Ratnaweera,

Faculty of Sciences and Technology, Norwegian
University of Life Sciences (NMBU), As, Norway

Michael Tritthart,

Institute of Hydraulic Engineering and River Research,
University of Natural Resources and Life Sciences
(BOKU), Vienna, Austria

Georgios E. Stavroulakis,

School of Production Engineering and Management,
Technical University of Crete, Chania, Greece

Barbara Karleuša,

Faculty of Civil Engineering, University of Rijeka,
Croatia

Milan Gocić,

Faculty of Civil Engineering and Architecture,
University of Niš, Serbia

Tamara Nestorović,

Faculty of Civil and Environmental Engineering,
Ruhr University Bochum, Germany

Ivan Damnjanović,

Zachry Department of Civil and Environmental
Engineering, Texas A&M University, United States

Blessen Skariah Thomas,

Ramanujan Faculty, Department of Civil Engineering,
National Institute of Technology Calicut, Kerala, India

Marija Nefovska Danilović,

Faculty of Civil Engineering, University of Belgrade,
Serbia

Thanongsak Imjai,

School of Engineering and Technology, Walailak University,
Thailand

Sudharshan N. Raman,

Faculty of Civil Engineering, Monash University, Malaysia

Ernesto Cascone,

Department of Engineering, University of Messina,
Messina, Italy

Dimitris Pitilakis,

Department of Civil Engineering,
Aristotle University of Thessaloniki, Thessaloniki, Greece

Paulo Santos,

Institute for Sustainability and Innovation in Structural
Engineering (ISISE), University of Coimbra, Portugal

Elena Lucchi,

Department of Architecture, Construction Engineering and
Built Environment (DABC), Politecnico di Milano, Italy

Proofreading:

Goran Stevanović, University of Niš, Faculty of Civil Engineering and Architecture

UDC Classification Associate: **Ana Mitrović**, Library of Faculty of Civil Engineering and Architecture, Niš

Computer support:

Mile Ž. Randelović, Head of Publishing Department, University of Niš, e-mail: mile@ni.ac.rs

Secretary:

Aleksandra Golubović, University of Niš, e-mail: saska@ni.ac.rs

Publication frequency – one volume, three issues per year.

Published by the University of Niš, Serbia

© 2024 by University of Niš, Serbia

Financial support: Ministry of Science, Technological Development and Innovation of the Republic of Serbia

Printed by ATLANTIS DOO, Niš, Serbia

Circulation 50

ISSN 0354 – 4605 (Print)
ISSN 2406 – 0860 (Online)
COBISS.SR-ID 98807559
UDC 71/72+62

FACTA UNIVERSITATIS

SERIES ARCHITECTURE AND CIVIL ENGINEERING
Vol. 22, N° 2, 2024



UNIVERSITY OF NIŠ

INSTRUCTIONS FOR CONTRIBUTORS

Contributions should be (preferably) in English, French or German.

Under the paper title, the name(s) of the author(s) should be given while the full name, official title, institute or company affiliation and the like should be placed at the end of the paper together with the exact mail and e-mail address, as well as short (running) title of paper.

Manuscript format. A brief abstract of approximately 100 to 150 words in the same language and a list of up to six key words should precede the text body of the manuscript. All the authors apart from foreign ones should also submit a complete manuscript in Serbian. Manuscripts should be prepared as doc. file, Word version 6.0 or higher. Manuscript should be prepared using a Word template (downloaded from web address <http://casopisi.junis.ni.ac.rs/index.php/FUArchCivEng/about/submissions#onlineSubmissions>).

Manuscript length. Brief articles and discussions (10 pages or less) are encouraged. Otherwise, papers should present well-focused arguments of approximately 16 pages.

Style requirements. Letters, figures and symbols should be clearly denoted.

Equations should be typewritten and, with the number, placed in parentheses at the right margin. References to equations should be in the form "Eq. (2)" or simply (2). For equations that cannot be entered in a single line, use the Equation Editor in MS Word. In equations and in the text, *italicize* symbols that are used to represent variables or parameters, including subscripts and superscripts. Only use characters and symbols that are available in the Equation Editor, in the *Symbol font* or in *Times New Roman*.

All illustrations (figures, photographs, line drawings, graphs) should be numbered in series and all legends should be included at the bottom of each illustration. All figures, photographs, line drawings and graphs, should be prepared in electronic form and converted in TIFF or JPG (max quality) file types, in 300 dpi resolution, for superior reproduction. Figures, line drawings and graphs prepared using elements of MS Drawing or MS Graph must be converted in form of pictures and unchangeable. All illustrations should be planned in advance so as to allow reduction to 12.75 cm in column width. Please review all illustrations to ensure that they are readable.

All **tables** should be numbered with consecutive Arabic numbers. They should have descriptive captions at the top of each table and should be mentioned in the text.

The **references** should be numbered in the order in which they appear in the text, at the end of the manuscript, in the same way as the following examples:

1. Kollbruner C. F., Hajdin N., Stipanić B.: *Contribution to the Analysis of Cable-Stayed Bridges* N. 48, Schulthess Verlag, Zürich, 1980, pp. 66-77.
2. Đuranović P.: Organizacija upravljanja projektima, Izgradnja N° 1/96, Beograd, 1996, str. 45-52.
3. Živković D.: Influence of front excavation on the state and deformity of montage lining of hydraulic pressure tunnels, Ph. D. University of Niš, 1988, pp. 95-108.
4. Kurtović-Folić N.: Typology of Architectural Forms-Strong and Weak Typological Characteristics, Facta Universitatis, University of Niš, Vol. 1, N° 2, 1995, pp. 227-235.

References should be quoted in the text by the corresponding number in square brackets.

Electronic submission. Papers for consideration should be submitted to the Series Editor in electronic form via the Journal's home page: <http://casopisi.junis.ni.ac.rs/index.php/FUArchCivEng/index>.

FACTA UNIVERSITATIS

Series
Architecture and Civil Engineering

Vol. 22, N° 2, 2024

Contents

- Artur Roshi, Golubka Nechevska-Cvetanovska, Julijana Bojadjieva, Jordan Bojadjiev**
SEISMIC PERFORMANCE OF RC BUILDING COLUMNS CONFINED WITH CFRP ...89-95
- Ljiljana Vasilevska, Magdalena Slavković**
URBAN RESILIENCE:
DEFINITIONS, UNDERSTANDING AND CONCEPTUALIZATION 97-103
- Maša Žujović, Jelena Milošević**
PARAMETRIC DESIGN OF 3D PRINTED RIBBED SLAB SYSTEM
BASED ON NATURE-INSPIRED PATTERNS 105-113
- Hartmut Pasternak, Yvonne Ciupack**
APPLICATION OF ADHESIVELY BONDED CFRP FOR REINFORCEMENT
AND REHABILITATION OF FATIGUE DAMAGED STEEL STRUCTURE -
ONLY A NICE IDEA? 115-126
- Zoran Grdić, Nenad Ristić, Dušan Grdić, Gordana Topličić-Ćurčić,
Dejan Krstić, Jelena Bijeljić**
HIGH STRENGTH CONCRETES BASED ON THE CHOICE
OF THE BEST PARTICLE SIZE DISTRIBUTION IN AGGREGATE 127-137
- Snežana Đorić-Veljković, Nikola Mitrović, Sandra Veljković, Vojkan Davidović,
Emilija Živanović, Ivica Manić, Danijel Danković**
THE ROLE OF OLED DEVICES IN THE DEVELOPMENT OF SMART CITIES.... 139-149
- Nemanja Bralović, Iva Despotović, Danijel Kukaras**
EXPERIMENTAL ANALYSIS OF THE BEHAVIOR
OF CAPPING BEAMS ACROSS THE PILES IN LOOSE SAND 151-163
- Nemanja Marinković, Elefterija Zlatanović, Nebojša Davidović, Zoran Bonić,
Nikola Romić, Branimir Stanković, Lazar Živković**
COMPARATIVE ANALYSIS OF ATTERBERG'S LIMITS
OF FINE-GRAINED SOIL DETERMINED BY VARIOUS METHODS 165-174

SEISMIC PERFORMANCE OF RC BUILDING COLUMNS CONFINED WITH CFRP*

UDC 699.841:691.87

Artur Roshi¹, Golubka Nechevska-Cvetanovska²,
Julijana Bojadjieva², Jordan Bojadjiev³

¹Metropolitan University, Tirana, Albania

²UKIM-IZIIS Ss. Cyril and Methodius University-Skopje, North Macedonia

³International Balkan University, Skopje, North Macedonia


ORCID iDs: Artur Roshi


Golubka Nechevska-Cvetanovska


Julijana Bojadjieva

Jordan Bojadjiev

 N/A

 <https://orcid.org/0000-0001-7546-932X>

 <https://orcid.org/0000-0003-4047-7500>

 <https://orcid.org/0000-0002-3688-8326>

Abstract. *It is a usual practice that traditional methods with traditional materials (most frequently jacketing of elements) are used for repair and strengthening of structures. However, lately, particularly in the last two decades, there have occurred new construction materials intended for strengthening and design referred to as composites strengthened by polymer fibers (FRP). These materials have special mechanical properties and special properties.*

In the paper part of the laboratory and quasi-static experimental investigations of designed models of RC columns confined with CFRP will be presented. Particular attention will be paid to behavior of these columns under quasi-static loads, whereat a number of comparative analyses of a number of parameters obtained from the experimental investigations of the tested models will be carried out. Some recommendations and outcomes will be given as to the approach and technology of practical application of these materials, particularly in seismically active regions.

Key words: *seismic strengthening, innovative materials, CFRP, quasi-static test.*

1. INTRODUCTION

The need for repair and strengthening of RC buildings and their structural elements occurs when their elements do not possess sufficient strength, stiffness and/or ductility out of different reasons or due to slighter or more severe damages that are most frequently caused by earthquakes. Within the frames of this paper, special emphasis will be put on RC buildings where, during construction, the built-in concrete has not achieved

Received June 30, 2023 / Revised August 1, 2023 / Accepted August 15, 2023

Corresponding author: Artur Roshi - Metropolitan University, Tirana, Albania

e-mail: artur.roshi@yahoo.com

*Selected paper presented at the International Conference Sinarg 2023 held in Niš, Serbia on 14-15 September 2023.

© 2024 by University of Niš, Serbia | Creative Commons License: CC BY-NC-ND

the designed concrete class and/or buildings that cannot satisfy the required strength, stiffness and deformation characteristics particularly in earthquake conditions, [1]. In these cases, it is necessary to take measures for repair and strengthening of both individual structural elements and whole structures, [2], [3].

To present the possibilities and the benefits of use of these innovative construction materials in strengthening of structural elements of buildings and integral building structures, ample laboratory research for definition of the characteristics of these materials and experimental investigations of RC columns strengthened by CFRP by variation of concrete class, reinforcement percentage and different technologies of strengthening by CFRP (Fiber Reinforced Polymers) materials are carried out at the Institute of earthquake Engineering and Engineering Seismology – IZIIS, Skopje, [4], [5] and [6].

In this paper, some of the laboratory and quasi-static experimental investigations of designed models of RC columns are presented.

2. LABORATORY TESTS ON MATERIALS BUILT-IN MODELS FOR EXPERIMENTAL RESEARCH CARRIED OUT AT UKIM-IZIIS

To realize the experimental quasi-static tests, two models were designed and constructed, namely Model M1 and Model M2, Figure 1. The models were with identical proportions (supporting beam proportioned 50/50/116 cm and a column proportioned 30/30/200cm), constructed to the scale of 1:1[1].

For the purpose of easier incorporation of the FRP materials, it was decided to build the models in vertical position.

Figure 1 shows photos taken during concreting of the foundation-beam and the columns of both models. In the first phase, concreting of the supports – foundations was done, while in the second phase, both columns were concreted.



Fig. 1 Construction of the column models for experimental tests and Photos taken during application of FRP on the mode

During concreting of the models, three trial specimens - concrete cubes proportioned 15/15/15 were taken from the supports - beams and three trial cubes proportioned 15/15/15 were taken from the columns, in addition to the nine (9) cylinders proportioned 15/30 cm Figure 2. To define compressive strength and concrete class, laboratory tests were performed at stock holding company-GIM-Skopje (for the cubes) and ZIM –Skopje (for the cylinders), while the tests for definition of the modulus of elasticity of the built-in concrete were done at ZIM – Skopje.



Fig. 2 Photos of taken trial concrete specimens

Using the trial concrete specimens – cylinders, three series of tests of compressive strength and tests for definition of the modulus of elasticity of the built-in concrete were carried out as follows:

- Series 0- concrete cylinders without FRP- plain concrete
- Series 1- concrete cylinders wrapped with 1 (one) FRP layer
- Series 2- concrete cylinders wrapped with 2 (two) FRP layers

Presented further are photos and results taken during laboratory tests for definition of compressive strength of concrete for the three series Figure 3. It must be pointed out that the collapse of the models from the first and the second series was explosive, with big crushing of concrete wrapped with FRP. This was particularly pronounced in Series 2 where concrete was wrapped with two CFRP layers.

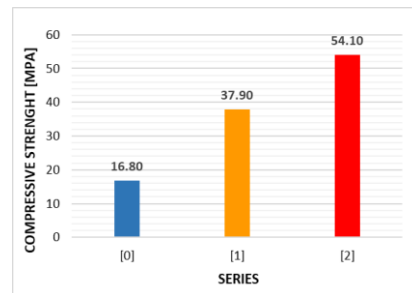


Fig. 3 Testing and results: a) Testing of compressive strength for the first series, b) Diagram of compressive strength for each series

In general, it can be concluded that the compressive strength and modulus of elasticity is higher with the number of FRP layers.

3. EXPERIMENTAL PROGRAM

For the needs of own experimental investigations, two column elements were designed. The column models were designed as fixed cantilever girders with a constant length of both models of 200 cm (the column was treated only up to the inflection point,

i.e., half of the total height) and cross-section of 30/30 cm. In both models, the varying parameters were the percentage of longitudinal and transverse reinforcement and the axial forces. The concrete class, i.e., the compressive strength of concrete and the type of the FRP was same for both models. The elements were designed to the geometrical scale of 1:1.

Presented further are photos taken during construction of the models (Model M1 and Model M2), Figure 4.

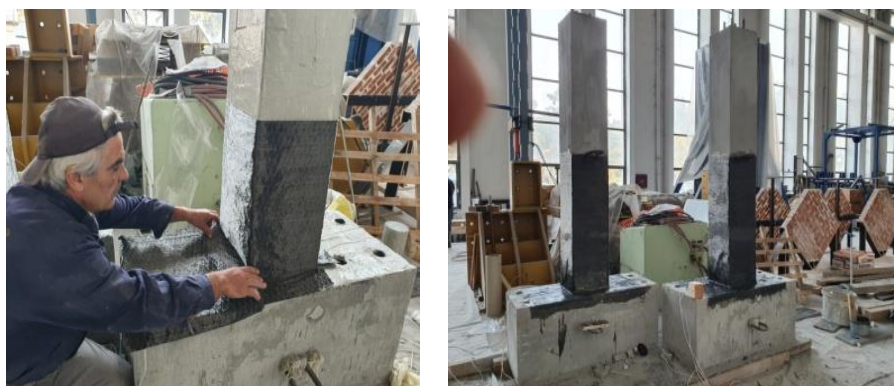


Fig. 4 Construction of the models: a) Model M1 and Model M2; b) Construction of the column models for experimental tests.

To define the real bearing and deformability capacity of the built column models, the values on quality of built-in concrete and reinforcement obtained for both vertical and transverse reinforcement, as well as the type of used CFRP were used. In the first phase, the real $M-\Phi$ (moment – curvature) relationships of the column cross-sections were computed by applying axial force, the real $M-N$ diagrams, and then, based on the obtained $M-\Phi$ diagrams, the strength and deformability capacity of each model was defined.

The strength and deformability characteristics ($M-N$) and ($M-\Phi$) at cross-section level were analytically defined by use of the SAP2000 computer software. All analyses were done by taking into consideration confinement of the cross-section of transverse reinforcement. Selected results are given in chapter 4.

4. RESULTS FROM EXPERIMENTAL INVESTIGATIONS AT UKIM-IZIIS

Presented further are photos and results from the process of quasi-static tests on Model M1 and Model M2 with photos of characteristic damage Figure 5 and Figure 6, respectively. Figure 7 and Figure 8 represent results from the testing in terms of Moment – curvature diagrams for the two models and series of testing.



Fig. 5 Quasi-static tests of Model M1: a) Shot during the quasi-static testing of column Model M1; b) Damage from quasi static testing of column Model M1



Fig. 6 Experimental set-up quasi static testing of column Model M2

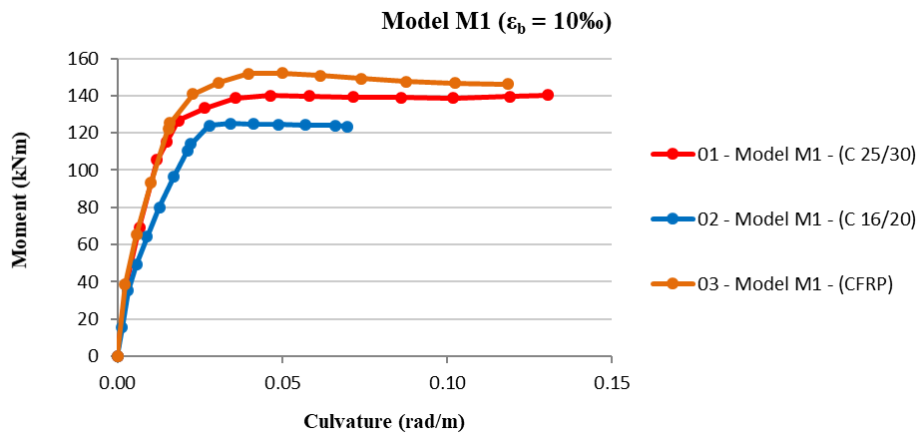


Fig. 7 M-φ Interaction Diagram for Model M1 – Comparison

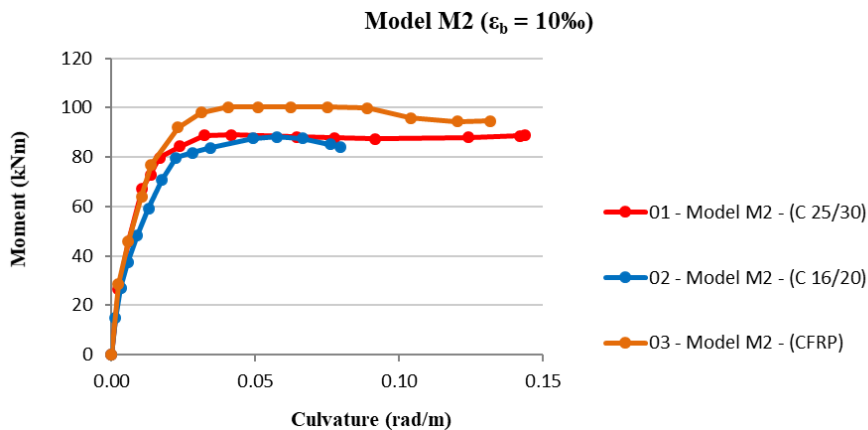


Fig. 8 M- ϕ Interaction Diagram for Model M2 – Comparison

The interaction diagrams clearly show the difference among the all series of analyses. The moment capacity for the 03 series (cross-section with CFRP) is higher than that of cross-section 02 (series with built-in concrete class of 16/20).

Based on the analyses of the results from Table 1, it can be concluded that the ductility to rotation for Model M1 is 2.049 greater for the model with CFRP, while the ductility to displacement is greater in respect to the ductility of Model M1 without CFRP for 76.7%.

In the case of Model M2, the ductility to rotation is higher in the case of the Model with CFRP for 64 %, while the ductility to displacements is higher compared to the ductility of the Model M2 without CFRP for 46.1%.

Table 1 Rotation and displacement capacity for Model M1 and Model M2

Specimen	Rotation		Ductility D_ϕ	Displacement		Ductility D_d
	ϕ_y [rad/m]	ϕ_u [rad/m]		d_y [cm]	d_u [cm]	
Model M1-02	0.0127	0.0696	5.48	1.056	2.626	2.487
Model M1-03	0.0154	0.1730	11.23	1.281	5.631	4.306
Model M2-02	0.0128	0.0663	5.18	1.065	2.542	2.387
Model M2-03	0.0231	0.1963	8.50	1.922	6.702	3.487

5. CONCLUSIONS

In the paper part of the analytical, laboratory and quasi-static experimental investigations of designed models of RC columns strengthened with FRP were presented. Based on the experimental investigations the following conclusions can be outlined:

- In general, it can be concluded that the compressive strength and modulus of elasticity is higher with the number of CFRP layers (Figure 3b).
- From the behavior of the tested elements it can be concluded that in both Models, the failure was sudden and explosive, but with sufficient ductility capacity (Figure 7).
- These tests are good basis for further analytical and numerical investigations, which can provide additional conclusions.

REFERENCES

1. Roshi, A., (2020). Application of innovative buildings materials for repair and strengthening of rc columns in seismically active regions, Doctoral dissertations, Ukim Izis Skopje, Macedonia
2. Sarafraz, M., & Danesh, F. (2008, October). Flexural enhancement of RC columns with FRP. In The 14th World Conference on Earthquake Engineering (pp. 1-7).
3. Chapragoski Goran, Nechevska-Cvetanovska Golubka. (2019). Strengthening Of Existing Building Using Cfrp Wrapping System, 18th International Symposium of Macedonian Association of Structural Engineers (MASE), Ohrid, Macedonia.
4. Roshi Artur, Nechevska-Cvetanovska Golubka Repair And Strengthening Of RC Buildings Using Traditional And Innovative Materials, 18th International Symposium of Macedonian Association of Structural Engineers (MASE), Ohrid, Macedonia.
5. Nechevska-Cvetanovska, G., & Roshi, A. (2019). Rehabilitation of RC buildings in seismically active regions using traditional and innovative materials. Građevinski materijali i konstrukcije, 62(3), 19-30.
6. Nechevska-Cvetanovska, G., Roshi, A., & Bojadjieva, J. (2019). Seismic strengthening of existing rc buildings structures using concrete jacketing and FRP materials. E-GFOS, 10(19), 68-80.

SEIZMIČKA OTPORNOST AB STUBOVA ZGRADA UTEGNUTIH UPOTREBOM CFRP

Uobičajena je praksa da se za popravku i ojačavanje konstrukcija koriste tradicionalne metode sa tradicionalnim materijalima (najčešće oblaganje elemenata). Međutim, u poslednje vreme, posebno u poslednje dve decenije, pojavljuju se novi građevinski materijali namenjeni za ojačavanje i dizajn koji se nazivaju kompoziti ojačani polimernim vlaknima (FRP). Ovi materijali imaju posebna mehanička svojstva i posebna svojstva.

U radu će biti prikazana laboratorijska i kvazistatička eksperimentalna istraživanja projektovanih modela RC stubova utegnutih CFRP-om. Posebna pažnja će biti posvećena ponašanju ovih stubova pod kvazistatičkim opterećenjima, pri čemu će se izvršiti niz uporednih analiza niza parametara dobijenih eksperimentalnim ispitivanjem testiranih modela. Daće se neke preporuke i rezultati u vezi sa pristupom i tehnologijom praktične primene ovih materijala, posebno u seizmički aktivnim regionima.

Ključne reči: seizmičko ojačavanje, inovativni materijali, CFRP, kvazi-statičko ispitivanje.

URBAN RESILIENCE: DEFINITIONS, UNDERSTANDING AND CONCEPTUALIZATION*

UDC 711.4:502/504
711.4:551.583

Ljiljana Vasilevska, Magdalena Slavković

University of Niš, Faculty of Civil Engineering and Architecture, Niš, Serbia

ORCID iDs: Ljiljana Vasilevska
Magdalena Slavković

<https://orcid.org/0000-0002-6836-0139>

<https://orcid.org/0009-0000-2775-5217>

Abstract. *Sustainability and resilience are the two main paradigms of planning and policy making in the past decades. Fostering resilience in the face of environmental, socio-economic and political uncertainty and risk has captured the attention of academics and decision makers across disciplines, sectors and spatial scales. Urban resilience has become an important goal for cities, especially from the point of view of adapting to climate change and reducing their ecological footprint. Urban resilience is conventionally defined as the measurable ability of any urban system, with its inhabitants, to maintain continuity through all shocks and stresses while positively adapting and transforming towards sustainability. However, in theory and practice there are different definitions that are often in conflict. This paper first provides an overview of existing definitions of urban resilience and highlights their main determinants. Then, the paper discusses definitions from the perspective of ways of incorporating key concepts found both in resilience theory and urban theory. In the following, similarities and mutual tensions are recognized between the key concepts. Finally, the paper concludes that a clearer conceptualization is needed to improve this developing field and create conditions for its further operationalization.*

Key words: *urban resilience, definition, resilience conceptualization*

1. INTRODUCTION

The two main challenges and risks at the global level today are rapid urbanization and climate change. By 2050, two thirds of the total population, which is about 6,5 billion people, will be urban. At the same time, the potential risks of climate change at the global level are: a) an increase in the average temperature by 3°C by 2070; b) reduction of

Received June 30, 2023 / Revised August 1, 2023 / Accepted August 15, 2023

Corresponding author: Ljiljana Vasilevska. University of Niš, Faculty of Civil Engineering and Architecture, Niš, Serbia
e-mail: ljiljana.vasilevska@gaf.ni.ac.rs

*Selected paper presented at the International Conference Sinarg 2023 held in Niš, Serbia on 14-15 September 2023.

© 2024 by University of Niš, Serbia | Creative Commons License: CC BY-NC-ND

average amounts of precipitation by 20-40% by 2070; c) an increase in sea level in conjunction with an increase in storm events, and d) an increase in the frequency and intensity of stormy periods in regional framework. Although urban areas (at least 50,000 inhabitants) cover less than 3% of the Earth's surface, they are responsible for about 71% of global energy-related carbon emissions [1]. With all that in mind, it is understandable why the UN (2010) recognized the following as three key challenges/goals at the urban level: 1) improving the quality of life in cities; 2) reducing their ecological footprint, and 3) adapting them to climate change. A few years later, they were translated and incorporated into the 11th Millennium Goal - Sustainable Cities and Communities [2].

In the broader discussions on urban sustainability and climate change adaptation, the promotion of urban resilience amidst environmental, socio-economic, and political unpredictability and vulnerability has garnered the interest of scholars and policymakers spanning various fields and urban levels. Urban resilience has become an increasingly favored concept [3] [4] and an important goal for cities. Its popularity has exploded, with numerous explanations for this dramatic rise [5]. However, the meaning of urban resilience remains malleable, allowing stakeholders to come together around a common terminology without necessarily agreeing on an exact definition [6]. In addition, this vagueness can make it difficult to operationalize urban resilience or develop generalizable indicators [7].

Therefore, the two objectives of this paper are as follows:

- systematize and provide an overview of current definitions of urban resilience and highlight their main determinants; and
- analyse and consider mutual similarities and tensions between key determinants and aspects of urban resilience at a conceptual level.

2. METHODOLOGY

The analytical framework in this research is based on the application of the descriptive method, analysis method and the comparative analysis method. The descriptive method and the analysis method were applied in the process of researching and systematizing the definitions of urban resilience, while the comparative analysis method was used in the research of similarities and tensions between the key determinants of urban resilience at the conceptual level.

3. URBAN RESILIENCE: DEFINITIONS AND UNDERSTANDING

According to Klein et al. [8], the term resilience is etymologically rooted in the Latin word *resilio*, which means "to bounce back". As an academic concept, its origins and meaning are more ambiguous [9], [10], [11], [12], [13]. Although the concept has a long history of use in the engineering, psychology and disaster literature [14], Meerow et al. [9] state that the research work of ecologist C.S. Holling's (1973) on the resilience of ecological systems is considered the originator of the modern theory of resilience. ¹

¹ "Holling used resilience to describe the ability of an ecological system to continue to function, or to "persist" when it changes, but does not necessarily remain the same. This contrasts with "engineering resilience", which focuses on a single state of equilibrium or stability to which a resilient system would revert after disruption" [10].

There are different definitions of urban resilience in the literature and practice. They are an expression of the multitude of disciplines dealing with the phenomenon of urban resilience, as well as the complexity of urban resilience itself. An overview of the most common current definitions is given in Table 1.

Table 1 Definitions of urban resilience – short overview

	Author/year	Discipline	Definition
1.	Alberti et al. (2003) (15)	Agricultural and biological sciences; Environmental science	“... the degree to which cities tolerate alteration before reorganizing around a new set of structures and processes”
2.	Godschalk (2003) (16)	Engineering	“... a sustainable network of physical systems and human communities”
3.	Campanella (2006) (17)	Social science	“... the capacity of a city to rebound from destruction”
4.	Wardekker et al. (2010) (18)	Business management and accounting; Psychology	“... a system that can tolerate disturbances (events and trends) through characteristics or measures that limit their impacts, by reducing or counteracting the damage and disruption, and allow the system to respond, recover, and adapt quickly to such disturbances”
5.	Ahern (2011) (19)	Environmental science	“...the capacity of systems to reorganize and recover from change and disturbance without changing to other states...systems that are “safe to fail””
6.	Leichenko (2011) (5)	Environmental science; Social science	“... the ability...to withstand a wide array of shocks and stresses”
7.	Tyler and Moench (2012) (20)	Environmental science; Social science	“...encourages practitioners to consider innovation and change to aid recovery from stresses and shocks that may or may not be predictable”
8.	Liao (2012) (21)	Environmental science; Social science	“...the capacity of the city to tolerate flooding and to reorganize should physical damage and socioeconomic disruption occur, so as to prevent deaths and injuries and maintain current socioeconomic identity”
9.	Brown et al. (2012) (22)	Environmental science; Social science	“...the capacity to dynamically and effectively respond to shifting climate circumstances while continuing to function at an acceptable level. This definition includes the ability to resist or withstand impacts, as well as the ability to recover and reorganize in order to establish the necessary functionality to prevent catastrophic failure at a minimum and the ability to thrive at best”
10.	Meerow et al. (2015) (9)	Environmental science; Urban studies; Social science	“...ability of an urban system-and all its constituent socio-ecological and socio-technical networks across temporal and spatial scales - to maintain or rapidly return to desired functions in the face of a disturbance, to adapt to change, and to quickly transform systems that limit current or future adaptive capacity”

4. URBAN RESILIENCE: CONCEPTUALIZATION AND DISCUSSION

The meaning and use of the concept of resilience in urban research and in the context of policy derives from the way of considering the following key relationships and determinants: 1) equilibrium vs. non-equilibrium resilience; 2) positive vs. neutral (or negative) conceptualizations of resilience; 3) mechanisms of changing the system into a resilient state; 4) specific adaptation vs. general adaptability; and 5) time and spatial scale of action [9].

Regarding the first relationship, there is a division in urban resilience between single-state equilibrium, multi-state equilibrium, and dynamic non-equilibrium. Their disciplinary orientations, as well as key characteristics are shown in Table 2.

Table 2 Notion of urban resilience equilibrium

Type of equilibrium	Discipline	Key characteristic
1. Single-state equilibrium or " <i>engineering resilience</i> "	Disaster management; Psychology; Economics	Refers to the capacity of a system to revert to a previous equilibrium post-disturbance
2. Multi-state equilibrium or " <i>ecological resilience</i> "	Environmental science	Posits that systems have different stable states and, in the face of a disturbance, may be transformed by tipping from one stability domain to another
3. Dynamic non-equilibrium	Ecology; Urban planning and design	Suggests that systems undergone constant change and have no stable state

Some of the definitions take an explicit position on this issue. Thus, Liao [21] argues that engineering resilience is an "outdated equilibrium paradigm" for communities exposed to risk from natural hazards, while Ahern [19] claims that resilient urban systems are "safe-to-fail" which is opposed to "fail-safe", reflecting an unbalanced perspective. Some definitions suggest that a return to a previous equilibrium may be possible, focusing on the city's ability to "renew" and "recover" [17]. Other definitions do not take an explicit position, but nevertheless recognize that cities are constantly changing and may not return to their previous state [9].

Regarding the second relationship - positive vs. neutral (or negative) conceptualization of urban resilience, the findings of a comparative analysis of existing definitions indicate that urban resilience is predominantly viewed as a positive concept. The idea that resilience is a positive feature that contributes to sustainability is widely accepted [3], [22]. However, there is debate as to whether resilience is always a positive concept. Within equilibrium focused definitions, based on the ability of the urban system to return to its original state after disturbance, doubts arise precisely as to how and for whom that original state is desirable (for example, what if it is poverty, car-dependence urban environment or dictatorship). Some social theorists consider that the concept can be used to promote a neoliberal agenda or retain systemic inequality [22] [9], and that therefore the determination of a desirable or undesirable state is a matter of political and social consensus and regulation.

The following can be recognized as key mechanisms for changing the system into a resilient state: 1) persistence; 2) transition; and 3) transformation. Their key characteristics are shown in Table 3.

Table 3 Mechanisms of urban resilience

Type of mechanism	Discipline	Key characteristic
1. Persistence	Engineering	Reflects the engineering principle that systems should resist disturbance and try to maintain the status quo
2. Transition	Environmental science; Social science; Urban planning and design	Refers to the system ability to incrementally adapt
3. Transformation	Environmental science; Social science; Urban planning and design	Refers to the system ability to more radically transform - when a system is in a robustly undesirable state, efforts to build resilience might seek to purposefully and fundamentally change its structures

The findings of a comparative analysis of this relationship indicate that definitions and concepts of urban resilience mostly focus on persistence, but there are also those that focus on transformation and transition [19]. There are few who explicitly identify two or all three mechanisms for achieving a state of urban resilience [22]. For example, Wamsler et al. [23], recognize that actions aimed at creating a resilient city can be both transitional and transformational. Some research focuses specifically on incremental change or transition [21], while others argue for transformation [22].

The understanding of the fourth relationship between so called “specific” adaptations vs. “general” adaptations also differs. Some studies argue that focusing on specific resilience can lead to undermining the system’s flexibility and its ability to respond to unexpected threats, while other definitions and conceptual approaches are based on the assumption that inherent (specific) qualities are better under normal conditions and adaptive (general) qualities during disasters [24]. A possible collision between short-term adaptation, which is highly specialized, and long-term adaptability, which is generalized, is also recognized. Scholars focusing on climate change resilience align with Brown et al. [22] in arguing that urban resilience should focus on adaptive capacity rather than specific adaptations.

Regarding the time and spatial scale of action, most definitions do not mention them. Those definitions based on the rapid recovery of the urban system as a key characteristic do not specify the meaning of “rapid” or the timescale of actions. Some definition and concepts note that the time it takes to return to a previous stable state after a disturbance can be used to measure resilience, but it also not clear what “rapid” exactly means. The spatial scale of the action - macro, meso and/or micro urban scale is also rarely mentioned.

Despite the differences in disciplinary and conceptual approaches, urban resilience can be recognized in practice through two dimensions - as “soft” resilience and “hard” resilience [25].

“Soft” resilience includes socio-economic resilience and organizational resilience of a certain urban area. Socio-economic resilience refers to economic diversity, the level and structure of employment of the population, the ability to operate economically in the event of risks, as well as the ability of the social community to face and respond to them [26]. Organizational resilience refers to the institutional context, primarily the ability to adapt institutions, social organizations and social communities to disaster risks.

“Hard” urban resilience can be viewed through two dimensions, as physical resilience and as natural resilience. Physical resilience refers to the resilience of the urban infrastructure

system in correlation with the urban system, including power and telecommunication systems, city water supply and sewage system, but also shelters, breakwaters and other elements of protection. Natural resilience includes ecological and environmental resilience [27]. As "hard" urban resilience is key in resilience simulations, there is an extensive literature on environmental resilience, risk assessment and vulnerability analysis, as well as infrastructure resilience simulation [25].

5. CONCLUSION

There is an increasing emphasis on enhancing the resilience of cities in the face of rapid urbanization and climate change. Academics and practitioners from different disciplines have adopted the term urban resilience. However, as the literature review and analysis demonstrate, definitions of urban resilience are often incoherent.

It could be said that urban resilience has certain theoretical inconsistencies and conceptual vagueness. On the one hand, that can be considered useful because it allows it to function as a link between different developmental dimensions. In this way, urban resilience can foster multidisciplinary scientific collaboration. This is especially important for cities, which are complex systems and therefore require the expertise of multiple disciplines and stakeholders. On the other hand, this conceptual ambiguity results in difficulties in operationalization, establishment of indicators and their measurability. As Klein et al. [8] consider, "the problem with resilience is the multitude of different definitions and turning any of them into operational tools...After thirty years of academic analysis and debate, the definition of resilience has become so broad as to render it almost meaningless."

Nevertheless, the importance of urban resilience is undeniable. It is considered a positive concept that contributes to urban sustainability. Building resilient urban systems requires different degrees of alteration, thus transitional, incremental, or transformational changes and types of actions may be relevant.

REFERENCES

1. International Panel on Climate Change, IPCC, 2014
2. UNDP, 2015. Sustainable Development Goals 2030. [https://www.undp.org/sustainable-development-goals/no-poverty?gclid=EAAIaQobChMIws63t4NwIVIM_F3Ch1xHwZIEAAYAiAAEgI4KDB wE \(8.6.2023.\)](https://www.undp.org/sustainable-development-goals/no-poverty?gclid=EAAIaQobChMIws63t4NwIVIM_F3Ch1xHwZIEAAYAiAAEgI4KDB wE (8.6.2023.))
3. Leichenko Robin: Climate change and urban resilience. *Current Opinion in Environmental Sustainability*, Vol. 3, No. 3, 164-168, 2011.
4. Brand Fridolin Simon, Jax Kurt: Focusing the Meaning(s) of Resilience: Resilience as a Descriptive Concept and a Boundary Object. *Ecology and Society*, Vol. 12, No 1, 23, 2007.
5. Meerow Sara, Newell Joshua Peter: Resilience and complexity: A bibliometric review and prospects for industrial ecology. *Journal of Industrial Ecology*, Vol. 19, No 2, 236-251, 2015.
6. Gunderson Lance: Ecological Resilience — In Theory and Application. *Annual Review of Ecology and Systematics*, Vol. 31, 425-439, 2000.
7. Klein Richard, Nicholls Robert, Thomalla Frank: Resilience to natural hazards: How useful is this concept? *Environmental Hazards*, Vol. 5, No. 1-2, 35-45, 2004.
8. Meerow Sara, Newell Joshua Peter, Stults Melissa: Defining urban resilience: A review. *Landscape and Urban Planning*, Vol. 147, 38-49, 2016.
9. Adger Neil: Social and Ecological Resilience: Are They Related? *Progress in Human Geography*, Vol. 24, No. 3, 347-364, 2000.
10. Friend Richard, Moench Marcus: What is the purpose of urban climate resilience? Implications for addressing poverty and vulnerability. *Urban Climate*, Vol. 6, 98-113, 2013.

11. Lhomme Serhe, Serre Damien, Diab Youssef, Laganier Richard: Urban technical networks resilience assessment. In R. Laganier (Ed.), *Resilience and urban risk management*, London: CRC Press. 2013.
12. Pendall Rolf, Foster Kathryn, Cowell Margaret: Resilience and regions: building understanding of the metaphor. *Cambridge Journal of Regions, Economy and Society*, Vol. 3, No. 1, 71–84, 2010.
13. Matyas David, Pelling Mark: Positioning resilience for 2015: The role of resistance, incremental adjustment and transformation in disaster risk management policy. *Disasters*, Vol. 39 Suppl. 1:S1-18, 2015.
14. Alberti Marina, Marzluff John, Schulenberger Eric, Bradley Gordon: Integrating Humans Into Ecology: Opportunities and Challenges for Studying Urban Ecosystems. *BioScience*, Vol. 53, No. 12., 1169-1179, 2003.
15. Godschalk David: Urban hazard mitigation: Creating resilient cities. *Natural Hazards Review*, Vol. 4, No. 3, 136–143, 2003.
16. Campanella Thomas: Urban Resilience and the Recovery of New Orleans. *Journal of the American Planning Association*, Vol. 72, No. 2, 141-146, 2006.
17. Wardekker Arjan, de Jong Arie, Knoop Joost, van der Sluijs Jeroen: Operationalising a resilience approach to adapting an urban delta to uncertain climate changes. *Technological Forecasting and Social Change*, Vol. 77, No. 6, 987–998, 2010.
18. Ahern Jack: From fail-safe to safe-to-fail: Sustainability and resilience in the new urban world. *Landscape and Urban Planning*, Vol. 100, No. 4, 341-343, 2011.
19. Tyler Stephen, Moench Marcus: A framework for urban climate resilience. *Climate and Development*, Vol. 4, No. 4, 311-326, 2012.
20. Liao, Kuei-Hsien: A theory on urban resilience to floods – A basis for alternative planning practices. *Ecology and Society*, Vol. 17, No. 4, 48, 2012.
21. Brown Anna, Dayal Ashvin, Rumbaitis Del Rio Christina: From practice to theory: Emerging lessons from Asia for building urban climate change resilience. *Environment and Urbanization*, Vol. 24, No. 2, 531–556, 2012.
22. Wamsler Christine, Brink Ebba, Rivera Claudia: Planning for climate change in urban areas: From theory to practice. *Journal of Cleaner Production*, Vol. 50, No. 2, 68-81, 2013.
23. Cutter Susan, Barnes Lindsey, Berry Melisa, Burton Christopher, Evans Elijah, Tate Eric, Webb Jennifer: A place-based model for understanding community resilience to natural disasters. *Global Environmental Change*, Vol. 18, No. 4, 598–606, 2008.
24. Han Xuehua., Wang Liang., Xu Dandan, Wei He., Zhang Xinghua, Zhang, Xiaodong: Research Progress and Framework Construction of Urban Resilience Computational Simulation. *Sustainability* Vol. 14, No.19, 11929, 2022.
25. Scherzer Sabrina, Lujala Paivi, Jan Ketil Rod: A community resilience index for Norway: An adaptation of the Baseline Resilience Indicators for Communities (BRIC). *International Journal of Disaster Risk Reduction*, Vol. 36, 101-107, 2019.
26. Ribeiro Paulo, Pena Luis Antonio JG: Urban Resilience: a conceptual framework. *Sustainable Cities and Society*, Vol. 50, 101625, 2019.
27. G. Eason, B. Noble and I. N. Sneddon, "On certain integrals of Lipschitz-Hankel type involving products of Bessel functions", *Phil. Trans. Roy. Soc. London*, vol. A247, pp. 529-551, April 1955.

URBANA OTPORNOST: DEFINICIJE, RAZUMEVANJE I KONCEPTUALIZACIJA

Održivost i otpornost su dve glavne paradigme planiranja i kreiranja politike u proteklih decenijama. Podsticanje otpornosti u suočavanju sa ekološkom, socio-ekonomskom i političkom neizvesnošću i rizikom privuklo je pažnju akademika i donosioca odluka u različitim disciplinama, sektorima i prostornim razmerama. Otpornost gradova je postao važan cilj za gradove, posebno sa stanovišta prilagođavanja klimatskim promenama i smanjenja njihovog ekološkog otiska. Urbana otpornost se konvencionalno definiše kao merljiva sposobnost bilo kog urbanog sistema, sa njegovim stanovnicima, da održi kontinuitet kroz sve šokove i stresove dok se pozitivno prilagođava i transformiše ka održivosti. Međutim, u teoriji i praksi postoje različite definicije koje su često suprotstavljaju. Ovaj rad prvo daje pregled postojećih definicija urbane otpornosti i ističe njihove glavne determinante. Zatim se u radu razmatraju definicije iz perspektive načina inkorporiranja ključnih pojmova koji se nalaze kako u teoriji otpornosti tako i u teoriji grada. U nastavku se prepoznaju sličnosti i međusobne tenzije između ključnih pojmova. Konačno, u radu se zaključuje da je potrebna jasnija konceptualizacija da bi se ova razvojna oblast unapredila i kako bi se stvorili uslovi za njenu dalju operacionalizaciju.

Ključne reči: *urbana otpornost, definicije, konceptualizacija otpornosti*

PARAMETRIC DESIGN OF 3D PRINTED RIBBED SLAB SYSTEM BASED ON NATURE-INSPIRED PATTERNS*



UDC 624.073.5

681.625.9:688.796.2

Maša Žujović, Jelena Milošević

University of Belgrade, Faculty of Architecture, Belgrade, Serbia

ORCID iDs: Maša Žujović
Jelena Milošević

 <https://orcid.org/0000-0001-6346-5102>
 <https://orcid.org/0000-0001-7293-8194>

Abstract. *The interest in pattern geometry and its application to architecture may be seen throughout history. While some authors were fascinated by pattern aesthetics, others were focused on their effectiveness and underlying principles of pattern formation. In continuing with the work of the second group of authors, this paper reviews opportunities for efficient ways of implementing patterns in the design of architectural elements, supported by recent developments in parametric design and digital fabrication techniques. This paper aims to analyze pattern configurations found in nature in order to determine the underlying generation principles and the potential of their application for 3D printed slab systems. Using case study methodology, selected patterns will be applied in developing a generative parametric design system, which will further be tested in creating and (small-scale) fabricating ribbed slab elements. The result of the research is the generalization of a design approach based on principles of natural pattern formation to produce sustainable design solutions that rely on the transposition of the inherent efficiency of natural systems, such as low energy or material consumption.*

Key words: *pattern design, pattern formation, bioinspired design, 3D printing, ribbed slab systems*

1. INTRODUCTION

Pattern geometry has long captivated architects and designers, serving as a source of inspiration and innovation throughout history. While some authors have been captivated by the aesthetic appeal of patterns, others have focused on their effectiveness and the underlying principles of pattern formation. Building upon the work of the latter group of authors, this study explores the effective pattern implementation in architectural design, leveraging recent developments in parametric design and digital fabrication techniques.

Received June 30, 2023 / Revised August 1, 2023 / Accepted August 15, 2023

Corresponding author: Maša Žujović - University of Belgrade, Faculty of Architecture, Belgrade, Serbia
e-mail: masa.zujovic@arh.bg.ac.rs

*Selected paper presented at the International Conference Sinarg 2023 held in Niš, Serbia on 14-15 September 2023.
© 2024 by University of Niš, Serbia | Creative Commons License: CC BY-NC-ND

By analyzing pattern configurations found in nature, this paper aims to determine the underlying generation principles and explore their potential application for 3D-printed ribbed slab systems. The main goal of this research is to develop a design approach based on the efficiency of natural systems, leading to sustainable design solutions that minimize energy and material consumption.

Throughout architectural history, numerous authors have recognized the profound impact of patterns on the built environment [1], [2]. One of the most notable authors in this area was architect Christopher Alexander, who explored patterns as fundamental building blocks in architectural design throughout his work, particularly in his book *A Pattern Language* [3]. Although his work focused more on the experiential qualities of patterns in architectural spaces rather than on the geometric and structural properties, his work paved the way for further exploration of this topic in later years. In contrast to Alexander's emphasis on aesthetics, even prior, another group of authors delved into the scientific principles underlying pattern formation and their potential application in architecture. Thompson, a mathematician, and biologist, investigated the mathematical properties of natural patterns in his book *On Growth and Form*, focusing on a relationship between physical forces and the formation of patterns in nature, highlighting pattern generation principles and the efficiency of natural patterns [4].

Recent technological advancements have opened new possibilities for integrating patterns into architectural practice [5], [6]. Parametric design, a computational design approach, allows architects to create complex and customizable designs by manipulating parameters and algorithms. Using parametric design enables the exploration of intricate patterns that can be tailored to specific contexts and performance criteria. Additionally, digital fabrication techniques, such as 3D printing, enable the realization of complex geometries with unprecedented precision and efficiency. These technological advancements provide a fertile ground for exploring the implementation of patterns in architectural elements with improved efficiency and sustainability.

Slabs are the structural building element with great potential for optimization regarding material efficiency. Today slabs are primarily made of concrete and take up most of it out of all construction elements in the standard building, making them a significant contributor to global CO₂ emission [7]. This comes as a result of the traditional building technology limitations where non-standard forms require complex formworks to cast concrete, making them cost-inefficient. For this reason, even though ribbed slabs have been proven more materially and structurally efficient, most floor systems are still constructed as flat slabs. To answer this problem, the use of digital fabrication technologies, especially 3D printing, has been extensively researched in recent years and has shown great potential for the fabrication of non-standard geometries through the printing of structural material or, more commonly, the printing of bespoke formworks [8].

Ribbed slabs are optimized alternatives to solid slabs. This study explores the possibilities of harnessing the inherent efficiency of nature-inspired pattern formation for non-standard slab design in order to assess the potential design and fabrication of more sustainable construction elements

2. METHODOLOGY

Starting with the literature review, this paper provides an overview of nature-inspired patterns by discussing underlying design principles, generation methods, and potential applications for 3D printed slabs. First, the key points and some of the main authors in the field are recognized in the brief historical review of the topic and some of the current architectural concepts influenced by pattern science. Then, main generation principles are identified and systematized along with their natural manifestations and corresponding mathematical models. Next, using case study methodology, several patterns are selected and applied through the digital design of non-standard ribbed floor systems. Designed slabs are then evaluated, against the standard solid slab, in terms of material efficiency by assessing specific rib configurations to exploit the inherent efficiency of natural patterns to create sustainable construction elements.

3. NATURE-INSPIRED PATTERNS

The first observations in the field of patterns came from the attempts of ancient Greek philosophers and mathematicians, such as Pythagoras or Plato, to understand and explain the universal laws in nature by observing natural phenomena. In the Middle Ages, Fibonacci introduced the Western world to the Fibonacci sequence in the book *Liber Abaci* [9]. Mathematics and the understanding of patterns experienced accelerated knowledge development from the 15th century with the transition to the Renaissance period. Thus, Leonardo Da Vinci analyzed the appearance of the golden section in nature, noticing, among other things, the spiral configuration of plant leaf patterns. Kepler applied the Fibonacci sequence to describe patterns in nature. The golden ratio and the Fibonacci sequence became two of the best-known mathematical rules that can be used to describe a large number of patterns in nature. During the 18th and 19th centuries, numerous scientists, such as Thomas Browne and Charles Bonnet, further developed these ideas [10]. For example, the problem of minimum area for a given contour was defined by studying soap bubbles. Based on these laws, William Thomson explained the system of efficient packing of cells, that is, one type of pattern formation in space [11].

Previous points to not only interest in aesthetic aspects of the natural patterns but also the significant interest in the underlying mathematical principles that lead to their formation. The attempts to understand naturally occurring visual patterns and their causes have interested many researchers during the last century. One of the first comprehensive research attempts to explain complex physical phenomena in nature was made by D'Arcy Wentworth Thompson from the position of natural science. He explained many phenomena that influence the formation of form and patterns in nature, such as the influence of scale on the formation of patterns [4]. His work emphasized the interconnectedness between mathematics, physics, and biology in understanding pattern formation. He proposed that physical forces, such as tension, pressure, and growth, play a crucial role in shaping natural patterns. Although it did not focus on establishing mathematical models describing pattern generation principles, this work is important from the architectural point of view as it offers a systematized insight into the formation of different structures found in nature and their morphogenesis. These principles were further researched in the following years. For example, Alan Turing, a pioneer of artificial intelligence, studied the mechanisms that influence the formation of patterns in living organisms broadening the understanding of

their morphogenesis [12]. Most of the natural patterns were subject to observation and exploration from an early age, but branching, which was noted early on, was explained only much later. First, Lindenmayer presented the L-systems, which can be used to describe the growth of plants in the form of fractals. Followed by Mandelbrot's introduction of the term fractal geometry [13]. The interest in this topic over time evolved and led to the formation of pattern theory, a branch of applied mathematics that analyzes the patterns that the world generates in any modality, in all their natural complexity, intending to reconstruct the processes, objects, and events that produced them [14]. This theory represents the theoretical basis of many disciplines, such as artificial intelligence, image and acoustic signal processing, and pattern recognition.

The concept of morphogenesis, or the creation of form, was originally used to describe biological processes of cellular formation. However, the concept of digital morphogenesis emerged with the development of digital technologies. It refers to applying computational techniques and algorithms to generate and explore complex architectural forms and structures, drawing inspiration from biological processes and natural systems [15]. Patterns in nature represent a source of inspiration for this research direction as they are often formed on principles that favor the logic of optimization, which can be highly beneficial when transposed in structural design [16]. Biomimetics, the design that draws inspiration from nature in terms of an organism's or ecosystem's functional notions, emerged from this concept. It focuses on the interpretation and implementation of natural principles for generating optimized structures through generative design [17].

3.1. Pattern formation principles

A pattern in mathematics refers to any system formed based on defined rules. For this work, visual patterns, those with a geometric manifestation, are relevant. Visual patterns and the rules by which they are formed are mostly present in nature. There were multiple attempts at categorizing natural patterns [18], [19]. According to the literature review, nature-based patterns can be classified into the following categories based on the main generation principles.

Self-Organization: A dynamic process in which complex structures and patterns emerge from numerous interactions, executed using only local information, among the individual lower-level components of the system.

Self-Similarity: Process of forming geometric patterns that exhibit self-similarity, meaning that they are formed by repeating a unit pattern through different scales, such as fractals.

Reaction-Diffusion Systems: A dynamic process naturally found in chemistry involving local chemical reactions and substance diffusion, leading to spatial pattern formation.

Growth and Morphogenesis: Biological growth processes are caused by the distribution of resources, cell proliferation, and physical constraints that determine the spatial arrangement of tissues and organs.

Physical Forces and Constraints: Process of forming patterns under the influence of physical forces (tension, compression, or gravity) or mechanical forces and growth constraints.

Optimization: The natural process of pattern forming under optimization and efficiency principles in nature exhibits remarkable adaptations for resource utilization, energy, and material efficiency, or functional optimization.

Table 1 Overview of patterns and generation principles in nature

Generation principle	Pattern	Computational models
Self-Organization	ant trails, flocking of birds, cell organization, ripple patterns	cellular automata, agent-based simulations
Self-Similarity	branching networks, coastlines, cloud shapes, crystals, waves	recursive algorithms
Reaction-Diffusion Systems	turing patterns, stripes, spots, travelling waves	partial differential equations
Growth and Morphogenesis	tissue and bone morphology, spirals, trees	finite element method
Physical Forces and Constraints	branching structures, honeycomb, spirals, banded patterns, voronoi	finite element method
Optimization	voronoi, packing patterns, Fibonacci sequence and the golden ratio, flow patterns, spider webs, sponges	biological algorithms / including evolutionary algorithms, genetic algorithms, neural networks

Every pattern in nature or its geometric approximation can be classified into at least one listed category (Table 1). However, it is important to note that patterns in nature are often the result of the combination of multiple factors. Patterns from each category can be applied to a surface; therefore, each can be applied as a rib configuration for slab systems. For example, standard rib configurations include regular networks of ribs belonging to regular geometric tessellations or ribs following isostatic lines representing force flows [20].

4. DESIGN OF RIBBED SLAB SYSTEM

In standard building practice, rib configuration selection is often influenced by construction technology limitations rather than achieving maximal efficiency. Previous results in using regular geometric patterns such as orthogonal or triangular grids as they do not require overly complex formworks and can be achieved using modular elements [21]. Pier Luigi Nervi has shown in his work that it is possible to achieve much greater material efficiency using rib configurations that follow isostatic lines of principal bending moments [22]. However, his approach was never widely used because of the needed formwork complexity. Digital fabrication and especially 3D printing techniques have shown a great potential for more efficient fabrication of complex form slabs by allowing bespoke formwork design [23]–[25].

This study explores the potential applications of nature-inspired patterns for the design of non-standard ribbed floor slabs for 3D printing. To do this, a design process, shown in Figure 1, was established and implemented, producing test slab models.

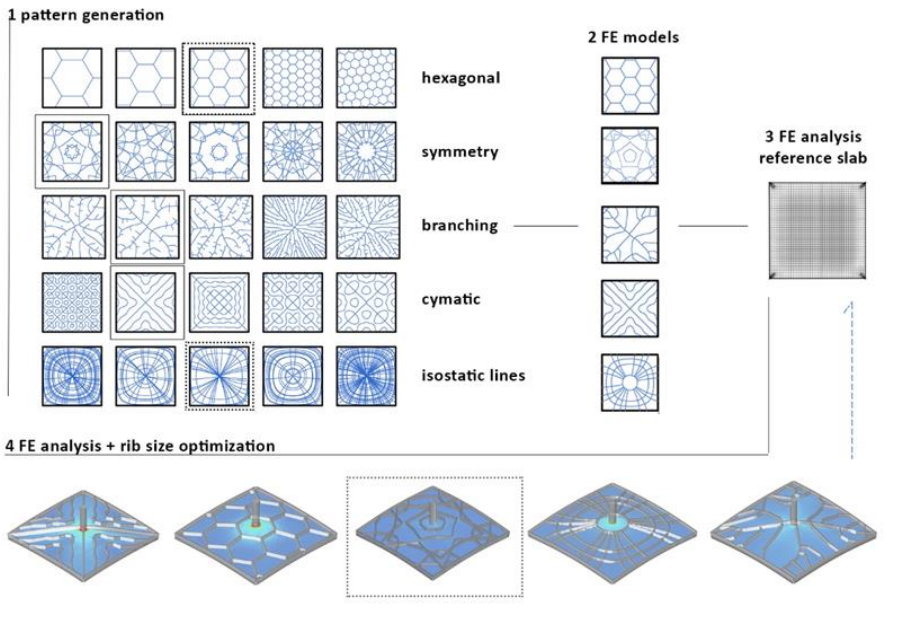


Fig. 1 Design process workflow

First, a model slab was selected as an 8x8m centrally supported two-way slab in reference to the Nervi's Gatti Wool Factory, which was proven to be one of the highly materially efficient built slabs [22], and because it represents a typical span for multistory buildings. The reference solid slab was tested with Finite Element Analysis (FEA) using the Millipede plugin for Rhinoceros 3D/Grasshopper. A solid slab with a thickness of $h=22\text{cm}$ was chosen as a reference.

Next, based on the literature review, several pattern generation principles were selected for the slab design. The selection was made considering the optimization potential and compatibility of said principle with the structural requirements of slab elements. Some natural patterns were discarded due to the overly complex geometric nature (e.g., Turing patterns), and some due to the formation principal incompatible with the selected design task. Several patterns were selected and parametrically generated, exploring different configurations and densities. Five pattern groups were then chosen for further testing based on their form, complexity, optimization potential, and aesthetic qualities, with one of them being an isostatic pattern generated through FEA. This pattern was included as a second reference since it is commonly considered an efficient configuration in the building industry.

For each group, one representative configuration was chosen for testing, each with a similar curve density. In the next step, these configurations were applied to the test slab, and digital models were made. These models were then tested using another FEA, and optimal rib size was determined based on the deflection. Finally, all test models were compared with the reference slab in terms of material efficiency.

In the final step, the most efficient configuration was selected, and a 3D model was generated. Based on this 3D model, a formwork for a small-scale prototype was designed

for 3D printing on a desktop PLA printer simulating a larger-scale production method of combining 3D printed formwork with traditional concrete casting techniques.

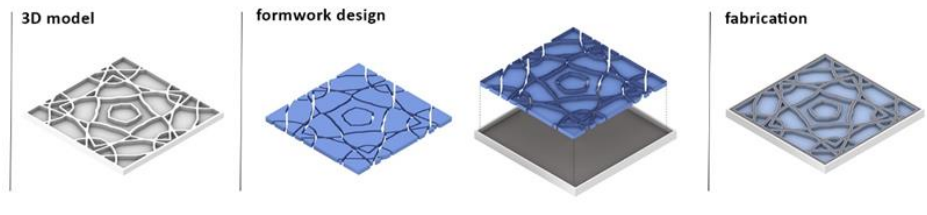


Fig. 2 Formwork design

5. DISCUSSION

The presented case study explored a variety of design solutions for non-standard rib configurations based on the selected generation principles. The results have shown that these rib configurations can lead to a more materially efficient design. Among the analyzed slab models, all had lower material consumption than the reference slab. The weight difference was between 16 - 42%, with the most efficient being rib configuration formed on the principles of multiple symmetry and reflections. Another important finding was that this configuration showed slightly better performance than the tested isostatic pattern, confirming the hypothesis that natural generation principles could lead to innovative and more optimized design solutions.

Although this study confirmed efficiency of ribbed slab systems based on nature-inspired patterns, some aspects could be further developed:

The results of this study can be further verified through the fabrication of small-scale prototypes and model testing.

Further research should consider reinforcement design as it was not included in this research; however, it is an important step for scaling up the prototypes and can potentially alter the design criteria.

The proposed design workflow could be developed in the future to include additional optimization algorithms in the form-finding stage to further improve the material efficiency of the proposed structures.

FEA for this study was done using a Millipede plugin; however, in the future, it would be beneficial to consider using other software that could provide more parameter control to increase optimization and precision.

In this study, designed structures were assumed to be standard reinforced concrete; to increase sustainability, exploring other material alternatives for both construction elements and digital fabrication would be necessary.

6. CONCLUSION

This paper explores the potential of implementing nature-inspired pattern generation principles in the structural element design workflow for creating non-standard ribbed floor systems. The literature review was first conducted to understand the development of the interest in the field of nature-inspired patterns, underlying principles, and their impact

on architectural design. The main groups of generation principles were then identified and systematized, along with the corresponding occurrences in nature. Among these, several with the most potential for use in the design of slab elements were selected and applied in the case study. Next, the design workflow was formed and applied to design several slabs with non-standard rib configurations and to compare them against a standard flat slab. Results have shown that using nature-inspired principles for rib configuration form-finding has excellent potential for reducing material consumption. The proposed design method, combined with the novel fabrication techniques, could be used to design more sustainable construction elements.

This study is part of an ongoing research effort into the digital fabrication of structurally optimized architectural elements, through which discussed further research directions and limitations will be addressed.

Acknowledgement. *This research was funded by the Ministry of Education, Science and Technological Development of the Republic of Serbia, grant number 451-03-68/2020-14/200090. The research was done under the research lab of the University of Belgrade, Faculty of Architecture—Laboratory for Innovative Structures in Architecture (LISA).*

REFERENCES

1. Uchiyama, Yuta, Eduardo Blanco, and Ryo Kohsaka: Application of Biomimetics to Architectural and Urban Design: A Review across Scales. *Sustainability*, vol. 12, no. 23, p. 9813, Nov. 2020, doi: 10.3390/su12239813.
2. Badamah, Lidia: Form Follows Environment: Biomimetic Approaches to Building Envelope Design for Environmental Adaptation. *Buildings*, vol. 7, no. 4, p. 40, May 2017, doi: 10.3390/buildings7020040.
3. Alexander, Christopher, Sara Ishikawa, and Murray Silverstein: *A pattern language: towns, buildings, construction*. New York: Oxford University Press, 1977.
4. Thompson, D'Arcy Wentworth: *On Growth and Form: The Complete Revised Edition*. Dover Publications, Incorporated, 1992.
5. Menges, Achim: Material Computation: Higher Integration in Morphogenetic Design. *Architectural Design*, vol. 82, no. 2, pp. 14–21, Mar. 2012, doi: 10.1002/ad.1374.
6. Iwamoto, Lisa: Digital fabrications: architectural and material techniques. in *Architecture briefs*. New York: Princeton Architectural Press, 2009.
7. Jayasinghe, Amila, John Orr, Will Hawkins, Tim Ibell, and William P. Boshoff: Comparing Different Strategies of Minimising Embodied Carbon in Concrete Floors. *Journal of Cleaner Production*, vol. 345, p. 131177, Apr. 2022, doi: 10.1016/j.jclepro.2022.131177.
8. Žujović, Maša, Radojko Obradović, Ivana Rakonjac, and Jelena Milošević: 3D Printing Technologies in Architectural Design and Construction: A Systematic Literature Review. *Buildings*, vol. 12, no. 9, p. 1319, Aug. 2022, doi: 10.3390/buildings12091319.
9. Salinger, Nikos A.: *Architecture, Patterns, and Mathematics*. *Nexus Network Journal*, vol. 1, pp. 75–85, 1999.
10. J. A. Adam, *Mathematics in Nature: Modeling Patterns in the Natural World*. Princeton University Press, 2011.
11. F. J. Almgren: Minimal surface forms. *The Mathematical Intelligencer*, vol. 4, no. 4, pp. 164–172, Dec. 1982, doi: 10.1007/BF03023550.
12. Turing, Alan: The Chemical Basis of Morphogenesis. *Philosophical Transactions of the Royal Society of London*, vol. 237, no. 641, pp. 37–72, 1952.
13. M. M. Novak, Ed., *Thinking in patterns: fractals and related phenomena in nature*. River Edge, N.J: World Scientific, 2004.
14. Mumford, David: Pattern Theory: A Unifying Perspective. in *Progress in Mathematics*, 1994, pp. 187–224. doi: DOI: 10.1007/978-3-0348-9110-3_6.
15. Kolarevic, Branko: *Digital Morphogenesis*. in *Architecture in the Digital Age*, Taylor & Francis, 2003.
16. Leach, Neil: Digital Morphogenesis. *Architectural Design*, vol. 79, no. 1, pp. 32–37, Jan. 2009, doi: 10.1002/ad.806.

17. Jamei, Elmira, and Zora Vrcelj: Biomimicry and the Built Environment, Learning from Nature's Solutions. Applied Sciences, vol. 11, no. 16, p. 7514, Aug. 2021, doi: 10.3390/app11167514.
18. P. S. Stevens: Patterns in Nature. in Atlantic Monthly Press book. Little, Brown, 1974.
19. Field, Mike, and Martin Golubitsky: Symmetry in chaos: a search for pattern in mathematics, art, and nature, 2nd ed. Philadelphia, PA: Society for Industrial and Applied Mathematics, 2009.
20. Nervi, Pier Luigi, Cristiana Chiorino, Elisabetta Margiotta Nervi, and Thomas Leslie: Aesthetics and technology in building. The twenty-First-Century edition. Urbana: University of Illinois Press, 2018.
21. Wight, James K: Reinforced concrete: mechanics and design. Seventh edition. Hoboken, New Jersey: Pearson, 2016.
22. Halpern, Allison B, David P Billington, and Sigrid Adriaenssens: The Ribbed Floor Slab Systems of Pier Luigi Nervi. Proceedings of the International Association for Shell and Spatial Structures (IASS) Symposium 2013, 2013, p. 8.
23. Burger, Joris, Tobias Huber, Ena Lloret-Fritsch, Jaime Mata-Falcón, Fabio Gramazio, and Matthias Kohler: Design and fabrication of optimised ribbed concrete floor slabs using large scale 3D printed formwork. Automation in Construction, vol. 144, p. 104599, Dec. 2022, doi: 10.1016/j.autcon.2022.104599.
24. Jipa, Andrei, Cristián CALVO Barentin, Gearóid Lydon, Matthias Rippmann, Matteo Lomaglio, Arno Schlüter, and Philippe Block: 3D-Printed Formwork for Integrated Funicular Concrete Slabs. Proceedings of the IASS Annual Symposium 2019 – Structural Membranes 2019, 2019.
25. Graser, Konrad, Marco Baur, and Hack Norman: DFAB House: A Comprehensive Demonstrator of Digital Fabrication in Architecture. in Fabricate 2020, UCL Press, 2020, pp. 130–139. doi: 10.2307/j.ctv13xpsvw.

PARAMETARSKI DIZAJN 3 D ŠTAMPANIH SISTEMA REBRASTIH PLOČA INSPIRISAN PRIRODNIM OBLICIMA

Kroz istoriju se može videti interes za geometriju uzoraka i njenu primenu na arhitekturu. Dok su neki autori bili fascinirani estetikom obrazaca, drugi su bili fokusirani na njihovu efikasnost i osnovne principe formiranja obrazaca. Nastavljajući rad druge grupe autora, ovaj rad razmatra mogućnosti za efikasne načine implementacije obrazaca u dizajn arhitektonskih elemenata, podržane najnovijim razvojem parametarskog dizajna i tehnikama digitalne izrade. Ovaj rad ima za cilj analizu konfiguracije obrazaca koje se nalaze u prirodi kako bi se utvrdili osnovni principi generisanja i potencijal njihove primene za 3D štampane sisteme ploča. Koristeći metodologiju studije slučaja, odabrani obrasci će biti primenjeni u razvoju generativnog parametarskog projektantskog sistema, koji će se dalje testirati u kreiranju i izradi (malih) elemenata rebrastih ploča. Rezultat istraživanja je generalizacija dizajnerskog pristupa zasnovanog na principima formiranja prirodnog obrasca za proizvodnju održivih dizajnerskih rešenja koja se oslanjaju na poziciju inherentne efikasnosti prirodnih sistema, kao što je niska potrošnja energije ili materijala.

Ključne reči: dizajn obrazaca, formiranje obrazaca, bioinspirisani dizajn, 3D štampa, sistemi rebrastih ploča



APPLICATION OF ADHESIVELY BONDED CFRP FOR REINFORCEMENT AND REHABILITATION OF FATIGUE DAMAGED STEEL STRUCTURE - ONLY A NICE IDEA? *

UDC 624.014.2:69.059.3
69.059.3:678.7

Hartmut Pasternak, Yvonne Ciupack

Brandenburg University of Technology, Cottbus, Germany

ORCID iDs: Hartmut Pasternak
Yvonne Ciupack

 <https://orcid.org/0000-0003-0473-0302>
 <https://orcid.org/0000-0002-4276-1356>

Abstract. *As an alternative to classic repair measures of fatigue-damaged steel structures, adhesively bonded CFRP lamellas are ideal. In this way, disadvantages of the established methods can be circumvented. Compared to bolted reinforcing measures, cross-sectional weakening by the bolt is avoided. Heat-induced residual stresses and distortions, as they usually occur during repair welding, can also be excluded. These disadvantages represent a weak point during cyclic loading due to the notch effect.*

To characterize the materials, tests are carried out on small scale specimens. With the help of tests on CT-samples a comparison with established methods such as drilling the crack tip and repair welding is realized. Based on the crack propagation, the great potential of bonded CFRP reinforcements can be deduced. By prestressing the lamellas, the remaining lifetime can generally be further increased. It should be noted, however, that with single-sided prestressing, a precamber of the specimen and, during loading, a secondary bending moment may occur. The combination of bonded CFRP with established methods can be described as particularly effective. With a reinforcement on both sides with pre-stressed plates, up to 7.9 times the remaining service life can be determined in comparison to unreinforced specimens.

The effectiveness of adhesively bonded CFRP lamellas is examined in a German research project. Selected results are presented in this paper.

Key words: steel structures, bonded CFRP, fatigue, repair, reinforcement.

Received June 30, 2023 / Revised August 1, 2023 / Accepted August 15, 2023

Corresponding author: Hartmut Pasternak - Brandenburg University of Technology, Cottbus, Germany
e-mail: Hartmut.Pasternak@b-tu.de

*Selected paper presented at the International Conference Sinarg 2023 held in Niš, Serbia on 14-15 September 2023.
© 2024 by University of Niš, Serbia | Creative Commons License: CC BY-NC-ND

1. INTRODUCTION

Many cyclic loaded steel structures, such as road and railways bridges or large conveyor systems, have an enormous need for rehabilitation. In particular, the average condition of bridges has deteriorated significantly in recent years. A study by the Federal Highway Research Institute in Germany shows that ca. 15% of the road bridges have to be renewed or rehabilitated in the near future [1]. Similar conditions can be observed in other countries. The main reasons for this are the increased volume of traffic, the proportion of heavy-duty traffic and the permissible axle loads in the last three decades, which clearly exceed the traffic load forecasts used for the design of bridges in the 1960s.

According to the current state of the art, fatigue damaged steel structures are strengthened by drilling the crack tip, repair welding or a combination of both. Partially, additional reinforcement measures, e.g. steel sheets or angles, are locally welded or bolted. The disadvantages of those common methods are the high heat input through welding and the associated negatively acting residual stresses as well as the cross-sectional weakening caused by bolts. Additionally, undefined notch details can originate from those repair methods. Frequently fatigue cracks again appear on these notch details after a short period of time.

The strengthening of cracked steel structures using adhesively bonded CFRP lamellas overcomes the before mentioned disadvantages and, as the experimental findings show, can even result in higher remaining lifetimes compared to common repair methods. It allows a strengthening of the existing structure without inducing additional, undefined notch details. Furthermore, it represents a repair method without significantly changing the dead weight. Figure 1 shows potential details for an application of adhesively bonded CFRP lamellas as a method of crack repair.

CFRP are characterized by a high tensile strength, a high modulus of elasticity, which can even exceed the stiffness of carbon steel, and a very low specific weight. Furthermore, they are corrosion and fatigue resistant [2]. First experiences on strengthening steel structures using CFRP materials regarding both quasi-static as well as fatigue behaviour were presented by [3] and [4]. In [5] the effectiveness of a rehabilitation of fatigue-damaged details using welded sheet metal was compared to the effectiveness of a rehabilitation using adhesively bonded CFRP laminates. Initial design recommendations for increasing the remaining service life of steel structures with externally bonded CFRP materials can be found in the "CIRIA Design Guide"[6].

A major advantage of the reinforcement with CFRP lamellas is the possibility of prestressing. The pretension force in the lamellas induces compressive stresses into the steel component superimposing the stresses caused by the fatigue loading and thereby reduces the stress intensity at the crack tip. Two methods of applying prestressed CFRP lamellas for strengthening cracked steel structures have to be distinguished. The pretension force can on the one hand be transmitted into the steel component by an adhesive layer. This way the compressive stresses are concentrated locally on the area around the crack tip. Since the level of prestressing is limited by the strength of the adhesive bond on the other hand pre-stressing systems with fixed anchor points can be used. This way the pretension force is transmitted into the steel component at two discrete points. For the rehabilitation of concrete structures various prestressing systems with fixed anchor points have been developed. As part of the ongoing research project, the influence of adhesively bonded prestressed and non-prestressed CFRP lamellas on the crack propagation rate as a local reinforcement of fatigue damaged steel components is being investigated.

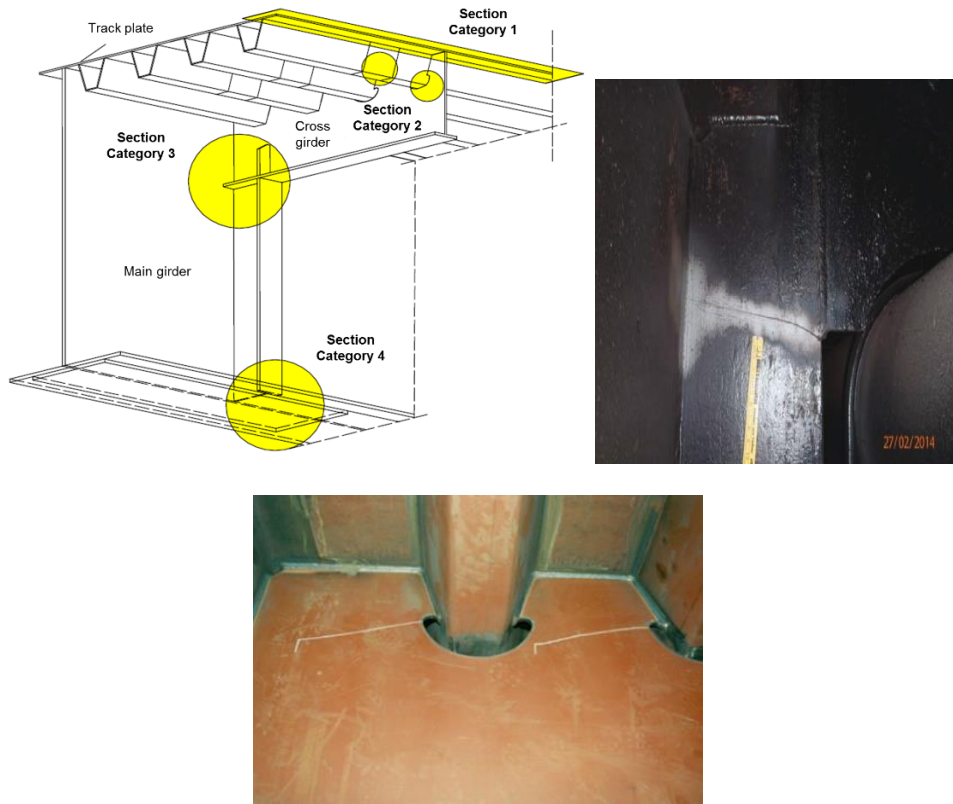


Fig. 1 Crack categories in orthotropic steel deck [7], cracks in categories 2 and 3

2. PRELIMINARY INVESTIGATIONS

The bonding behaviour and the mechanical properties of the used materials highly influence the efficiency of the repair method. For this reason, experimental investigations are carried out to determine the material characteristics of the CFRP lamella and five different adhesives as well as the strength of the adhesive bond between steel and CFRP. To characterize the CFRP's mechanical properties tensile tests according to DIN EN ISO 527-4 are carried out at the BTU in Cottbus. On average, the 20 mm wide and 1.4 mm thick lamella has an ultimate strength of 3400 MPa and a Young's modulus of 192 GPa. The mechanical properties of five preselected epoxy-based adhesives are determined by tensile tests on injection moulded dumbbell specimens in accordance with DIN EN ISO 527 and by lap shear tests based on DIN EN 14869-2 at the RWTH Aachen. The specimens used in the lap shear tests are modified according to [8] in order to take into account the adhesion between the adhesive and the CFRP. Figure 2 shows the geometry of the modified sample and the used testing device.

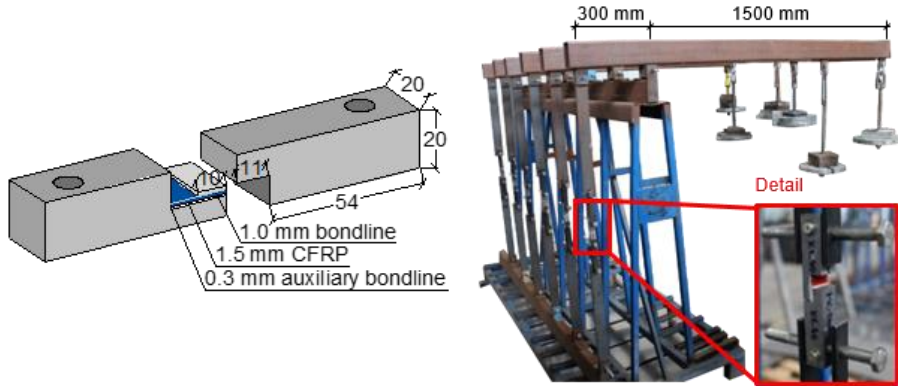


Fig. 2 Modified lap shear specimen [8] and creep testing device [9][10]

The experimental determination of the tensile properties is carried out strain-controlled with a rate of 1 %/min, while the shear properties are determined displacement-controlled with 0.09 mm/min. Based on the results, two adhesives are selected for the use in the following experimental investigations. Table 1 summarizes the mean values of the mechanical properties for the two chosen adhesives.

Table 1 Mechanical properties of the chosen adhesives (Epoxy 1= MC DUR 1280, Epoxy 2= SIKAdur 370)

	Epoxy 1	Epoxy 2
Tensile strength [MPa]	33.5	23.1
Young's Modulus [MPa]	8812	3858
Shear strength [MPa]	32.6	24.4
Shear Modulus [MPa]	1780	450

As can be seen from the Table 1, Epoxy 1 has a higher stiffness and a higher tensile and shear strength. Epoxy 2 in contrast has a higher deformation capacity in the quasi-static tests, which is regarded as beneficial concerning a possible detachment of the lamella under fatigue loading. In the installed condition, the bondline is stressed by permanent loads, such as the prestressing force and the mean fatigue load. Therefore, creep tests on the modified lap shear specimens (see Figure 2) are carried out at the BTU to investigate the deformation behaviour under a long-term loading. It is known that the creep behaviour of adhesive layers is significantly influenced by the ambient temperature. For this reason, the tests are carried out at four temperatures, which are shown in Table 2.

Table 2 Experimental conditions for creep tests

Temperature	<u>Lap shear strength</u>	<u>Stress level</u>
	quasi-static test	creep test
	Epoxy 1 / Epoxy 2	Epoxy 1 / Epoxy 2
80°C	3.4 / 9.9 MPa	1.4 / 4.0 MPa
50°C	4.8 / 14.9 MPa	1.9 / 6.0 MPa
23°C	32.6 / 24.4 MPa	11.3 / 9.5 MPa
-30°C	33.3 / 37.2 MPa	13.3 / 14.9 MPa

The thermal conditions reflect the expected operating conditions of the adhesive joint according to EC3. The determination of the load level of the permanent load is based on 40% of the quasi-static shear strength, which has also been determined at the corresponding temperatures. Figure 3 shows the mean curves of the deformation for a long-term loading of 1000 hours for various temperatures and adhesives.

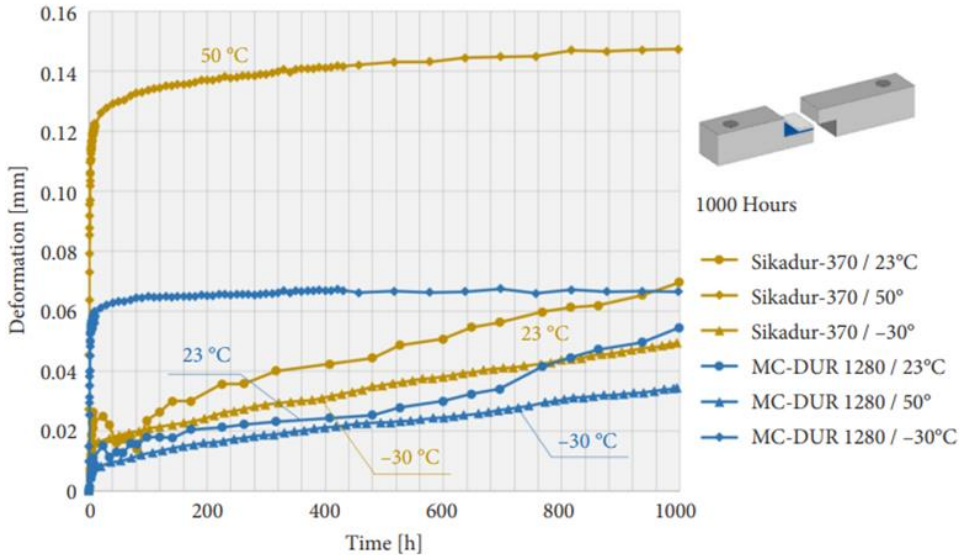


Fig. 3 Results of the creep tests [10]

In general, the characteristic increase of creep deformations with an increasing temperature can be derived from the diagram. For the design of adhesively bonded prestressed CFRP lamellas as a reinforcement measure, it is of particular importance to know the operating temperature range. Furthermore, it can be seen that Epoxy 2 allows larger creep deformations, suggesting a greater degradation of the pretension force compared to Epoxy 1. Both adhesives show distinct primary creeping. It is not solely attributable to the solving of secondary valence bonds and repositioning of chain segments. This behaviour is superimposed by load eccentricities due to the experimental setup, which result in twisting of the sample halves.

3. TESTS ON CENTRE-NOTCHED SPECIMENS

3.1. Specimen

In order to investigate the influence of adhesively bonded CFRP lamellas on the crack propagation rate in steel components, fatigue tests are carried out on centre-notched specimens at BTU. The test specimen consists of a 10 mm thick steel sheet made from S355 J2 with a length of 700 mm and a width of 105 mm. In order to create an initial crack, which subsequently is to be strengthened, a notch is induced in the middle of the specimen using the method of wire erosion. The bond length is dependent on the mechanical

properties of the adhesives and is chosen according to [11]. For Epoxy 1 the bond length is 150 mm and for Epoxy 2 the bond length is 220 mm. Figure 4 schematically shows the test specimen for Epoxy 1 with end anchoring, which are to prevent a failure at the end of the lamellas due to high peel stresses.

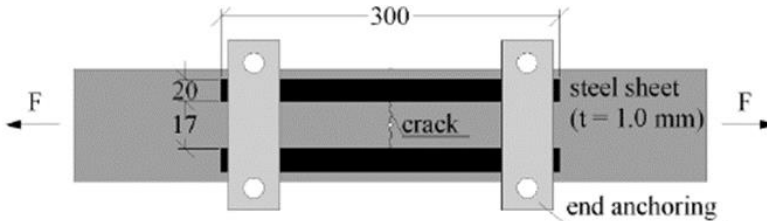


Fig. 4 Centre-notched specimens with single-sided adhesively bonded CFRP strips and end anchoring [10]

The CFRP lamellas are applied under laboratory conditions to the blasted steel surface (Sa 2½ according to DIN EN ISO 8501-1). Before applying the adhesive, the surfaces need to be thoroughly cleaned with acetone and lint-free cloths. In order to realize the bondline thickness of 1 mm, glass beads with the corresponding diameter are sprinkled into the not yet cured adhesive layer. After the joining process, the samples cure for 7 days under normal climatic conditions (temperature of $23^{\circ}\text{C} \pm 2^{\circ}\text{C}$ and relative humidity of $65\% \pm 4\%$) and under uniform contact pressure. If the CFRP strips are to be prestressed, this is done directly before the application of the lamella to the adhesive layer. Within the scope of the research project, a special prestressing device was developed at KIT Karlsruhe for this purpose. It consists of a substructure in form of a profile U240 and fixed anchorages at its ends. Clamping jaws, that are connected to the anchorages over a system of threaded rods, nuts and linkages, are used to fix the CFRP lamellas. Intermediate blasted aluminium plates provide a more uniform distribution of the clamping force on the lamellas and a higher coefficient of friction in order to prevent slippage of the CFRP lamellas. The pretension force is applied by tightening nuts at the anchorages and monitored by a combination of load cells at the preload point of the device and strain gauges on the lamellas. After the curing process and before releasing the sample, end anchors are applied to prevent a detachment of the lamella ends (see Figure 4).

3.2. Test setup and procedure

The influence of the adhesive stiffness, the pretension force and the load level on the remaining lifetime of the centre-notched specimens is investigated. The experimental matrix is summarized in Table 3.

Herein LL stands for the load level, P for the prestress grade, $\Delta\sigma$ for the stress range in MPa and R for the stress ratio. The pretension force specified in kN applies to each CFRP lamella.

The test procedure is divided into three phases: In the first test phase, an initial crack with a length of 40 mm is created by applying a fatigue load according to Table 3. At KIT Karlsruhe a method to repeatedly produce the same initial crack length in each specimen was developed. Using a copper wire, bonded onto the specimen at the point of the desired

Table 3 Test conditions and number of specimens respectively for the experimental investigations on centre-notched steel sheets

	Epoxy 1			Epoxy 2		
	P1	P2	P3	P1	P2	P3
kN	0	5	10	0	3	6
LL 1						
$\Delta\sigma = 50$ MPa	2	2	2	2	2	2
R = 0.5						
LL 2						
$\Delta\sigma = 70$ MPa	2	2	2	2	2	2
R = 0.5						
LL 3						
$\Delta\sigma = 100$ MPa	2	2	2	2	2	2
R = 0.1						

crack tip, and a voltage source linked to an electric circuit an input signal is placed into the test machine. When the initial crack tip reaches the copper wire a drop in voltage occurs. Using a shutoff criterion, the test machine automatically stops when a defined voltage value is undercut. In the second test phase each cracked specimen is strengthened by applying two CFRP lamellas on one side of the specimen following a fatigue test of each strengthened specimen in the third test phase. The fatigue test is carried out until the crack reaches a total length of 80 mm. The experiments run force-controlled with a frequency of 8 Hz. During the tests the machine force, the surface strains in the middle of the lamellas as well as the crack propagation to both sides are registered continuously.

3.3. Test results

The evaluation of the crack propagation during the third experimental phase is of particular interest, since the efficiency of the reinforcement measures is in the foreground of the investigations. For load level 1 (LL 1) the crack propagation curves are exemplary shown in Figure 5. For reasons of clarity, only the mean curves derived from the measurements of the crack propagation to both sides are given.

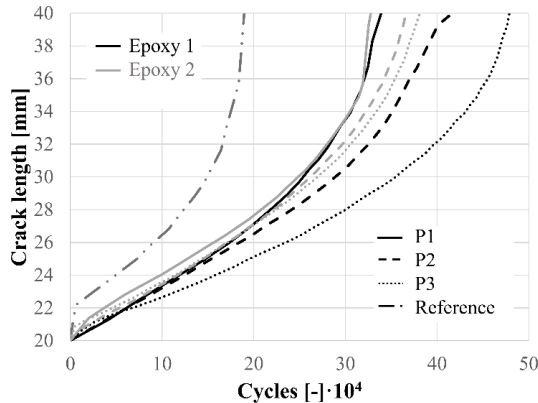


Fig. 5 Mean crack propagation curves for LL 1

A comparison of the results for the CFRP reinforced specimens with the results for unreinforced reference specimens shows the effectiveness of the developed repair method. A decrease in the crack growth rate can be observed with an increase in the pretension force. Whether this observation is generally valid for other load levels will be examined below. When plotting the number of cycles for the achieved crack length of 80 mm over the prestress grades, the curves in Figure 6 are obtained. In order to allow statements about the efficiency, the results are compared with the reference tests at the respective load levels.

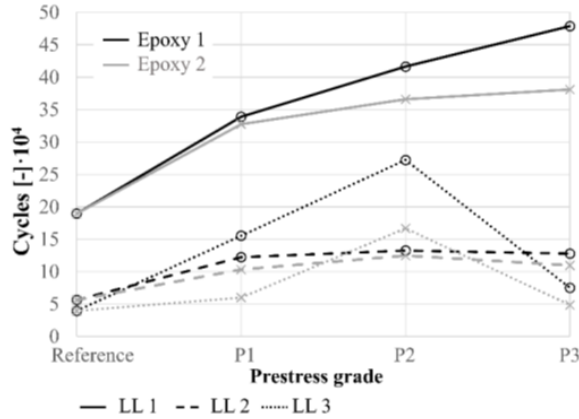


Fig. 6 Influence of the prestress grade on the remaining life-time of the centre-notched specimens

There is generally an increase in the remaining life-time with an increase in the pretension force for load level 1. In the cases of LL 2 and 3, the increase in the number of cycles can only be observed for the prestressing levels P1 and P2. If the prestress force is further increased, the remaining service life decreases. This phenomenon can be explained by the negative influence of single-sided reinforcement. The introduction of an eccentric tensile force on the 10 mm thick steel sheet creates a secondary bending moment causing a precamber, which increases with an increasing pretension force. For all test results, it can be observed that longer remaining lifetimes are achieved using Epoxy 1. It is assumed, that the reason for this behaviour lies in the higher stiffness of Epoxy 1 compared to Epoxy 2. A comparison of the remaining lifetimes as a function of the load level results in the curves shown in Figure 7.

Remarkable is the strong decrease of the remaining lifetime for LL 2. The stress range is lower than for LL 3, but a higher stress ratio R and thus a higher mean stress counteracting the prestress seam to lead to a decrease in the remaining lifetime. Also, in the comparison in Figure 7 the negative influence of the single-sided prestressed reinforcement with an increasing prestressing grade can be observed. For these reasons, it is desirable to realise a two-sided reinforcement with prestressed CFRP lamellas, if this is possible in the respective application. Tests with double-sided bonded and prestressed CFRP lamellas are currently performed at the KIT and confirm the negative influence of the secondary bending moment. Table 4 summarizes the results of the normalized remaining lifetimes of the specimens for the experiments presented here. The reference test (without bonded CFRP lamella) of the respective load level is assumed to be the reference value.

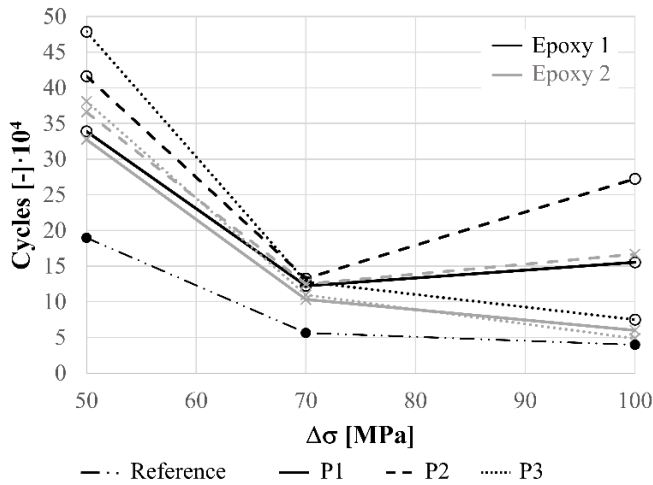


Fig. 7 Influence of the load level on the remaining life-time of the centre-notched specimens

Table 4 Normalized test results for the remaining lifetimes of the centre-notched specimens

	LL 1	LL 2	LL 3
Epoxy 1 – Single-sided reinforced			
P1	1.8	2.2	3.9
P2	2.2	2.4	6.9
P3	2.5	2.3	1.9
Epoxy 2 – Single-sided reinforced			
P1	1.7	1.8	1.5
P2	1.9	2.2	4.2
P3	2.0	1.9	1.2

4. OPTIMIZATION OF THE CRACK REPAIRING METHOD

If in practice higher demands are placed on the remaining service life than can be achieved by the sole application of bonded CFRP strips or conventional methods, it is possible to combine different repair methods. The gain that can be obtained by combining different methods is experimentally investigated on CT (compact tension, Fig. 8) specimens with an a/W -ratio of 0.6 according to ASTM E 399 at the BTU. Repair welding, drilling of the crack tip, single-sided bonding of prestressed and non-prestressed CFRP lamellas as well as combinations of these methods are considered. The test procedure is analogous to the investigations of centre-notched samples. A force amplitude of 10 kN, a stress ratio of 0.5 and a test frequency of 14 Hz are used. More detailed information on the experiment can be found in [9]. Figure 8 shows the results for the third test phase.

The standardization for the illustration in Figure 9 is based on a reference experiment in which the crack in the third test phase was created without any repair measure. The high potential of adhesively bonded CFRP lamellas can be confirmed for all test results. Prestressing of the lamellas (prestressing level P2 is used) leads to a further increase in the

sustainable number of load cycles. The remaining life can be further enhanced by combining different repair methods, such as drilling of the crack tip, repair welding and bonding of prestressed CFRP lamella (M1+M3+M4 in Figure 9).

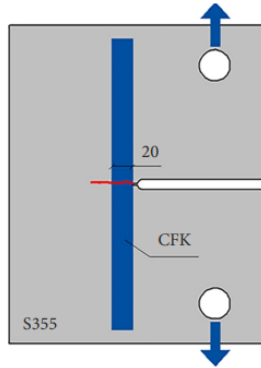
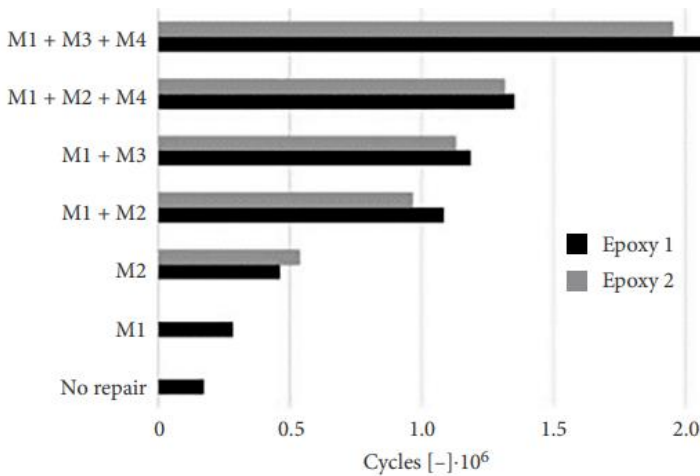


Fig. 8 CT specimen [10]



M1 – Drilling of crack tip; M2 – Non-prestressed CFRP;
M3 – Prestressed CFRP; M4 – Repair welding

Fig. 9 Comparison of the remaining lifetimes of CT specimens strengthened by various crack repairing methods

The standardization for the illustration in Figure 9 is based on a reference experiment in which the crack in the third test phase was created without any repair measure. The high potential of adhesively bonded CFRP lamellas can be confirmed for all test results. Prestressing of the lamellas (prestressing level P2 is used) leads to a further increase in the sustainable number of load cycles. The remaining life can be further enhanced by combining different repair methods, such as drilling of the crack tip, repair welding and bonding of prestressed CFRP lamella (M1+M3+M4 in Figure 9).

5. CONCLUSION AND OUTLOOK

The presented test results clearly show the high potential of adhesively bonded CFRP lamellas for a crack repair of cyclically loaded steel components. Depending on the adhesive and the loading conditions, the remaining lifetime of the specimens can be extended up to 690 %. For an application, it is essential to know the load level and define the material properties and the prestress grade, so that negative influences from the secondary bending moment are avoided. Further research needs to be done to design the reinforcement measure accordingly. If possible, a double-sided reinforcement is recommended. A combination of bonded CFRP lamellas with established methods, allows a further increase of the sustainable load cycles and is particularly suitable for high demands on the remaining service life of fatigue damaged steel constructions.

As could be shown in creep tests, it can be assumed that the pretension force is reduced by the primary and secondary creeping. The creep deformations increase with increasing temperature. In order to verify the effectiveness of the developed repair method in a practical application, measurements should be carried out on a selected bridge structure after the application of a local CFRP reinforcement.

Acknowledgement. *The IGF research project (IGF-No. 19032 BG/ DVS-no. 09.072) of the "Research Association on Welding and Allied Processes of the DVS, Aachener Straße 172, 40223 Düsseldorf" has been funded by the AiF within the program for sponsorship by Industrial Joint Research (IGF) of the German Federal Ministry of Economic Affairs and Energy, based on an enactment of the German Parliament.*

REFERENCES

1. difu Deutsches Institut für Urbanistik. (2013). Infrastruktur: Viele kommunale Straßenbrücken müssen bis 2030 neu gebaut werden. Medieninformation vom 30. September 2013. Retrieved from, <http://www.difu.de/presse/2013-09-30/infrastruktur-viele-kommunale-strassenbruecken-muessen-bis.html>
2. Dehn, F. 2005. Faserverbundwerkstoffe: Innovationen im Bauwesen – Beiträge aus Praxis und Wissenschaft. Berlin: Bauwerk.
3. Hollaway, L.C. & Cadei, J. 2002. Progress in the technique of upgrading metallic structures with advanced polymer composites. Progress in Structural Engineering and Materials 4 (2): 131-148.
4. Shaat, A., Schnerch, D., Fam, A. & Rizkalla, S. 2004. Retrofit of steel structures using Fiber-Reinforced Polymers (FRP): State-of-the-art. Transportation research board (TRB) annual meeting.
5. Jiao, H., Mashiri, F. & Zhao, X-L. 2012. A comparative study on fatigue behaviour of steel beams retrofitted with welding, pultruded CFRP plates and wet layup CFRP sheets. Thin-Walled Structures 59: 144-152.
6. Cadei, J. M. C., Stratford, T. J., Hollaway, L. C. et al. Strengthening metallic structures using externally bonded fibre-reinforced polymers. London: CIRIA 2004.
7. Sedlacek, G., Paschen, M. 2008. New ways in the reinforcement of orthotropic bridge decks, expert discussion, "New developments in steel construction" BAST.
8. Meschut, G., Teutenberg, D. & Wünsche, M. 2015. Prüfkonzept für geklebte Stahl/CFK-Strukturen. adhäsion KLEBEN & DICHTEN 59 (3): 16-21.
9. Sahellie, S., Pasternak, H. 2015. Expectancy of the lifetime of bonded steel joints due to long-term shear loading. Archives of Civil and Mechanical Engineering. Vol.15, Issue 4, page 1061-1069.
10. Kasper, Y., Albiez, M., Ciupack, Y., Gebler, A., Ummenhofer, T., Pasternal, H., Feldmann, M. 2020. Verstärkung von ermüdungsbeanspruchten Stahlbauteilen mit aufgeklebten CFK-Lamellen. Bauingenieur 95(3) 79-84 (part 1) and 95 (5) 166-173 (part 2).
11. Xia, S. H., Teng, J. G. 2005. Behaviour of FRP-to-steel bonded joints. Proceedings of the International Symposium on Bond Behaviour of FRP in Structures (BBFS 2005).

PRIMENA LEPLJENOG CFRP-A ZA OJAČANJE I REHABILITACIJU ČELIČNIH STRUKTURA OŠTEĆENIH ZAMOROM MATERIJAL – SAMO LEPA IDEJA?

Lepljene CFRP lamele su idealne kao alternativa klasičnim merama popravke čeličnih konstrukcija oštećenih zamorom. Na ovaj način nedostaci standardnih metoda se mogu zaobići. U poređenju sa merama za ojačanje sa zavrtnjima, izbegava se slabljenje poprečnog preseka zavrtnjem. Zaostali naponi i izobličenja izazvana toplotom, koja se obično javljaju tokom popravnog zavarivanja, takođe se mogu izbeći. Ovi nedostaci predstavljaju slabu tačku tokom cikličnog opterećenja zbog efekta zareza.

Da bi se okarakterisali materijali, ispitivanja se sprovode na uzorcima malih razmera. Uz pomoć testova na CT-uzorcima se realizuje poređenje sa utvrđenim metodama kao što su bušenje vrha pukotine i remontno zavarivanje. Na osnovu širenja prsline može se zaključiti da lepljene CFRP armature imaju veliki potencijal. Prednapretnjem lamela, preostali životni vek se generalno može dodatno produžiti. Treba, međutim, napomenuti da kod jednostranog prednapretnjanja može doći do preklapanja uzorka i, tokom opterećenja, do sekundarnog momenta savijanja. Kombinacija lepljenog CFRP-a sa tradicionalnim metodama može se opisati kao posebno efikasna. Sa obostranim ojačanjem sa prednapretnutim pločama, može se odrediti i do 7,9 puta preostali vek trajanja u poređenju sa neojačanim primercima.

Efikasnost lepljenih CFRP lamela se ispituje u nemačkom istraživačkom projektu. Odabrani rezultati su predstavljeni u ovom radu.

Ključne reči: čelične konstrukcije, lepljeni CFRP, zamor, popravka, armature.

HIGH STRENGTH CONCRETES BASED ON THE CHOICE OF THE BEST PARTICLE SIZE DISTRIBUTION IN AGGREGATE*

UDC 666.982.24:666.972.5

Zoran Grdić¹, Nenad Ristić¹, Dušan Grdić¹,
Gordana Topličić-Ćurčić¹, Dejan Krstić¹, Jelena Bijeljić²

¹University of Niš, Faculty of Civil Engineering and Architecture, Niš, Serbia

²College of Applied Technical Science, Niš, Serbia

ORCID iDs: Zoran Grdić

Nenad Ristić


Dušan Grdić


Gordana Topličić-Ćurčić


Dejan Krstić

Jelena Bijeljić

 <https://orcid.org/0000-0002-0653-210X>

 <https://orcid.org/0000-0002-8201-892X>

 <https://orcid.org/0000-0002-2651-7388>

 <https://orcid.org/0000-0001-5967-4964>

 N/A

 N/A

Abstract. *The requirements of the modern (high-end) construction industry demand the development of new types of concrete of high, and especially very high strength and with significantly improved properties in terms of durability. They provide new possibilities in the field of concrete technology of high strength and performance. When designing the composition of high-strength concrete (HSC), a special attention should be paid to the particle size distribution of aggregates, which should be chosen so as to achieve an "optimal" packing of the aggregate grains. The maximum grain size has been reduced to 2 mm. The Funk-Dinger formula was used to calculate the particle size distribution, which also takes into account fine particles of mineral powder additives. CEM I 52.5R, pure quartz sand, quartz filler, silica fume, powerful superplasticizer and low water/binder ratio were chosen for making HSC. In total, five different concrete mixtures were made. The paper presents the results of testing important properties of hardened concrete at ages from 1 day to 90 days and statistical processing of the obtained test results.*

Key words: *high strength concretes, aggregate particle size distribution, compressive strength, tensile strength*

1. INTRODUCTION

The review of the literature reveals different possible classifications of concrete, regarding the compressive strength, in terms of ranges which define concretes according to this property. Table 1 provides the classification of concrete based on the value of the

Received June 30, 2023 / Revised August 1, 2023 / Accepted August 15, 2023

Corresponding author: Zoran Grdić - University of Niš, Faculty of Civil Engineering and Architecture, Niš, Serbia
e-mail: zoran.grdic@gaf.ni.ac.rs

*Selected paper presented at the International Conference Sinarg 2023 held in Niš, Serbia on 14-15 September 2023.
© 2024 by University of Niš, Serbia | Creative Commons License: CC BY-NC-ND

compressive strength which is to a large degree in agreement with the classifications stated by other authors [1].

Procedures employed when selecting the material for making HCS, as well as for calculating the mix composition of HCS differ from the procedures employed for normal strength concretes. In the case of normal strength concretes, the procedures are even defined by ASTM and BS standards while this is not the case for HSC. In the literature, there are recommendations for the choice of materials and specific principles have been established, although, there are also some contrasting opinions. In general, authors agree about the following: It is necessary to

- select the particle size distribution of aggregate which provides the highest possible compactness of concrete when using fillers
- use the highest class cement, or energetically modified cement
- use silica fume and other suitable mineral admixtures
- make concrete with as low w/c factor as possible
- use high range water reducer (HRWR)
- use steel microfibers

Table 1 Classification of concrete based on the compressive strength value

Concrete type	Compressive strength [MPa]
Normal strength concretes	20 - 50
High strength concretes (HSC)	50 - 100
Ultra-High Performance Concrete (UHPC)	100 - 150
Reactive Powder Concrete (RPC)	> 150

As for the HSC mix design, a special attention should be paid to the particle size distribution of aggregate, which must be selected so as to achieve the optimal packing of aggregate grains. A well-chosen particle size distribution should provide a higher packing of grains in a given volume, i.e. the void between the grains should be minimal. After a number of modifications in the approach to the calculation of an “ideal” particle size distribution which would provide the packing of aggregate grains, including fine particles, Funk and Dinger [2] produced the following mathematical expression (1):

$$CPFT = \frac{d^n - d_s^n}{d_{max}^n - d_s^n} \cdot 100 \% \quad (1)$$

where:

- d – is the sieve opening in mm,
- d_s – is the finest sieve opening in μ mm (finest filler particle),
- d_{max} – is the highest nominal value of aggregate grain in mm,
- n – is the distribution modulus 0.2 to 0.4,
- CPFT** – **Cumulative Percent Finer Than d**

Chu & all researched mechanical properties and microstructure of UHPC while consistently implementing the principles listed in the previous text [3]. The result of their experimental research were concretes which had the flexural strength from 22 MPa to 24 MPa and compressive strength from 126 MPa to 155 MPa at the age of 28 days.

It is recommended to use CEM I of the 52,5 R strength class for making UHPC. Requirements of the contemporary (high-end) construction industry demand the development

of new kinds of binding materials with improved properties, specially designed for concretes of high, and particularly of very high strength, with considerably improved characteristics in terms of durability. They provide a new potential in the field of high strength concrete technology and performance. One of such innovative binders is the Energetically Modified Cement - EMC. The Energetically Modified Cement is produced by intensive grinding – mechanical activation of pure Portland cement (CEM I) together with various kinds of mineral admixtures. This technology was developed at the Department of Civil engineering at the Luleå University of Technology, Sweden [4]. Additional intensive grinding achieves a number of goals: activity of cement, pozzolanic activity of fly ash and chemical reactivity of ground granulated slag are all increased. EMC cements have grinding fineness of 5500 to 6000 cm^2/g by Blaine. The use of EMC cement can provide an increase of concrete strength of up to 100% at the same age in comparison with the high strength concretes made with “ordinary” PC.

In their experimental research Artega & all investigated the effects of energetically modified cement on achieving high concrete strengths [5]. They concluded that the replacement of CEM I with 30% to 35% EMC provides concretes with 50% higher strengths than the reference concrete.

The indispensable ingredient of UHPC is the silica fumes. In addition to the so-called micro silica fume, whose specific surface area ranges between 15 m^2/g and 35 m^2/g , for making of UHPC also is used the nano silica fume with the specific surface area from 100 m^2/g to as much as 400 m^2/g . Nano silica fume “completes” the particle size distribution curve in the area of finest particles and provides a great contribution to early strengths of UHPC concrete. Authors who investigate high strength concretes agree that replacing a part of cement with silica fumes contributes to the increase of strength, including those at the earliest age. In the paper [6] the authors published the results which indicate that the replacement of 10% of cement with silica fumes produces concretes which have up to 40% higher strength than the reference concrete.

The following two principles which are observed when designing the composition of UHPC are mutually related, and it is the use of a very low water-binder ratio and the obligatory use of powerful superplasticizers (HRWR) of the latest generation. The water/binder ratio value is usually about 0.25 or even less. For this reason, in HSC and UHPC it is common to use a higher percentage of superplasticizer (around 3%, and even more) than in the normal strength concretes (0.6% to 1.2%) in order to achieve the desired workability which facilitates their practical application. Zhang & all studied the effects of the water-to-binder ratio on the properties of UHPC [7]. The presented results indicate that the reduction of the water/binder ratio from 0.22 to 0.16 (in 0.02 increments) contributes to the increase of the UHPC strength for 50%, and even slightly higher.

In classical concretes, fibers, including steel ones, are used in order to increase the ductility of concrete and of certain increase of tensile strength, which nevertheless remains low. It is considered that the addition of fibers in normal strength concretes has almost no effect on the increase of compressive strength. In the case of UHPC the addition of steel microfibers having length (l) up to a maximum of 25 mm, but usually between 13 mm and 16 mm provides a great contribution to the increase of strength. The fiber diameter (D) is usually 0.20 to 0.30 mm. Aspect ratio l/D is most commonly between 60 and 70. Fang & all in the paper [8] investigated the effects of the percentage of addition of steel microfibers and their geometrical characteristics on the properties of UHPC. The addition of steel microfiber in the amount of 1%, 2% and 3% facilitates the increase of the compressive strength for 10% to 15%, and of the uniaxial tension resistance of up to 300%.

On the basis of the stated principles, the authors of this paper carried out an experimental investigation (which to a great extent can be considered initial) for the purpose of obtaining UHPC which could be implemented in practice. All the principles laid out in the introduction were observed and the results obtained in the experiment are presented hereinafter.

2. EXPERIMENTAL RESEARCH

Results of the experimental research presented in this paper are obtained in the Laboratory for Building Materials of the Faculty of Civil Engineering and Architecture of the University of Niš. The experimental research program is conceived so as to verify all previously mentioned principles for making of UHPC which can have practical application. It is planned to vary the type and amount of cement, as well types and amounts of mineral powder admixtures, in combination with low values of the water/binder ratio and different thermo-hygrometric conditions of concrete curing, especially at an early age of concrete. This paper presents only the results obtained so far on the reference concrete, concretes with the addition of silica fume and concretes with the addition of micro-reinforcing steel fibers at the age of up to 28 days. All other results are to be published on future occasions when they become available.

2.1. Materials used in the experiment

2.1.1. Cement

Cement CEM I of the 52.5 R class manufactured by “Moravacem” Novi Popovac was used for making concrete. The cement in question meets all the quality conditions prescribed by the standard SRPS EN 197-1 and they can be considered generally known. The chemical composition of cement is presented in table 2.

Table 2 Chemical composition of cement, silica fume and aggregate

Chemical composition	CEM I 52.5 R	Sikafume XR/TU	Quartz aggregate
	Quantity %		
SiO ₂	20.61	94.0	min. 99.00
Al ₂ O ₃	5.45	-	max. 0.40
Fe ₂ O ₃	3.36	-	max. 0.10
CaO	63.42	-	-
MnO	3.84	-	-
SO ₃	0.80	-	-
Na ₂ O	0.2	-	-
K ₂ O	1.00	-	-
Na ₂ O _{eq.}	0.86	-	-
Loss of ignition	1.00	3.0	max. 0.20
Moisture content	-	1.0	-

2.1.2. Silica fume

Silica fume Sikafume XR/TU was used as a mineral admixture for increasing the early strengths of concrete. The specific surface area of concrete was cca. 22 m²/g. The chemical composition of silica fume is provided in table 2.

2.1.3. Aggregate

Quartz sand produced by “Jugo Kaolin” at the Divci screening plant was used for making concrete. Three aggregate fractions were made: 0/0.5 mm, 0.4/0.8 mm and 1.4/4 mm, from which, all the subfractions of the full set of sieves were screened starting from < 0.063 mm to 2 mm. Rock flour obtained by grinding quartz from the screening plant Rgotina, also by “Jugo Kaolin” was used to provide the presence of the finest particles. This created the potential to compose the particle size distribution according to the Funk-Dinger formula with the modulus $n = 0.365$. The particle size distribution is shown in figure 1, while the chemical composition is presented in table 2.

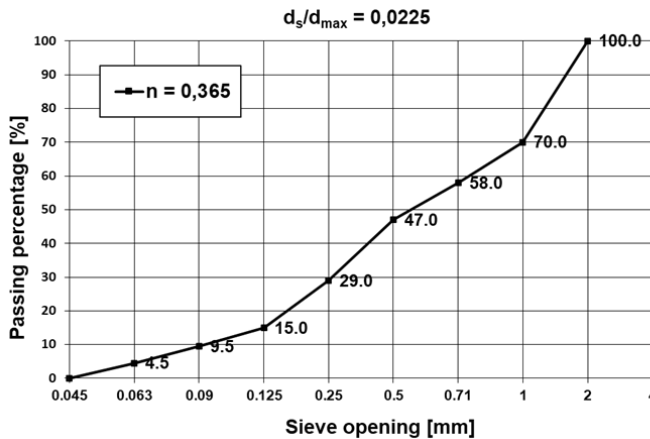


Fig. 1 Particle size composition of aggregate for concrete making

2.1.4. Steel micro fibers

In the experiment were used true steel micro fibers of circular cross-section from the cold drawn wire labeled as SA/M 0.22 x 13 mm manufactured by “Spajić” d.o.o. Negotin. Factor ratio is 59. The strength of the fibers at uniaxial tension is ≥ 2100 N/mm².

2.1.5. Superplasticizer

Superplasticizer of the last generation MC -PowerFlow 3100 produced by MC Bauchemie was used for the purpose of lowering the water/binder ratio and achieving the workability which facilitates the practical use of concrete. This high performance superplasticizer is based on the latest polycarboxylate terpolymer technology, and, among other things, it is designed exactly for making UHPC.

2.2. Composition, making method and curing regime of concrete mixtures

In this phase of experimental research, six concrete mixtures were made: reference (E), concrete mixtures with 10% (SF10) and 20% (SF20) of cement replaced by silica fume, concrete mixtures with 1%, 2% and 3% of addition of steel microfibers labeled as SMF1, SMF2 and SMF3 respectively. Compositions of concrete mixtures are presented in table 3.

For each type of concrete, 4 series of prisms having dimensions 40 x 40 x 160 mm were made so that the required number of specimens would be available for testing the density of the hardened concrete, as well as flexural and compressive strength at the ages of 1, 7, 28 and 90 days. Therefore, the total number of specimens is 72. Spreading on the shaking table was from 200 mm to 220 mm and it was maintained constant by varying the amount of superplasticizer.

Table 3 Concrete mixtures composition

Material	E	SF10	SF20	SMF1	SMF2	SMF3
	Quantity for 1 m ³					
Cement CEM I 52.5 R	735	662	589	735	735	735
Silica fume	-	73	146	-	-	-
Aggregate 0.09/2 mm	1330	1330	1330	1330	1330	1330
Quartz filler < 0.09 mm	140	140	140	140	140	140
Water	184	184	184	184	184	184
Superplasticizer	22.0	25.7	30.6	22.0	22.0	29.5
Steel microfibres	-	-	-	81.7	163.4	245.1
Water/binder ratio*	0.25	0.25	0.25	0.25	0.25	0.25

* without superplasticizer

Concrete mixing procedure was considerably modified, and it lasted longer than the standard procedure for the normal concrete. Firstly, sand and filler fractions were dry mixed for 3 minutes, then cement (and silica fume) were added, and it was all mixed for another 3 minutes. Finally, the superplasticizer previously mixed with water was added, after which the mixing continued for 4 minutes to allow the superplasticizer to exhibit its effects. Steel fibers were added only after 10 minutes of mixing when concrete already achieved the desired consistency. After adding fibers, the mixing continued for another 3 minutes. Concrete was placed into the steel moulds in two layers. Vibrating lasted 120 sec. with 3000 vibrations per minute, and amplitude of 0.75 mm.

For the first 24 h, specimens were cured in the moulds in the air having the relative humidity > 90% and temperature 20 ± 3 °C. From then on, up to the day of testing, all specimens were cured in the water having temperature 20 ± 2 °C.

3. EXPERIMENTAL RESEARCH RESULTS

In this initial phase of the research, the specimens were tested for: density of hardened concrete, flexural strength (Fig. 2 and 3) and compressive strength (Fig. 4). The tests were performed at the age of 1, 7 and 28 days. The specimens planned for the testing at 90 days did not reach this age at the moment of writing of this paper. The test results are presented in table 4.

It should be mentioned that the parts of the prism-shaped specimens remain connected after failure owing to the presence of steel microfibers – the so-called ductile failure. Figure 3 aims to show the uniform distribution of steel microfibers in the concrete mass and their proper orientation achieved during pouring in the moulds.



Fig. 2 Test setup for flexural strength testing



Fig. 3 Appearance of the concrete with steel microfibers at the failure point after testing the flexural strength



Fig. 4 Disposition during testing the compressive strength (left) and the appearance of the sample exposed to compression until failure (right)

Table 4 Test results of density, flexural and compressive strengths

Concrete label	E	SF10	SF20	SMF1	SMF2	SMF3
	Flexural strength [MPa]**					
1 day	10.3	9.7	10.0	11.4	17.5	22.8
7 days	15.3	16.1	16.8	17.5	24.2	26.7
28 days	18.0	19.2	20.3	22.4	26.7	28.9
Density at 28 days* kg/m ³	2411	2415	2420	2454	2474	2576
Compressive strength [MPa]**						
1 days	63.6	63.7	64.9	80.2	88.8	95.5
7 days	98.2	103.8	109.5	113.7	124.6	127.7
28 days	106.4	114.1	120.4	129.3	137.0	143.5

* water saturated surface dry concrete

** results in the table represent the mean value of three individual results

Considering the values of the achieved strengths, both flexural and compressive, the choice of the specimen dimension was fully justified. The available capacity of hydraulic presses used for testing of mechanical strength of concretes at the faculties and institutes in Serbia is most often 3000 kN, so they could not be used to test the cube shaped specimens, having sides of 150 mm.

4. TEST RESULTS DISCUSSION

The discussion of the test results is based on the comparison of the achieved strengths of individual concretes with the strengths of the reference concrete. The values of flexural and compressive strengths at all ages are adopted as the unit values, while the strengths of other concretes are expressed as a change in respect to the unit value. The test results comparison is provided in table 5.

Table 5 Comparison of the flexural and compressive strength testing

Concrete label	E	SF10	SF20	SMF1	SMF2	SMF3
	Flexural strength [MPa]					
1 day	1	0.94	0.97	1.11	1.70	2.21
7 days	1	1.05	1.05	1.14	1.58	1.75
28 days	1	1.07	1.13	1.24	1.48	1.61
Compressive strength [MPa]						
1 day	1	1.00	1.02	1.26	1.40	1.50
7 days	1	1.06	1.12	1.16	1.27	1.30
28 days	1	1.07	1.13	1.22	1.29	1.35

It can be established that the reference concrete has respectable values of flexural and compressive strength at all ages. The replacement of a part of cement with silica fume in the amount of 10% and 20% contributes to the further increase of flexural and compressive strengths. The increase of the flexural strength, and also the compressive strength at the age of 28 days amounts to 7% in the case of replacing 10% of cement, i.e. to 13% in the case of replacing 20% of cement with silica fume. Silica fume, due to its exceptional fineness and high content of amorphous silicon dioxide, is highly reactive and efficient

puzzolanic material. In addition to the pozzolanic reaction, an extremely small size of silica fume particle size also helps increase the density of the binding paste by filling in the voids between the cement grains, which enhances the packing of particles and distribution of pore sizes, and which is particularly important, the quality of the transit zone, figure 5 [9].

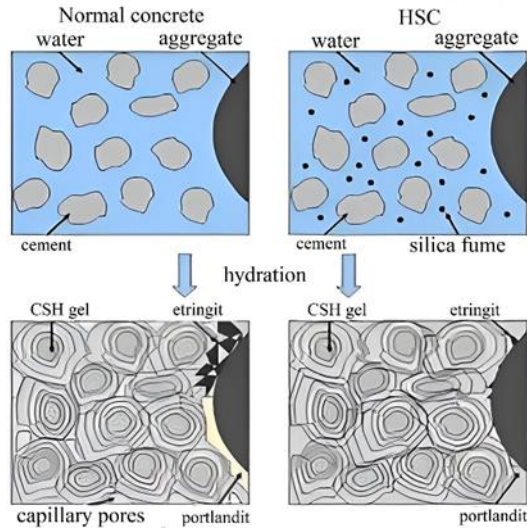


Fig. 5 Role of silica fume in fresh and hardened concrete

For the reasons of its exceptional fineness, silica fume increases the required amount of water for making concrete, see table 3. For this reason, the use of the chemical admixture (additive) such as superplasticizer is necessary, as it is high range water reducer (HRWR). It should be mentioned that the replacement of cement in the amount 20% with silica fume is very high, and that it was done only for the purpose of providing base research in the initial phase of the experiment. It is common to replace the cement up to 10%, very rarely up to 15%.

The effect of addition of steel microfibers in terms of increasing strength of fine grain concretes is more than justified, and it is much more efficient than the addition of silica fume. The increase of flexural and compressive strength is much more prominent at young age of concrete (1 day or 7 days) but this contribution remains considerable at a later date, too. Also, the effect of the increase of strengths is higher if the percentage of addition of fibers is higher, table 5. The addition of 1% of steel microfibers at the age of 28 days causes the increase of the compressive strength for cca. 20%, the addition of 2% fibers for cca. 30%, and the addition of 3% of fibers increases the compressive strength for around 35%. This was also the highest measure compressive strength, amounting to 143.5 MPa. The addition of 3% of steel microfibers can also be considered extreme, and on this occasion the first problems with mixing of fresh concrete occur, that is, one should use the appropriate high energy mixer.

5. CONCLUSION

Based on the obtained results of the experimental research a number of conclusions can be drawn, which can be used as a good basis for the future experimental work. In brief, the following conclusions can be made:

- By observing the fundamental and widely accepted principles, (mentioned in the introduction) UHPC can be successfully made
- With a proper choice of material for making concrete, using only CEM I in a fairly simple way, the compressive strength of 100 MPa and higher can be achieved
- Replacement of a part of cement using silica fume contributes to the further increase of flexural and compressive strengths
- Addition of steel microfibers provides a particularly high contribution to the strengths of concrete, whose increase can be up to 35% at the age of 28 days in relation to the reference concrete (addition of 3% of fibers)

The use of certain industrial byproducts which would have the role of fillers, different forms of curing, particularly in the initial period are in the plan of the future experimental research. Also, a considerable expansion in terms of types of test is planned, primarily concerning the resistance of such concretes to the adverse environmental effects.

Acknowledgement. *The work reported in this paper is a part of the investigation within the research project 451-03-47/2023-01/200095 supported by the Ministry for Science and Technology, Republic of Serbia. This support is gratefully acknowledged.*

REFERENCES

1. American Concrete Institute® - ACI 363R-10: Report on High-Strength Concrete. Reported by ACI Committee 363, First Printing March 2010.
2. James E. Funk, Dennis R. Dinger: Predictive Process Control of Crowded Particulate Suspensions Applied to Ceramic Manufacturing. Kluwer Academic Publishers, Boston, MA, pp. 786, 1994.
3. H. Chu, L. Gao, J. Qin, J. Jiang, D. Wang: Mechanical properties and microstructure of ultra-high-performance concrete with high elastic modulus. *Construction and Building Materials*, <https://doi.org/10.1016/j.conbuildmat.2022.127385>.
4. V. Ronin, L. Elfgren: Energetically Modified Cement (EMC) – Performance Mechanism. Center for High Performance Concrete, Luleå University of Technology, March 01, 2003, Sweden
5. J. C. Arteaga-Arcos, O. A. Chimal-Valencia, H. T. Yee-Madeira, S. D. de la Torre: The usage of ultra-fine cement as an admixture to increase the compressive strength of Portland cement mortars. *Construction and Building Materials*, <https://doi.org/10.1016/j.conbuildmat.2013.01.017>
6. J. C. Lim, T. Ozbakkaloglu: Influence of silica fume on stress-strain behavior of FRP-confined HSC. *Construction and Building Materials*, <https://doi.org/10.1016/j.conbuildmat.2014.03.044>
7. C. Zhang, Z. Wu, C. Luo, X. Hu, K. Li, C. Shi, N. Banthia: Size effect of ultra-high-performance concrete under compression: effects of steel fiber characteristics and water-to-binder ratio. *Construction and Building Materials*, <https://doi.org/10.1016/j.conbuildmat.2022.127170>
8. H. Fang, M. Gu, S. Zhang, H. Jiang, Z. Fang, J. Hu.: Effects of Steel Fiber and Specimen Geometric Dimensions on the Mechanical Properties of Ultra-High-Performance Concrete. *Materials*, 2022, 15, 3027. <https://doi.org/10.3390/ma15093027>
9. M. Muravljov, D. Jevtić: Građevinski materijali II, Akademska misao, ISBN 978-86-7466-527-5, Beograd, 2014.

BETONI VISOKIH ČVRSTOĆA BAZIRANI NA IZBORU NAJBOLJEG GRANULOMETRIJSKOG SASTAVA AGREGATA

Zahtevi savremene (vrhunske) građevinske industrije zahtevaju razvoj novih vrsta betona visoke, a naročito veoma visoke čvrstoće i sa značajno poboljšanim svojstvima u pogledu trajnosti. Oni pružaju nove mogućnosti u oblasti tehnologije betona visokih čvrstoća i performansi. Prilikom dizajniranja sastava betona visokih čvrstoća (HSC) posebnu pažnju treba posvetiti granulometrijskom sastavu agregata koji treba izabrati tako da se postigne „optimalno“ pakovanje zrna agregata. Veličina maksimalnog zrna je smanjena na 2 mm. Za izračunavanje granulometrijskog sastava koršćena je Funk – Dingerova formula, koja u obzir uzima i fine čestice mineralnih praškastih dodataka. Za spravljanje HSC izabrani su CEM I 52.5R, čist kvarcni pesak, kvarcni filer, silica fume, powerfull superplasticizer i low water/binder ratio. Ukupno je napravljeno pet različitih betonskih mešavina. U radu su prikazani rezultati ispitivanja važnih svojstava očvrslog betona pri starostima od 1 dana do 90 dana i statistička obrada dobijenih rezultata ispitivanja.

Ključne reči: *betoni visokih čvrstoća, granulometrijski sastav agregata, čvrstoća pri pritisku, čvrstoća pri zatezanju*

THE ROLE OF OLED DEVICES IN THE DEVELOPMENT OF SMART CITIES*

UDC 711.45:004.7

721:004.7

621.385.2:535.37

Snežana Đorić-Veljković¹, Nikola Mitrović², Sandra Veljković²,
Vojkan Davidović², Emilija Živanović², Ivica Manić², Danijel Danković²

¹University of Niš, Faculty of Civil Engineering and Architecture, Niš, Serbia

²University of Niš, Faculty of Electronic Engineering, Niš, Serbia

ORCID iDs: Snežana Đorić-Veljković

Nikola Mitrović

Sandra Veljković

Vojkan Davidović

Emilija Živanović

Ivica Manić

Danijel Danković

<https://orcid.org/0000-0003-0475-040X>

<https://orcid.org/0000-0001-8981-637X>

<https://orcid.org/0000-0001-9510-7465>

<https://orcid.org/0000-0003-3889-9595>

<https://orcid.org/0000-0001-9011-7111>

<https://orcid.org/0000-0003-3047-6790>

<https://orcid.org/0000-0002-0214-2606>

Abstract. *In the course of the last few years, interest in the development of smart cities and progress of smart buildings has increased significantly. This development has been significantly increased due to the development of new technologies, innovative functional materials, electronic components and other products. At the same time, it is imperative to use those products that contribute to the preservation of the environment, and above all to energy saving. Thus, new technologies are becoming increasingly attractive, such as the one based on OLED (Organic Light Emitting Diode) technology, which is used in the production of mobile phones, tablet computers, other devices, as well as light sources. Although this technology has been generally known for more than half a century, commercial application of OLED components was not possible due to insufficient efficiency of products based on it. However, the continuous improvement of characteristics and efficiency enabled their more significant application in the past few years. The aim of this work is to provide adequate information about the possibilities of applying some innovative technologies in the planning and development of smart cities. Especially, becoming more familiar with the basic properties and application possibilities of OLED devices can lead to the life quality improvements of city spaces users.*

Key words: *Development of smart cities, OLED devices, application of device.*

Received June 30, 2023 / Revised August 1, 2023 / Accepted August 15, 2023

Corresponding author: Snežana Đorić-Veljković - University of Niš, Faculty of Civil Engineering and Architecture, Niš, Serbia

e-mail: snezana.djoric.veljkovic@gaf.ni.ac.rs

*Selected paper presented at the International Conference Sinarg 2023 held in Niš, Serbia on 14-15 September 2023.

© 2024 by University of Niš, Serbia | Creative Commons License: CC BY-NC-ND

1. INTRODUCTION

Creating a smarter planet can be achieved by applying a concept which involves: Instrumented, Interconnected and Intelligent. This concept of three I - 3I, promoted by IBM, implies that there are three basic pillars of forming a smarter planet [1, 2]. At the same time, Instrumented means that by using a remote sensor, information can be collected wherever it exists. Interconnected means that the collected information can be sent, received, or simply moved to where it will be useful. The third part of this concept - Intelligent, means that obtained information can be processed, analysed and based on it certain procedures that can be carried out in order to obtain the appropriate knowledge, which can be further used, applied... According to this, in Fig. 1 is presented the 3I concept.

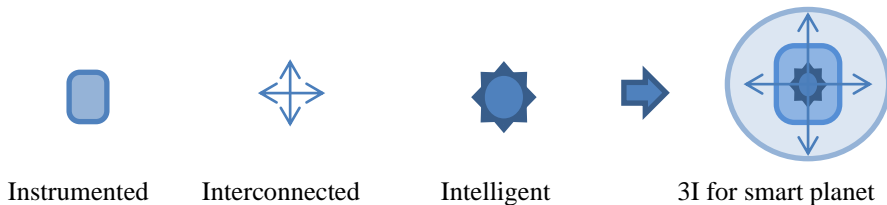


Fig. 1 Concept of 3I - three pillars for smarter planet

One of the elements in realizing the vision of a smarter planet, is certainly the formation of smart cities, in which the focus is especially on preserving the environment, available resources, saving energy, as well as ensuring efficient transport and communications. In such a city, the application of smart technologies is increasingly pronounced. Thereby, the application of the Internet of Things (IoT) system is very important and plays an increasingly pronounced role. Moreover, all these new technologies and novel products aim, above all, to improve people's quality of life.

It is important that one of progressively present novel technical achievements is OLED (Organic Light Emitting Diode). Namely, OLED devices are new electronic devices that, due to their characteristics, can have a really wide application in many areas. As it is known, they have significant applications for displays, televisions, tablets, mobile phones, screens for digital cameras, dashboards, in the automotive industry. These new systems and technologies based on the use of OLED devices have great advantages when it comes to production and design [3]. For instance, TVs made with OLED technology are only 4 mm thin, and they are thinner than those made with LED technology, because fewer layers are required to produce them.

In addition, the application of OLED devices as light sources, illuminating infrastructure and especially the decoration of a certain space is particularly important [4]. Thus, it is possible to install ones with transparent OLED elements instead of classic windows, so that they can serve as an artificial light source when there is no daylight. Application of these OLED components, as well as new equipment being perfected, can lead to significant reduction of energy consumption, but above all, artificial light would become more similar to daylight and more pleasing to the eye. Besides, innovative products, discovered innovations and quality solutions that were not available until now contribute to the improvement of automatic operation and control, as well as people's comfort and fast and better communication.

This paper presents the potential of applying some innovative technologies in the planning and development of smart cities, and especially some properties and possibilities of

applying OLED devices that can lead to an improvement in the quality of life of users of urban areas.

2. INTRODUCTION PROPERTIES AND ADVANTAGES OF OLED DEVICES

An important property of OLEDs is that they do not contain hazardous materials (such as mercury) making them environmentally friendly devices [5]. Also, the light emitted by OLED is pleasant and contains less "blue light" in its spectrum, which can be harmful because the light is of higher energy. Namely, if the eye is exposed to this light for a long time, it can lead to the degradation and damage of the vision, as well as sleep disturbance. Unlike LED light sources (which are point sources and therefore have glare), OLED sources emit significantly uniform light, which is similar to natural light and therefore more pleasant to the eye, while the source efficiency is greater than 150 lm / W and colour reproduction rate is higher than 90 [6].

These devices have the advantages of being low cost, light, flexible, and easy to modify, making them ideal materials for various applications. Principally, OLED devices are made of several thin organic layers that are placed between two electrode layers and when current flows through them, light appears. Thereby, there are a several types of OLED devices, which can be classified into some categories: bottom emission, top emission, and both side emission-transparent (from the point of view of emitting directions) as well as normal and inverted structures (from the point of view of the stacking order of the electrodes) [7].

It is important to note that research on the properties of OLED devices is very important, especially in scientific studies, in order to achieve the best possible performance of these devices for practical application. Very important for OLED devices are current performances, like efficiencies, lifetimes, luminance-current, and especially current-voltage (I-V) characteristics. Typical I-V characteristic of the OLED device with the structure of glass/ITO(150nm)/MoO₃(10nm)/ α -NPD(40 nm)/Alq₃(30 nm)/DPB: Liq(25wt%)(43.5 nm)/Al(100 nm) are shown in Fig. 2. This I-V characteristic is presented in lin-lin (Fig. 2a) and log-lin (Fig. 2b) scale.

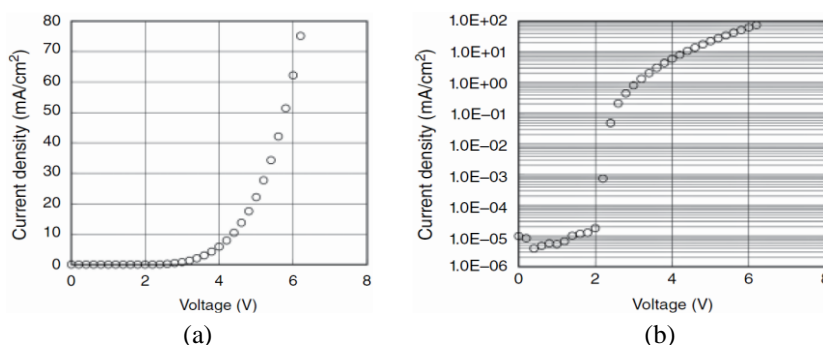


Fig. 2 Typical current-voltage characteristic of the OLED device with the structure of glass/ITO/MoO₃/ α -NPD/Alq₃/DPB/Al in lin-lin (a) and log-lin (b) scale, [7]

It can be seen that the turn-on voltage is 2.0 V and that the leakage level of this OLED device is close to 10^{-5} mA/cm². Standard OLED devices have a tendency to display a lower current level than 10^{-4} mA/cm² if they are properly made-up. Therefore, the information about the device failure can be obtained from the I-V characteristic (especially from the current presentation in a logarithmic scale) [7].

Owing to their improved lifetime, in addition to other good properties and the unique features, OLED devices show a promising potential not only for display and lighting uses, but for many other innovative applications [8].

Due to the great similarity in the operation of OLED devices and solar cells, flexible organic photovoltaic solar cells were realized. Namely, the organic material is coated over the surface or a layer of that mixture is sprayed on the surface, and uses the solar energy to create thin film organic photovoltaic solar cells. In addition, new technologies are creating engineering innovations, so it is now possible for organic solar cells and light-emitting diodes to be unified - combined in a single device [9]. Investigators succeeded in producing an organic solar cell that can simultaneously function as an efficient OLED, and current-voltage characteristic of such device is presented in Fig. 3. It can be achieved that below the open circuit voltage the diode functions as a solar cell, and above as an OLED. This organic optoelectronic diode absorbs ultraviolet and blue photons.

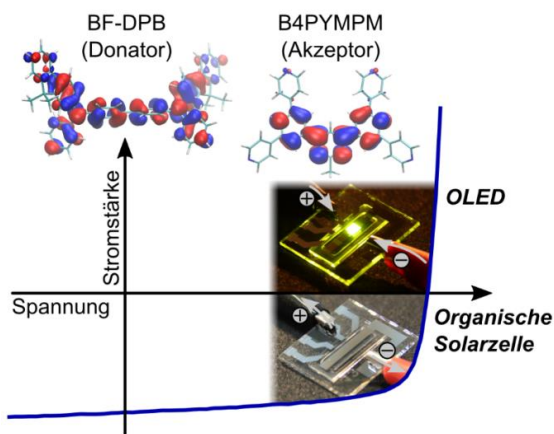


Fig. 3 Current-voltage characteristic of an organic optoelectronic diode that absorbs ultraviolet and blue photons, [9]

The molecular structures show the charge carrier distribution in the organic semiconductors used as electron donor BF-DPB (N₄,N₄'-Bis(9,9-dimethyl-9H-fluoren-2-yl)-N₄,N₄'-diphenylbiphenyl-4,4'-diamine) and as electron acceptor B4PYMPM (4,6-Bis(3,5-di(pyridin-4-yl)phenyl)-2-methylpyrimidine).

These discoveries can contribute to the development of more energy-efficient OLEDs in screens of television or displays of smartphone. The developed photovoltaic devices can be used for the efficient conversion of ultraviolet and blue photons (the high energy part of the optical electromagnetic spectrum) into the electrical power or as semi-transparent solar cells in glass facades. Also, in indoor applications they can be used for the electrical supply of Internet-of-Things devices which are increasingly present in ordinary life, and are an indispensable part of smart cities.

3. APPLICATION OF OLED DEVICES

It is clear that there is a constant search for better, more efficient solutions that can be applied, and the existing ones are improved. All these solutions and products are in the function of ensuring more efficient functioning and better quality of life for people, especially those in cities.

In Fig. 4a are presented flexible thin film solar cells which can be integrated into the building envelope and in Fig. 4b are presented transparent solar power windows, which can be a part of the building envelope [10]. Flexible thin-film solar cells can replace conventional materials in places such as roofs, skylights or facades and can represent an integrated photovoltaic unit in a building.



Fig. 4 Flexible thin-film solar cells (a) and transparent solar power surfaces (b), [10]

Transparent solar power surfaces can replace parts of windows. In this case, there are no moving parts involved in photovoltaic embedded systems and there is no associated electrical or acoustic noise. Also, it is obvious that these solar power surfaces use parts of existing surfaces of buildings or constructions. These characteristics show that there is a significant advantage of this use of solar energy compared to other green technologies.

In the upcoming smart cities, the challenge may be new infrastructures and networks, what requires innovation in providing novel facilities that will be able to receive, store and transmit information. At the same time, such facilities should provide the necessary energy for independent functioning. In addition, they could illuminate the environment and have other functions. In Fig. 5 is presented the cantilevering hybrid vertical structure that works as a stand-alone or a grid-connected smart tower-like object [11]. It can be used for multiple services, for integrative urban signage or lighting system.

The outer surface of the tower consists of three spirally twisted strips in which triangular plates are embedded. These panels cover the outer sides of the tetrahelix, which consists of tubular thin steel beams connecting the solid six-sided steel structure. The panels are made of an internal laminated glass structural panel with rounded edges. For this type of construction, glass was chosen as the optimal material due to its durability and other properties. Namely, regarding the possibilities offered by the lamination and bonding, electronic devices, such as photovoltaic cells, sensors, OLEDs and other lighting devices can easily be incorporated in the glass panels. Fig. 5 shows the tower, where photovoltaic panels (Fig. 5a), luminescent panels (Fig. 5b), and screens and sensors (Fig. 5c) are installed in the glass panels.

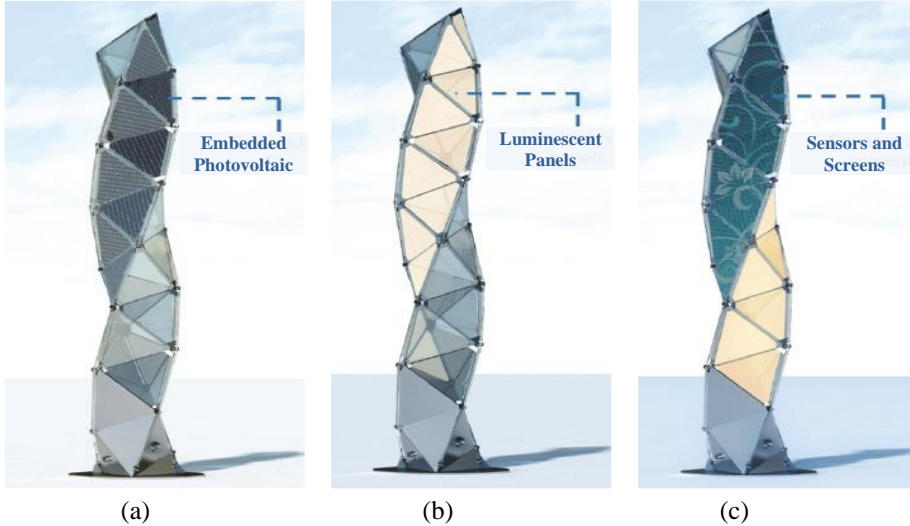


Fig. 5 Presentation of multifunctional towers where in glass panels are embedded photovoltaic (a), luminescent panels (b) and screens and sensors (c), [11]

The use of sensors is definitely necessary in smart cities because they collect data that is further distributed and used for further actions, which can contribute to making urban spaces comfortable and safe for people. That is why new, more efficient and cheaper solutions are constantly being developed to collect data. Special attention is paid to data transmission in a wireless sensor network [12].

Thus, sensor nodes can be placed alongside roads in order to collect relevant data that is valuable for road users during the driving duration. Thus, Fig. 6 presents one of the solutions for sensor nodes, using IoT, which can collect data such as air pollution on the road, weather parameters such as temperature and humidity, road description, speed limit, conditions such as traffic volume, activities maintenance and so on [13]. The data obtained with this device is displayed on an OLED-based screen that is used as the device's display. Fig. 6a presents an existing sign (small figure) and the name of the road

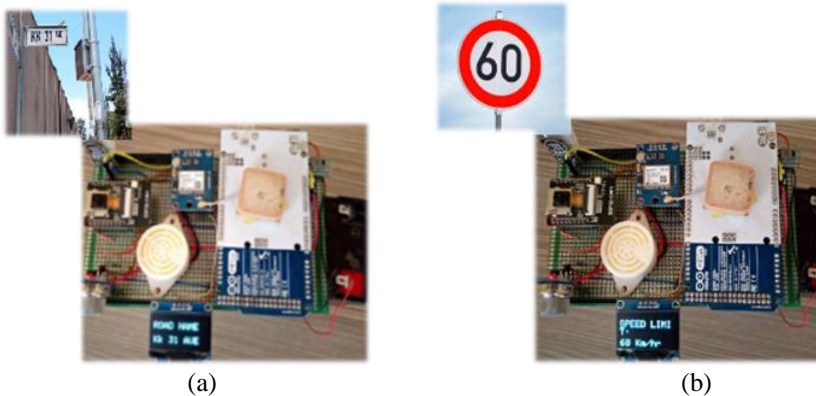


Fig. 6 Existing sign (small figure) and the presentation on OLED display for name of the road (a), and speed limit (b), [13]

that is shown on the sensor display, while Fig. 6b presents an existing sign (small figure) and speed limit that is shown on the sensor display.

Also, monitoring the weather forecast is very important in many cases, and the possibilities of cheaper and more efficient solutions for obtaining data are continuously being explored. In Fig. 7 is shown a low-cost weather monitoring system that extracts weather conditions (and weather forecasting) of any location that can be obtained from a cloud database management system and displays the obtained results on an OLED display.

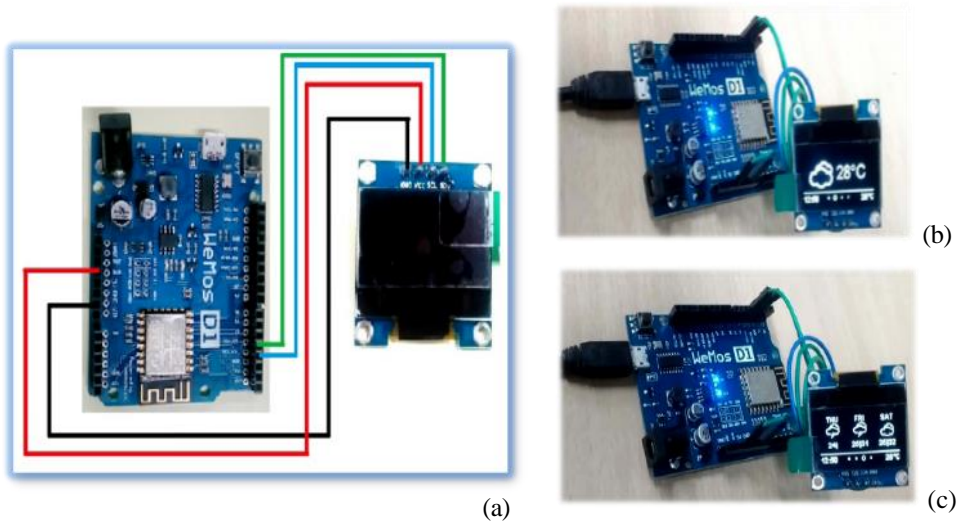


Fig. 7 Representation diagram of the system (a), temperature presentation on OLED display (b), and 3 days weather forecasting presentation on OLED display (c), [2]

In Fig. 7a is presented a schematic diagram of the system, while, in Fig. 7b and Fig. 7c are shown temperature and 3 days weather forecasting, respectively. For this system an ESP8266-EX microcontroller based Wemos D1 board is used and it is implemented on Arduino platform with which is possible to download the data from the cloud. In this way, it is possible to observe the weather conditions at any location and it is possible to access the current data of any station.

In addition to the mentioned presentations, the applications of transparent OLED that are applied to some other surface, such as a mirror, are especially attractive. The transparent OLED light source can completely cover the surface of the mirror or only a part of it. When it is off, it is transparent and practically a part of the mirror, and when it is on it becomes a source of pleasant white light. Interactive mirrors are innovative solutions that actually represent an OLED display. The advantages of interactive mirrors are enormous, and they can be integrated into both modern and traditional interiors. Such a mirror provides multiple possibilities and can be used for better organization or entertainment. It can be used for streaming music, YouTube videos, streaming TV, and exercise classes with the built-in Wi-Fi and high-quality bluetooth speakers. The mirror can also contain motion sensors to detect movement, so the mirror turns on when someone is nearby. In Fig. 8 are presented two different touch screen smart mirrors [14].

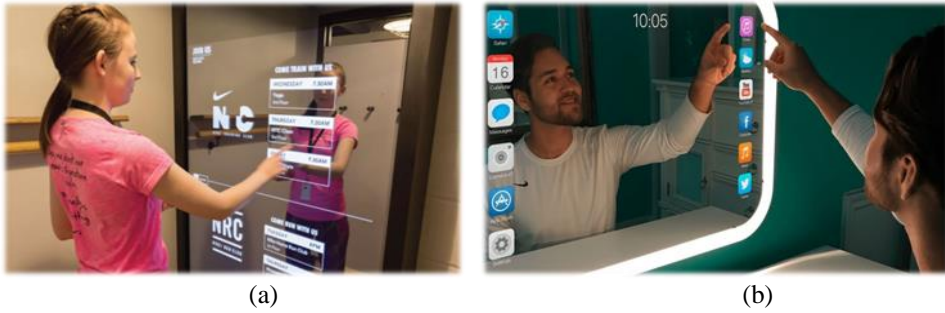


Fig. 8 Touch screen smart mirrors, [14]

Also, contemporary circumstances, as well as unpredictable ones, have forced remote and hybrid work to become more ubiquitous. Therefore, there is a strong need for multifunctional office space. Although the concept of open and shared office space is becoming dominant, it has been observed that in many situations, there is a need for a certain degree of privacy. Transparent OLED can play a dominant role in meeting these requirements because it can be flexibly used in many ways, as it is presented in Fig. 9.

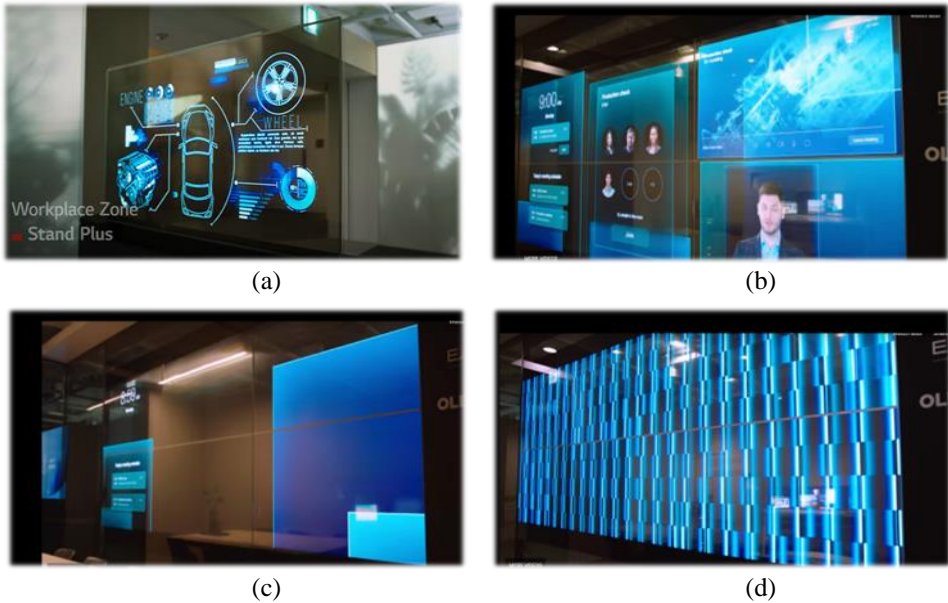


Fig. 9 Transparent OLED device used as a monitor on the glass wall of the office during live meetings (a), online meetings (b), part of the open workspace (c) and private space in the same workspace (d), [15]

Thus, it can be used as a monitor on the glass wall of the office for meetings [15], whereby data can be presented on it as standard during live meetings (Fig. 9a) or online meetings (Fig. 9b). At the same time, when it is turned off, it can represent a part of the

open workspace (Fig. 9c). However, by turning on the privacy mode, appropriate privacy can be ensured in part of that open space (Fig. 9d).

In this way, transparent OLED enables communication to take place freely in a space that is not segmented and has no opaque partitions. Thus, this transparent (glass) partition can at any time represent a screen on which appropriate contents can be found. In this manner, offered innovative application of OLED components enables the transformation of a certain space, representing a futuristic medium that is in harmony with the surroundings.

It is clear that the application of transparent OLED enables the achievement of completely new visual effects and ensures the formation process of innovative space [15]. This achieves the transformation of a space into a unique and superior space through sophisticated design and cutting-edge technology. Apart, transparent OLED can contribute to an innovative shopping experience (Fig. 10).

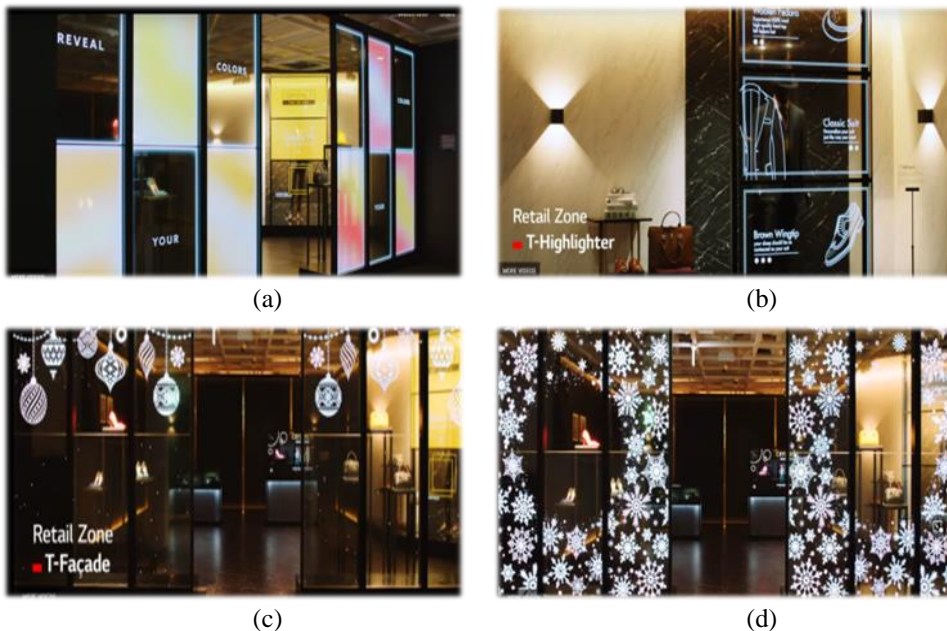


Fig. 10 Transparent OLED device displays detailed information about the respective brands and their products (a), (b), and contribute to an innovative shopping experience (c), (d), [15]

Namely, offline retail stores are increasingly accepted by customers and are developing because they provide customers with a different shopping experience and provide very detailed information about the respective brands and their products. Transparent OLED captures customers' attention by keeping the store open while overlaying various product information (Fig. 10a,b) providing an innovative approach to shopping (Fig. 10c,d). In this way, a new context for product advertisements is obtained and promotional effects are maximized.

4. CONCLUSION

Over the past few years, there has been a significant increase in interest in the advancement of smart cities and the evolution of intelligent buildings. This was possible thanks to the rapid development of new technologies, innovative functional materials, electronic components and various other products. OLED components play a special role in this, which can be used as screens in mobile phones, tablet computers, displays, various devices, and as light sources. These components have emerged as particularly promising because they are in line with environmental protection and energy efficiency, which has become the most important. This study aimed to provide the insight into the potential application of innovative technologies in the planning and construction of smart cities. In particular, gaining a deeper understanding of the basic properties and possibilities of different applications of OLED devices can contribute to improving the quality of life of city dwellers. As the journey toward smart cities continues, the integration of cutting-edge technologies like OLEDs can undoubtedly illuminate a path to a more sustainable and enhanced urban experience. In particular, new possibilities are offered by the integration of organic solar cells and diodes that have already been achieved, i.e. they are combined into one device. Additionally, the possibility of using OLEDs as displays that display data collected by appropriate sensors is significant, because the collection, distribution and presentation of a large amount of data is of particular importance in smart cities. The additional quality of these components, especially the transparent OLED, represents the possibility of using them for completely innovative applications. These devices make it possible to simultaneously provide the conditions imposed by the modern concept of working in offices, but also for the needs of people as users of the space for an appropriate degree of privacy. Innovative applications of transparent OLED can contribute to an innovative shopping experience, as well as a virtual experience in museums, various institutions, and homes.

Acknowledgement. *The work is the part of investigations supported by the Ministry of Science, Technological Development and Innovations of Republic of Serbia, within the research projects 451-03-47/2023-01/200095 and 451-03-47/2023-01/200102.*

REFERENCES

1. Valerie Lampkin, Weng Tat Leong, Leonardo Olivera, Sweta Rawat, Nagesh Subrahmanyam, Rong Xiang, "Building Smarter Planet solutions with MQTT AND IBM WebSphere MQ Telemetry", Books.google.co.in IBM RedBooks, 2012.
2. Ravi Kishore Kodali and Archana Sahu, "An IoT based Weather Information Prototype Using WeMos. Proc 2nd International Conference on Contemporary Computing and Informatics (ic3i)", Amity University, Noida, India, pp. 612-616, 2016.
3. Sandra Veljković, Aleksandra Čurčić, Vojislav Mitić, Gordana Topličić-Čurčić, "OLED Light Sources in Architecture", V International Symposium for Students of Doctoral Studies in the Fields of Civil Engineering, Architecture and Environmental Protection, PHIDAC 2019, pp. 199-205, Nis, Serbia, 24-25 October 2019.
4. Kanae Matsui, Katsutoshi Saito, "IoT-based OLED lighting control system for providing comfort space", IEEE SmartWorld, Ubiquitous Intelligence & Computing, Advanced & Trusted Computed, Scalable Computing & Communications, Cloud & Big Data Computing, Internet of People and Smart City Innovation, San Francisco, CA, USA, Accession Number: 17878639, 04-08 August 2017.

5. Snezana Đorić-Veljković, Jugoslav Karamarković, “Challenges and Possibilities of Application of Oled Light Sources”, Proc. International conference - Innovation as a Function of Engineering Development (IDE 2011), Niš, 103-108, 2011.
6. <https://www.energy.gov/eere/ssl/world-record-white-oled-performance-exceeds-100-lmw> [Accessed 15.7. 2023].
7. Mitsuhiro Kodan, “OLED Displays and Lighting”, John Wiley & Sons, Chichester, UK; Hoboken, NJ: 2016.
8. Snežana Đorić-Veljković, Nikola Mitrović, Sandra Veljković, Predrag Janković, Danijel Danković, “Innovative Applications of OLED Components in Architecture”, Proc. Building services & Architecture, University of Belgrade, Faculty of Architecture, Belgrade, pp. 139-147, 2021.
9. <https://www.led-professional.com/technology/light-generation/organic-solar-cells-and-light-emitting-diodes-united> [Accessed 15.7. 2023].
10. Patrizio Primiceri and Paolo Visconti, “Solar-Powered LED-based Lighting Facilities: an Overview on Recent Technologies and Embedded IoT Devices to Obtain Wireless Control, Energy Saving and Quick Maintenance”, Journal of Engineering and Applied Sciences, 12 (1), pp. 140-150, 2017.
11. Maurizio Froli, Francesco Laccone, “Hybrid GLAss-Steel Stele (HYGLASS): Preliminary Mechanical Study on a Smart Tetrahelical Cantilevering Tall Structure”, Conference on Architectural and Structural Applications of Glass, pp. 6.2181-1-6, 2018.
12. Sateesh Gudla, NageswaraRao Kuda, “A Reliable Routing Mechanism with Energy-Efficient Node Selection for Data Transmission Using a Genetic Algorithm in Wireless Sensor Network”, Facta Universitatis, Series: Electronics and Energetics, vol. 36, no 2, pp. 209 – 226, 2023.
13. Evariste Twahirwa, James Rwigema, and Raja Datta, “Design and Deployment of Vehicular Internet of Things for Smart City Applications”, Sustainability, 14, 176, pp. 14010176-1-16, 2022.
14. <https://prodisplay.com/touch-screens/interactive-screens/smart-mirror-touch-screen/> [Accessed 15.7. 2023].
15. <https://www.oledspace.com/en/products/transparent-oled/> [Accessed 15.7. 2023].

ULOGA OLED KOMPONENATA U RAZVOJU PAMETNIH GRADOVA

Tokom posljednjih nekoliko godina značajno je poraslo interesovanje za razvoj pametnih gradova i napredak u izgradnji pametnih zgrada. Ovaj razvoj je značajno povećan zahvaljujući razvoju novih tehnologija, inovativnih funkcionalnih materijala, elektronskih komponenti i drugih proizvoda. Istovremeno, neophodno je koristiti one proizvode koji doprinose očuvanju životne sredine, a pre svega uštedi energije. Zbog toga nove tehnologije postaju sve atraktivnije, poput one zasnovane na OLED (Organic Light Emitting Diode) tehnologiji, koja se koristi u proizvodnji mobilnih telefona, tablet računara, drugih uređaja, kao i izvora svetlosti. Iako je ova tehnologija opšte poznata više od pola veka, komercijalna primena OLED komponenti nije bila moguća zbog nedovoljne efikasnosti proizvoda zasnovanih na njoj. Međutim, kontinuirano unapređenje karakteristika i efikasnosti omogućilo je njihovu značajniju primenu u posljednjih nekoliko godina. Cilj ovog rada je da pruži adekvatne informacije o mogućnostima primene inovativnih tehnologija, kao što je i ova OLED, u planiranju i razvoju pametnih gradova. Posebno, upoznavanje sa osnovnim svojstvima i mogućnostima primene OLED uređaja može dovesti do poboljšanja kvaliteta života korisnika gradskih prostora.

Ključne reči: razvoj pametnih gradova, OLED komponente, primena komponenata

EXPERIMENTAL ANALYSIS OF THE BEHAVIOR OF CAPPING BEAMS ACROSS THE PILES IN LOOSE SAND*

UDC 624.154

Nemanja Bralović¹, Iva Despotović², Danijel Kukaras¹

¹University of Novi Sad, Faculty of Civil Engineering, Subotica, Serbia

²University of Kragujevac, Faculty of Mechanical and Civil Engineering, Kraljevo, Serbia

ORCID iDs: Nemanja Bralović

Iva Despotović

Danijel Kukaras

<https://orcid.org/0000-0001-5971-8031>

<https://orcid.org/0000-0002-4452-1372>

<https://orcid.org/0000-0003-4726-2799>

Abstract. *The test program was conducted on 1G models capping beams over the tops of the group of 2x2 piles, the purpose of which was to reduce the settlement of the structure. The test program included six experiments, three of which were conducted on capping beams without piles and three on capping beams across the tops of the piles, with pile distances 3d, 4d and 5d, where d is the pile diameter and the pile length is 40 d. Test results show that the current conventional approach to the design of capping beams across the tops of the piles, where the entire load is entrusted to the piles, is too conservative and irrational. Instead, it is more economical to apply a low bearing capacity factor for piles as settlement reducers and maximize use of raft bearing capacity to carry part of the external load.*

Key words: *raft foundation, pile foundation, piled raft foundation, settlement, Eurocode.*

1. INTRODUCTION

In geotechnical engineering, funding facilities on shallow foundations is not always possible due to the great deformability of the soil. Accordingly, alternative funding methods are used, such as deep funding. The calculation of the pile group is based on the assumption that the entire load from the aboveground part of the structure is taken over by the piles, not taking into account the load-bearing capacity of the capping beam. This approach to calculation is very conservative and irrational – the basic principle of calculation should be based on the fact that the foundation structure contains as many piles as would be needed to reduce settlement to an acceptable level, so that the load from the aboveground structure is transferred over the capping beam to the ground and partly

Received June 30, 2023 / Revised August 1, 2023 / Accepted August 15, 2023

Corresponding author: Nemanja Bralović, University of Novi Sad, Faculty of Civil Engineering, Subotica, Serbia
e-mail: nemanjabralovic@hotmail.com

*Selected paper presented at the International Conference Sinarg 2023 held in Niš, Serbia on 14-15 September 2023.

© 2024 by University of Niš, Serbia | Creative Commons License: CC BY-NC-ND

over the piles. Such a calculation approach would aim to contribute to the rationalization of the foundation structure, thus reducing the number of piles.

Assuming that the load is evenly distributed over the entire raft foundation, a deflection will occur in the middle of the raft foundation, as schematically shown in Figure 1a. By adding a certain number of piles under the raft foundation, settlement and differential settlement will reduce, Figure 1b. Using piles to reduce settlement is an idea that originated earlier, in the 1970s [2]. There is a number of studies that deals with the behavior of cap-ping beams and capping beams across the top of the piles [3], [4], [5], [6], [7] as well as with the settlement of capping beams across the top of the piles [8], [9], [10].

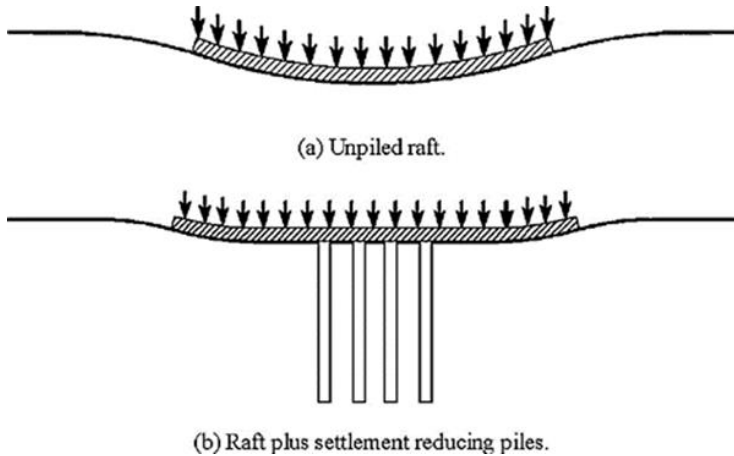


Fig. 1 Piles required to reduce differential settlement [1]

Muhammad Rehan Hakaro [11] investigated capping beams across the top of the piles in multilayer soil of different stiffness exposed to different loads using a software package Plaxis 2D.

O. Reul and M. Randolph [12] deal with the influences of certain parameters on the load distribution between the capping beam and the piles, such as the number and arrangement of piles, the piles length and the capping beam stiffness. They conclude that when using longer piles there may be less settlement than when using a larger number of piles, and that bending moments in the capping beam cannot be reduced by supporting it with piles. Phung [13] concludes that the conventional practice of designing beams across the tops of the piles is based on the assumption that external load is carried by piles and any contribution of the capping beam is neglected. Therefore, the approach is too conservative because the capping beam carries a significant part of the load due to direct contact with the ground. Bayad and others [14] say that in tests conducted on the capping beams across the tops of the piles 2x2, 3x3 and 4x4, when the capping beam settles 10 mm, 60% of the total load is taken over by piles. Fleming [15] states that when designing capping beams across the tops of the piles, capping beams have an appropriate capacity. Due to not taking into account the contribution of the load-bearing capacity of the capping beam, when designing capping beams across the tops on the piles, a larger number of piles is calculated than is actually needed [16].

Assel Zhanabayeva et al. [17] compared the capping beams on the piles, applying Euro-code 7 and Kazakhstan regulations. Thea concluded that Eurocode 7 was more conservative, provided a higher level of security [18], [19]. The system of foundation of capping beams across the tops of the piles is a fundamental structure that combines the effective bearing capacity of capping beams and piles taking into account the interactions pile-soil, pile-pile, capping-beam-soil, pile-capping beam.

The interaction between soil and structure has an impact on soil behavior as well as the behavior of piles under load [20], [21]. The behavior of the pile-soil system is mostly nonlinear. The load in the horizontally loaded pile is resisted by the pile-ground interaction, which depends on pile diameter, pile material [22]. Bourgeois [23] investigated the influence of the pile-soil interaction in a vertically loaded group of piles.

Based on experimental results, Phung Duc Long and other [24] authors propose a simplified method that can be used in design. The experiment shows that at the beginning of the loading of the capping beam, piles take over most of the load and after reaching the bearing capacity of the pile, the load is transferred to the capping beam. This method can give effective results if used with the finite element method for estimating the settlement of capping beams across the tops of the piles.

In this paper, the results of experimental analysis of 1G model of the capping beam across the tops of the piles, conducted for the purpose of writing a doctoral thesis, were used. The aim of the research was to point out that when designing these types of foundation structures on loose sand, the load-bearing capacity of the capping beam should not be neglected, while the number of piles required to receive vertical force would be reduced and thus a more rational foundation structure would be achieved. Together with the interaction of capping beams and piles, group effect was also examined.

2. MATERIALS AND METHODS

Laboratory tests were performed on a 1g model for a group of four piles, assembled in a 2x2 pile configuration. The test program consisted of six experiments, three of which were performed on piles of length $L/d=40$, with pile distances of 3d, 4d, 5d, and three experiments with a system of capping beams directly resting on a raft foundation, i.e. capping beams without piles. Pile arrangement, as well as capping beam dimensions, are shown in Figure 2.

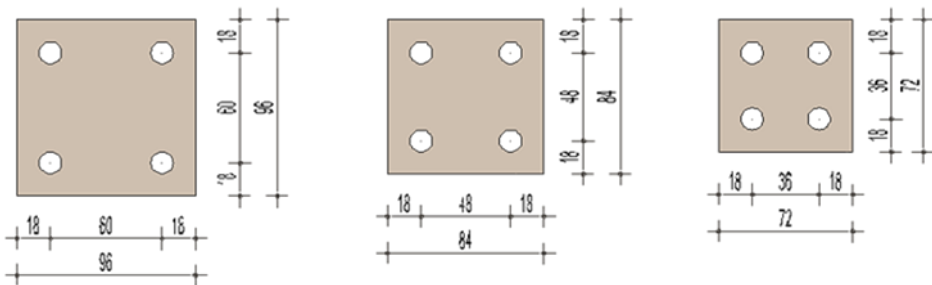


Fig. 2 Pile arrangement and capping beam dimensions (in mm)

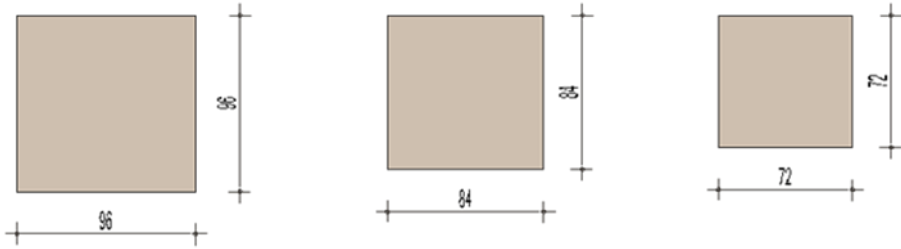


Fig. 2 Pile arrangement and capping beam dimensions (in mm)

2.1. Soil parameters

Dry sand was used in the experiment. Granulometric experiments were performed to determine the granulometric curve of the soil used. The granulometric curve parameters are: $D_{10} = 0.11\text{mm}$, $D_{30} = 0.15\text{ mm}$, $D_{60} = 0.23\text{ mm}$, the uniformity coefficient is $C_u = 2.1$ and the curvature coefficient $C_z = 0.8$, Figure 3.

Based on the United Soil Classification (USCS), the tested soil sample is classified as poorly graded SP sand. By direct shear test it is determined that the angle of internal friction is 30° .

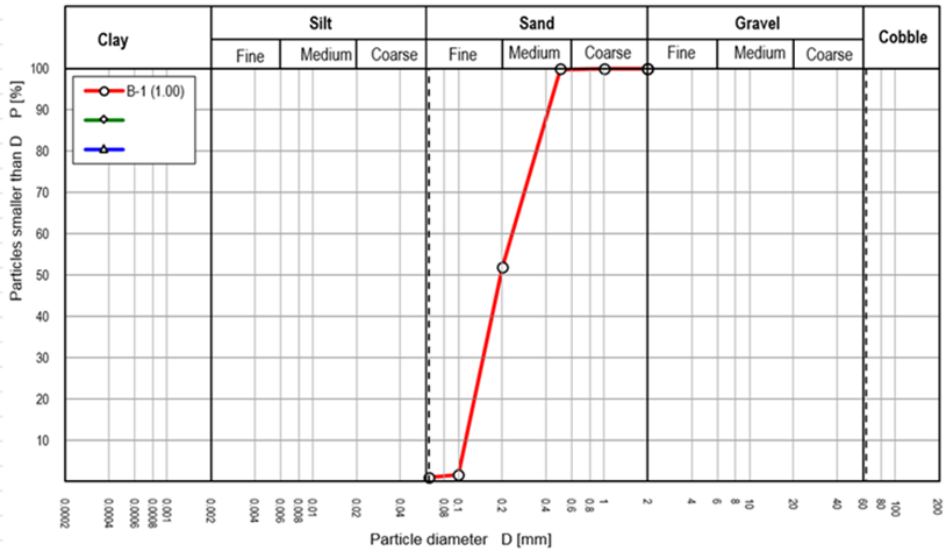


Fig. 3 The granulometric curve

2.2. Models of Capping Beams and Piles

The model of the capping beam across the tops of the piles is composed of a square capping beam. The capping beam is made of steel S 235, plate thickness 10 mm, which is an absolutely rigid body that is not subject to bending under forces occurring in the experiment. 9 mm diameter holes are drilled in the capping beam, arranged depending on

the configuration of the piles, through which the pile head passes, at the top of which a thread is incised, in order to tighten the piles with a nut from the upper side of the capping beam and thus achieve a rigid connection between the capping beam and the piles, Figure 4. Piles are made of steel S 235 with a diameter of 12 mm, and for easier and simpler installation, they are composed of three parts. The base of the pile is conical, in order to facilitate the breaking of the piles, while in the upper part of the pile, a so-called adapter is placed, over which the connection between the capping beam and the pile is made. In the adapter, the axial force in the pile head is measured via a miniature force sensor.

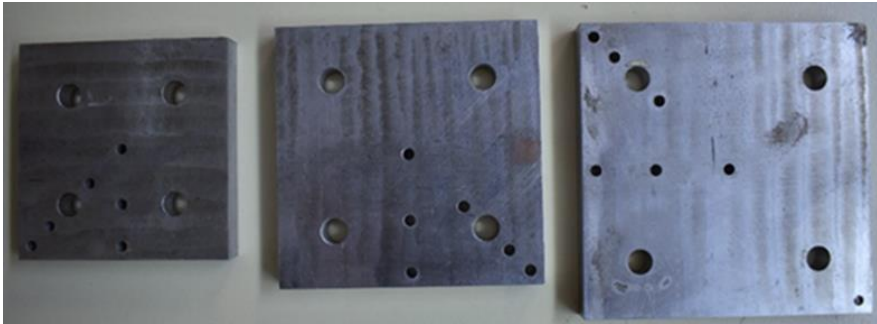


Fig. 4 Capping beams for group of 2x2 piles

2.3. Measuring Instruments and Equipment

2.3.1. Test box

Model testing was performed in specially designed test boxes. The box is made of steel L profiles and the dimensions of the box are 75x75x100 cm. In the corners of the mobile platform, four pillars of L profiles, which are interconnected by L profiles 35x35x2 mm, every 25 cm by the height of the pillars, are welded. They form a stable structure with prevented lateral deformations of the box walls. The inside of the box is coated with 3 mm thick Plexiglas, to make it easier to determine the height of the filled sand, as well as to eliminate friction between the sand and the walls of the box, as Mosa and others have observed in their experiments [25].

2.3.2. Measuring instruments

A data logger with one parallel analog board and eight serial analog boards is used to collect data from measuring instruments. On the parallel board, there is a digital-analog switch that generates an excitation signal for Winston measuring bridges. There is also an eight-channel analog-to-digital converter on the parallel board. Six channels are used on the parallel board, while signals from serial analog boards are fed to the remaining two channels. Serial boards have eight analog inputs, with a total of 64 channels.

2.3.3. Digital scrolling scale

To monitor the movement of the capping beam due to load, digital verniers with an accuracy 1/1,000 are used. Three verniers of model 601/SA, with a measuring length of 150 mm, are attached to a special frame construction over flexible magnetic stand.

2.3.4. Force Probe (a probe that measures the vertical force acting on the capping beam)

To determine the vertical force acting on the capping beam, a force probe with a measuring capacity of 350 kg is used, with measurement error of 0.2%, Figure 5. Force probe is used to measure static and dynamic forces. Probe calibration was done before use in the experimental analysis. The probe was calibrated to the pressure force by placing weights on the probe and thus its response to increasing load was measured. The basic element of the probe is the wall of the probe which is elastically deformed after the action of force. Four measuring tapes connected to the full Winston bridge, are placed inside the probe.

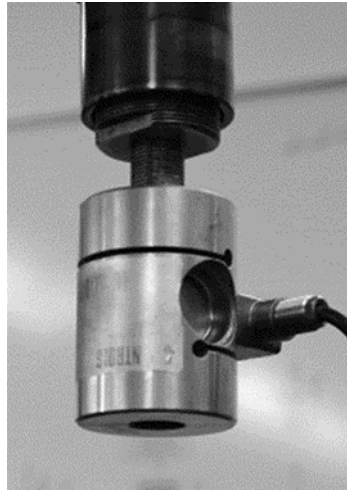


Fig. 5 Force probe with a measuring capacity of 350 kg

2.3.5. Sensor for measuring the force in the pile

A miniature force sensor, with a total measuring capacity of 30 kg, was used to measure the force in the pile. The diameter of the sensor is \varnothing 12 mm, and it has connection necks with notched threads M6. Four measuring tapes, connected to the full Winston bridge, are placed in the sensor. Sensors are placed under the capping beam, in place of the connection adapter. Calibration was performed in the measuring range of the sensor, i.e. from 0 N to 300 N, where the load was gradually increased and maintained for a certain time interval, in order to more clearly establish the step of changing the response with increasing load.

2.3.6. Spreader

For the purpose of testing the capping beams across the tops of the piles, grounded in loose sand, a self-propelled spreader, 70 cm wide, was made to fill the boxes with sand, in the form of rain from sand, Figure 6.

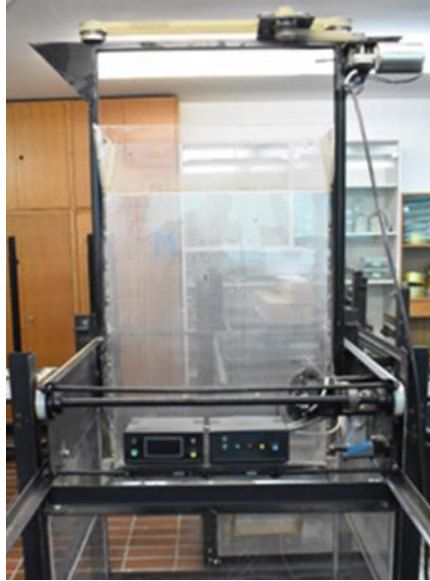


Fig. 6 Spreader

The spreader has two control panels through which the machine is controlled. One control panel serves to control the movement of the support brace within the box, with a programmer for adjusting the speed of movement. The second control panel controls the support brace box, adjusting the direction of movement of the box in the z-direction, as well as the speed of movement of the box.

2.4. Examination procedure

1. Before testing, the test box is filled with sand by means of a spreader, pouring sand in the form of sand rain at a height of 10 cm, so that the sand remains loose after filling the box.

2. The filled sandbox is placed under the previously installed test frame on which the engine with the mounted hydraulic piston is mounted. A force probe, that registers the vertical force on the system when pressing a group of piles into the sand, is mounted at the end of the piston.

3. The pre-assembled configuration of the capping beams across the tops of the piles is mounted on the force probe and the measuring equipment is connected to the measuring instrument.

4. Before pressing the capping beam across the tops of the piles into the sand, spacers are placed between the piles at certain heights, ensuring that the piles remain vertical when pressed and do not be skewed.

5. After the spacers are installed, the measuring instrument is started and it is checked whether all measuring equipment gives responses. The piles are pressed into the sand at a speed of 10.5 cm/min, until the capping beam reaches the height of 10 mm above the sand.

6. When the capping beam reaches the height of 10 mm above the surface of the sand, the pressing speed is reduced to 1 mm/min and the pressing continues until the ground breaks, or until the capping beam is pressed into the sand to a depth of $0.1B$, where B is the width of the beam.

3. RESULTS AND DISCUSSION

3.1. Capping beam without the piles

Load-bearing curves for capping beams without the piles, in the case of capping beams pressing to a depth of $0,1B$, where B is the capping beam width, for capping beam dimensions $72 \times 72 \times 10$ mm, $84 \times 84 \times 10$ mm, $96 \times 96 \times 10$ mm, are shown in Figure 7.

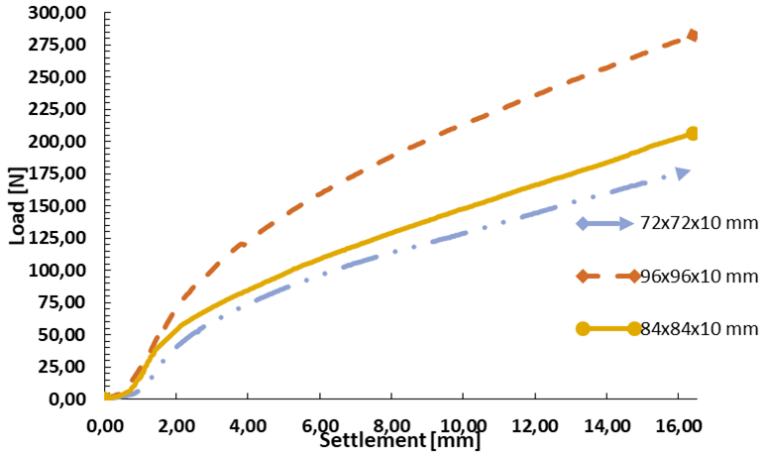


Fig. 7 Load-bearing curves for capping beams without the piles

The results of the experiment show that capping beams that have a smaller contact surface at the same forces, have higher differential settlements. Such results are expected.

3.2. Capping beams across the piles

In the next part, the relationship of load distribution between capping beams and piles during sand pressure, will be analyzed. Figures 8-10 show diagrams force – movement of the capping beams across the tops of the piles for pile length $L/d = 40$, which is often applicable in practice with pile distances of $3d$, $4d$, $5d$. From the diagrams shown, it can be noticed that when the settlement increases, mobility of the capping beam occurs and as the settlement further increases, the part of the force carried by the capping beam, becomes larger. The final settlement criterion is a settlement size of $0,1B$, measured from the moment the capping beam touches the sand, where B is the width of the capping beam. The diagram shows the proportion of the load taken by the capping beam. In the group where the piles are at a distance $e/d=3$, approximately 24% of the total force is taken by the capping beam, for piles at a distance $e/d=4$, the percentage of force taken over by the capping beam is approximately 40%, and for piles at a distance $e/d=5$, the capping beam takes up as much as 49% of the force.

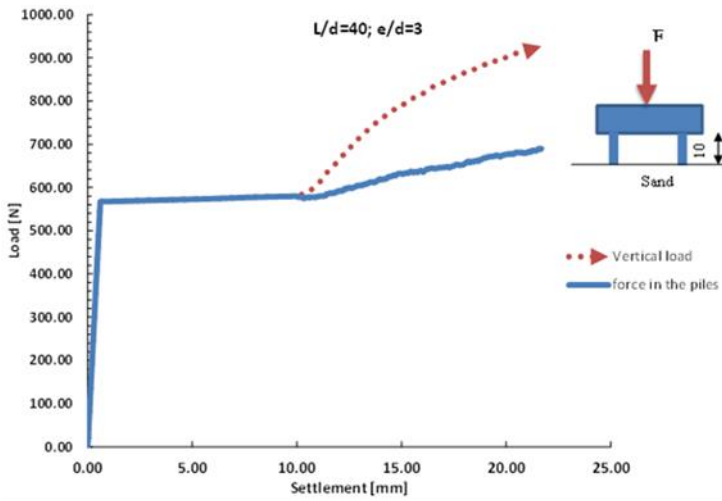


Fig. 8 Diagram force – movement of the capping beams across the piles $L/d=40$, $e/d=3$

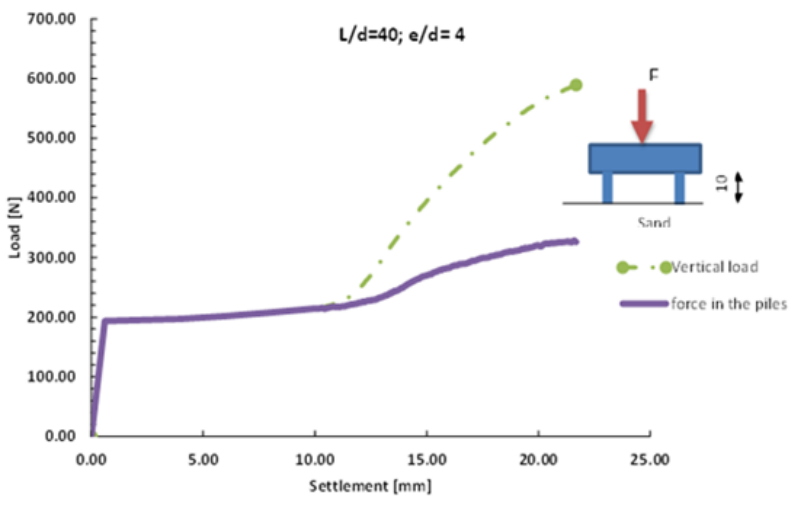


Fig. 9 Diagram force – movement of the capping beams across the piles $L/d=40$, $e/d=4$

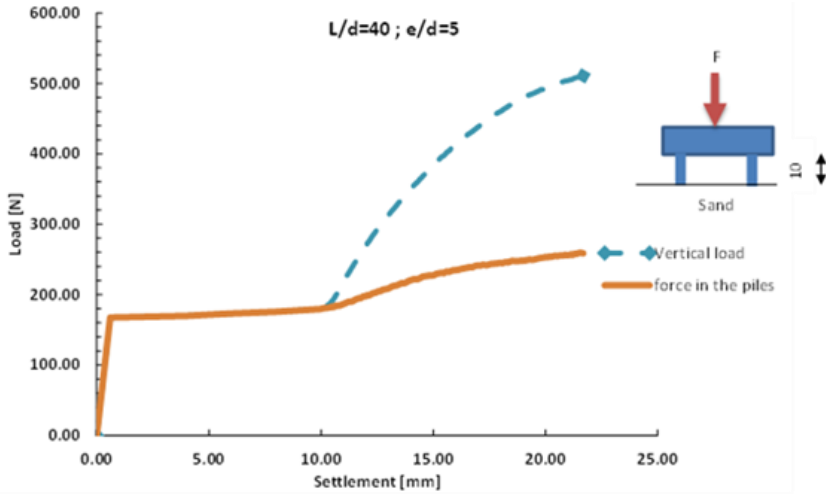


Fig. 10 Diagram force – movement of the capping beams across the piles $L/d=40, e/d=5$

Previous diagrams show that when designing these types of foundations, the calculation should not be based on the required number of piles that should accept the entire load, but on the number of piles needed to reduce the settlement to the allowable limits.

3.3. Influence of Distance – Group Effect

Within the experiment, the influence of pile spacing on the relationship between load and settlement in a combined system of foundation of capping beams across the tops of the piles, was investigated, as well as the distribution of forces between piles and the capping beam.

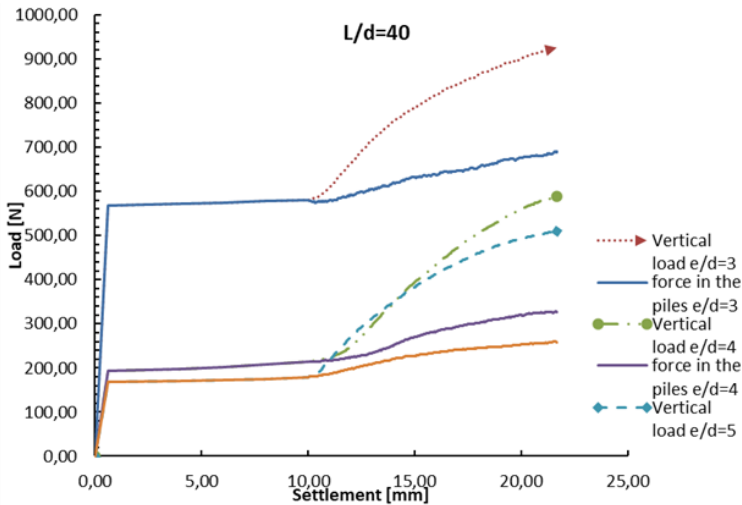


Fig. 11 Diagram force – movement of the capping beams across the piles $L/d=40, e/d=3;4;5$

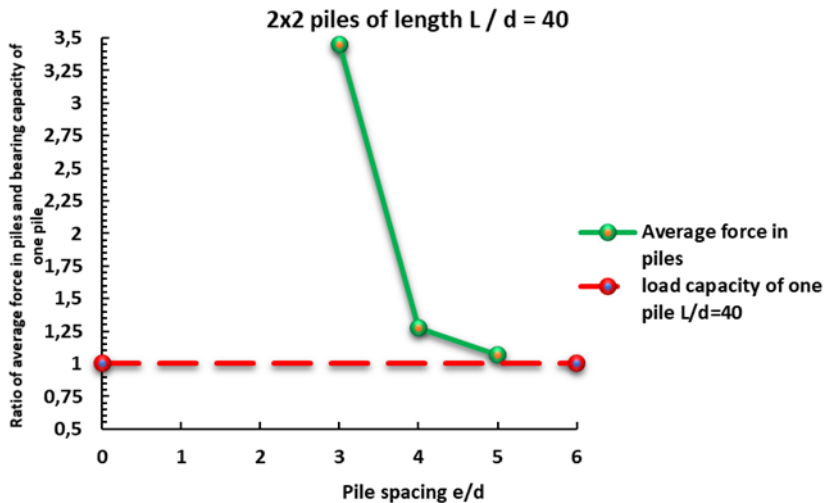


Fig. 12 The effect of the group of 2x2 piles, for piles length $L/d = 40$

The diagram in Figure 11 shows that pile spacing has an effect on the relationship between load and settlement in a combined foundation system, so that it is much more pronounced at the spacing $e/d=3$ and smaller at the spacing $e/d=4$ and 5. A smaller pile spacing will provide a significant improvement in the performance of the combined system and accordingly, increasing the spacing of the piles leads to an increasing settlement of the foundation. Pile spacing also affects the redistribution of force between the piles and the capping beam. The diagram in Figure 12 shows that the effect of the group is very pronounced in piles that are at a distance of $3d$. It can also be concluded that as the spacing increases, the group effect decreases, which is to be expected. At a pile distance of $4d$ there is a group effect but this effect is much smaller, about 2.8 times. As the spacing of the piles increases to $5d$, the group effect slowly begins to be lost and the piles behave as if they were individual. It can be concluded that the final distance between the piles in the group is $5d$ and that at greater distances the group effect is lost.

4. CONCLUSIONS

Based on experimental results, conclusions follow:

1. Capping beams that have smaller contact surface have higher differential settlements at the same forces; increasing the contact surface improves the load-bearing capacity of the capping beam at the same settlements.
2. When pressing a group of piles, immediately after the moment the capping beam touches the sand, a capping beam mobilization occurs and it increases as the settlement increases.
3. It was concluded that in the case of $0.1B$ capping beam settlement, where B is the width of the capping beam, the part of force taken by the capping beam ZA $3d$ pile spacing, was approximately 24%. As the distance increased, the part of the force taken by

the capping beam was higher, so at a pile spacing of $4d$ it was approximately 40%, and at a pile spacing of $5d$, the capping beam took approximately 49% of the total force.

4. At $3d$ pile distances the group effect is very pronounced but as the spacing increases, the group effect decreases. As the final distance to which the piles behave as a group, a distance of $5d$ is established.

REFERENCES

1. El-Garhy, A. Abdel, Abdel-Fattah Youssef i M. Abo: Behavior of raft on settlement reducing piles: Experimental model study. *Journal of Rock Mechanics and Geotechnical*, pp. 389-399, 2013.
2. Burland et al: Behaviour of foundations and structures. *Proc. 9th ICSMFE, Tokyo, 1977.*
3. V. Berezantzev: Load Bearing Capacity and Deformation of Piled Foundations. *Proceedings of the Fifth International Conference on Soil Mechanics and Foundation Engineering, Paris, France, 17–22 July 1961.*
4. J. Burland: Shaft Friction of Piles in Clay—A Simple Fundamental Approach. *London, Ground Engineering, 1973.*
5. Poulos, H.G: Pile Behaviour—Theory and Application. *Geotechnique*, 39, 365–415, 1989.
6. Poulos, H.; Small, J.; Chow, H: Piled Raft Foundations for Tall Buildings. *Geotech. Eng. J. SEAGS AGSSEA 2011*, 42, 78–84, 2011.
7. Poulos, H.G.; Bunce, G: Foundation Design for the Burj Dubai—The World’s Tallest Building. *Proceedings of the 6th International Conference on Case Histories in Geotechnical Engineering, Arlington, VA, USA, 11–16 August 2008.*
8. Chow, H.; Small, J: Behaviour of piled rafts with piles of different lengths and diameters under vertical loading. *Austin, TX, USA, 2005.*
9. De Azevedo et al: Effect of the Addition and Processing of Glass Polishing Waste on the Durability of Geopolymeric Mortars. 2021.
10. Gad, M.A.; Riad, A.M.; Nikbakht, E.; Ali, M.; Ghanem, G.M: Structural Behavior of Slender Reinforced Concrete Columns Wrapped with Fiber Reinforced Polymers Subjected to Eccentric Loads. *Proceedings of the 2020 Second International Sustainability and Resilience Conference, Technology and Innovation in Building Designs, Sakheer, Bahrain, pp 1-5, 11–12 November 2020*
11. Muhammad Rehan Hakro et al: Numerical Analysis of Piled-Raft Foundations on Multi-Layer. *Buildings*, 12, 356, 2022.
12. Reul O., Randolph M: Design Strategies for Piled Rafts Subjected to Nonuniform Vertical Loading. *Journal of Geotechnical and Geoenvironmental Engineering*, pp. 1125-1128, 2004.
13. Phung Duc Long: Piled Raft – A Cost-Effective Foundation Method for High- Rises. *Geotechnical Engineering Journal of the SEAGS & AGSSEA*, 2010.
14. Bajad S., Sahu R: An Experimental Study on the Behaviour of Vertically Loaded Piled. *International Association for Computer Methods and Advances in Geomechanics, Goa, 2008.*
15. Fleming and Randolph: *Piling Engineering*, Taylor & Francis Group: New York, NY, USA, p. 95, 2009.
16. Clancy and Randolph: An Approximate Analysis Procedure for Piled Raft Foundations. *International Journal for Numerical and Analytical Methods in Geomechanics*, pp. 849-869, 1993.
17. Zhanabayeva Assel et al: Comparative Analysis of Kazakhstani and European Design Specifications: Raft Foundation, Pile Foundation, and Piled Raft Foundation. *Appl. Sci.*, 11, 3099, 2021.
18. Burland J., Burbidge M., Wilson E., Terzaghi K: Settlement of Foundations on Sand and Gravel. *Proc. Inst. Civ. Eng*, 1985.
19. Ali M. et al: Experimental Validation of Mander’s Model for Low Strength Confined Concrete Under Axial Compression. *Proceedings of the 2020 Second International Sustainability and Resilience Conference Technology and Innovation in Building Designs, Sakheer Bahrain, November 2020; pp.1–6.*
20. Mandolini, A., Laora R, Mascarucci Y: Rational Design of Piled Raft. *Procedia Eng.* 57, 45–52, 2013.
21. Chu Y.M. et al: Combined Impact of Cattaneo-Christov Double Diffusion and Radiative Heat Flux on Bio-Convective Flow of Maxwell Liquid Configured by a Stretched Nano-Material Surface. *Appl. Math. Comput.*, 419, 126883, 2021.
22. Kavitha P.E., Beena K.S., Narayanan K.P: A review on soil–structure interaction analysis of laterally loaded piles. *Innov.Infrastruct.Solut.*, 1, 14, 2016.
23. Bourgeois E. et al: Settlement Analysis of Piled-Raft Foundations by Means of a Multiphase Model Accounting for Soil-Pile Interactions. *Comput. Geotech.* 46, 26–38, 2012.

24. Long Duc P., Bakar A: Settlement analysis for piled raft foundations - A case study. Geotechnics for Sustainable Development, 2013.
25. Mosa J., Mohammed Y: Experimental observations on the behaviour of a piled raft foundation. Journal of Engineering, pp. 807-828, 2011.

EKSPERIMENTALNA ANALIZA PONAŠANJA NAGLAVNIH GREDA NA ŠIPOVIMA U RASTRESITOM PESKU

Program testiranja je sproveden na 1G modelima naglavnih greda preko vrhova grupe šipova 2Xx2, čija je svrha bila smanjenje sleganja konstrukcije. Program testiranja uključivao je šest eksperimenata, od kojih su tri izvedena na naglavnim gredama bez šipova i tri na naglavnim gredama na vrhovima šipova, sa rastojanjem šipova 3d, 4d i 5d, gde je d prečnik šipa, a dužina šipa 40 d. Rezultati ispitivanja pokazuju da je postojeći konvencionalni pristup projektovanju naglavnih greda preko vrhova šipova, gde je celokupno opterećenje na šipovima, previše konzervativan i iracionalan. Umesto toga, ekonomičnije je primeniti nizak faktor nosivosti za šipove kao reduktore sleganja i maksimizirati korišćenje nosivosti naglavica za nošenje dela spoljašnjeg opterećenja.

Ključne reči: pločasti temelj, temelj na šipovima, ploča na šipovima, sleganje, Evrokod

COMPARATIVE ANALYSIS OF ATTERBERG'S LIMITS OF FINE-GRAINED SOIL DETERMINED BY VARIOUS METHODS

UDC 624.131.3

**Nemanja Marinković, Elefterija Zlatanović, Nebojša Davidović,
Zoran Bonić, Nikola Romić, Branimir Stanković, Lazar Živković**

University of Niš, Faculty of Civil Engineering and Architecture, Niš, Serbia

ORCID iDs: Nemanja Marinković
Elefterija Zlatanović
Nebojša Davidović
Zoran Bonić
Nikola Romić
Branimir Stanković
Lazar Živković

 <https://orcid.org/0000-0001-5834-7910>
 <https://orcid.org/0000-0001-6783-1325>
 N/A
 <https://orcid.org/0000-0002-7452-6756>
 <https://orcid.org/0000-0002-1075-2738>
 N/A
 <https://orcid.org/0000-0002-0765-4854>

Abstract. *Determination of the Atterberg's limits is necessary for the classification of fine-grained soil. That limits can be determined according to the valid standard SRPS EN ISO 17892-12. Two methods are prescribed by the standard for determining the liquid limit: the Casagrande cup and the Fall Cone test, and one method for determining the plasticity limit: the thread-rolling method. In this paper the Fall Cone method was also used as an alternative method to determine the plastic limit. Ten samples of various fine-grained materials, originating from the wider area of the city of Niš, were tested. The classification of all samples was performed based on the results obtained by the methods prescribed by the standard and alternative methods. Comparative analysis shows that the results obtained by applying standard and alternative methods are close, but also that the scattering of results obtained by the Fall Cone method is significantly less, whereas the reproducibility is higher.*

Key words: *fine-grained soil, liquid limit, plastic limit, plasticity index, Fall Cone method*

1. INTRODUCTION

The Atterberg's limits (Liquid Limit LL, Plastic Limit PL, Shrinkage Limit SL) are related to the amount of water attracted to the surface of the soil particles and are predominant factors for identifying and classifying a fine-grained soil. The cohesive soil can be in various physical states, i.e. of different consistency (solid, semi-solid, plastic, liquid) (Fig. 1).

Received June 30, 2023 / Revised August 1, 2023 / Accepted August 15, 2023

Corresponding author: Nemanja Marinković - University of Niš, Faculty of Civil Engineering and Architecture, Niš, Serbia

e-mail: nemanja.marinkovic@gaf.ni.ac.rs

*Selected paper presented at the International Conference Sinarg 2023 held in Niš, Serbia on 14-15 September 2023.

© 2024 by University of Niš, Serbia | Creative Commons License: CC BY-NC-ND

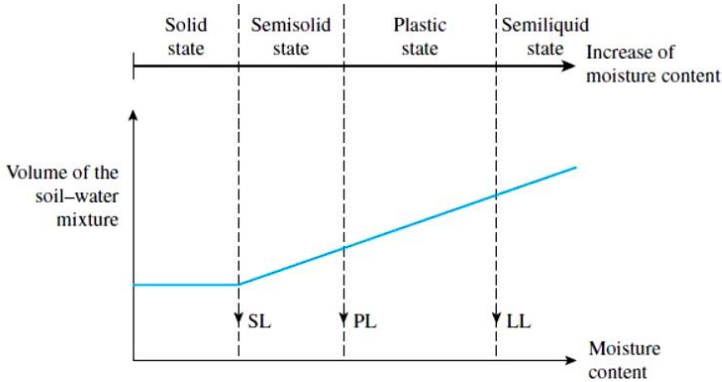


Fig. 1. Diagram of soil consistency

In nature, the soil often occurs in a plastic state. Plasticity Index (PI) represents the difference between the Liquid Limit and Plastic Limit ($PI = LL - PL$). The LL value, which may vary over a wide range, is used in the classification and preliminary evaluation of fine-grained soils in engineering works. If the LL is incorrectly defined, it can lead to the rejection of satisfactory materials, even the acceptance of unsuitable materials [1]. To determine LL two methods can be used according to SRPS EN ISO 17892-12 [2]: the Casagrande method and the Fall Cone method. The Fall Cone method, on the other hand, is easier, faster and less sensitive to the subjective factors (better repeatability of the test) and from this point of view this method was accepted as a standard method for LL determination in the European Standard EC7 [3]. A number of studies have been dealing with comparing the results obtained by applying these two methods [4–10]. Unlike the liquid limit, the plastic limit test is prescribed in a unique way – thread-rolling method. This paper presents an analysis of the results obtained using the standard and alternative method for PL determination proposed by Wood and Wroth [11]. Despite its wide use, thread-rolling method is often criticized for the influence of the assessment by the laboratory technician during the applying of the method as well as insufficiently good results for sandy clays. According to Whyte [12] when applying the standard method, the result is affected by several factors: the pressure applied to the soil thread; the geometry, i.e. the contact area between hand and thread; the friction between the soil, hand and base plate; the rate of rolling. None of these variables is controlled easily, and consequently the standard plastic limit test does not provide a direct measurement of soil strength. A modified Fall Cone method, proposed by Wood and Wroth [11] using a heavier cone, is very current. It differs from the standard cone for determining the liquid limit in the weight and the angle of the cone (cone characteristics: apex angle 60° , weight 240 g). The advantages and disadvantages of methods for testing the Atterberg limits using Fall Cone method are presented in the case studies [12,13].

The necessary values for the classification of materials were obtained in two ways in this paper. Namely, first the liquid limit was obtained using two methods prescribed by the standard, and then the plasticity limit was obtained using two methods (one method prescribed by the standard, the other alternative). The classification was performed in two ways: (1) using Casagrande cup and thread-rolling method, and (2) using the Fall Cone method. The obtained results are compared and their dependence is shown.

2. MATERIALS AND EXPERIMENTAL METHODS

As part of the research presented in this paper, 10 samples (S1–S10) were tested in order to determine the liquid limit and the plastic limit. The soil samples used in this analysis were taken from different places within the wider area of the city of Niš (Fig. 2). The samples are fine-grained materials that are typical for this area. Table 1 contains the labels of all samples, the locations from which they originate, the description of the sample material and the laboratory-determined values of specific gravity (G_s).

Table 1 Samples used for testing

Sample	Origin	Description	G_s [1]
S1	Babin Kal–Bela Palanka	Crushed stone (fine-grained fractions)	2.650
S2	Ličje–Gadžin Han	Crushed stone (fine-grained fractions)	2.666
S3	Doljevac 1	Sandy clay	2.648
S4	Aleksinac 1	Light brown clay	2.639
S5	Doljevac 2	Light brown clay	2.642
S6	Bancarevo 1	Brown clay	2.635
S7	Aleksinac 2	Sandy clay	2.634
S8	Bancarevo 2	Brown clay	2.630
S9	Ostrovica 1	Light brown clay	2.624
S10	Ostrovica 2	Brown clay	2.619

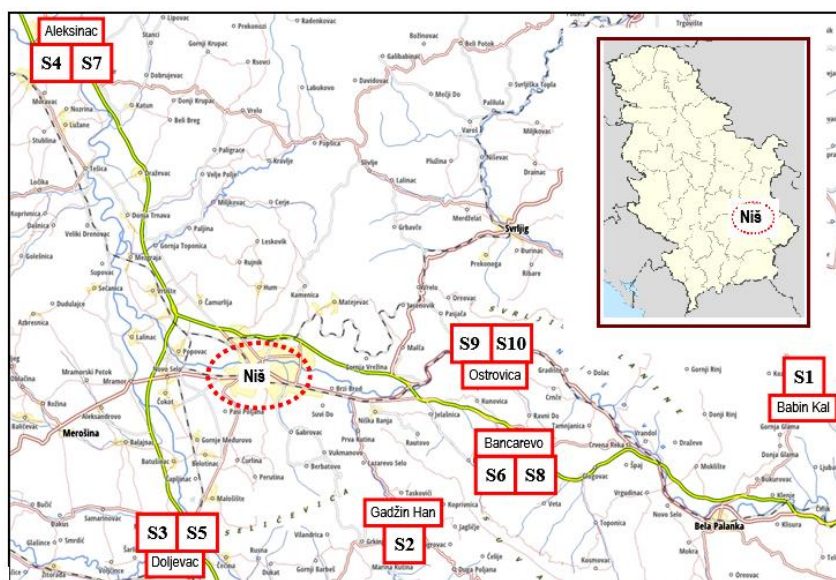


Fig. 2 Sample labels and locations in the wider area of the city of Niš where they were taken

For each sample the liquid limit was determined using two different procedures - the Casagrande method (results labeled LL_{cup}) and the Fall Cone method (results labeled LL_{cone}). For each sample, the Plastic Limit was determined using 2 different procedures -

the thread-rolling method (results marked by PL_{rolling}) and the Modified Fall Cone method (results marked PL_{cone}).

The obtained results were compared and discussed. Based on the comparative analysis, the relationship between LL_{cone} and LL_{cup} values, and then PL_{rolling} and PL_{cone} which is relevant for fine-grained soils from this area, should be defined by mathematical expression.

According to SRPS EN ISO 17892-12, each sample of soil material is sieved through a 0.5 mm sieve to remove larger particles. The sample is then mixed with distilled water and homogenized with metal blades, with the aim that the whole sample has the same moisture content. Each sample was tested 10 times. For all samples, the classification was performed on the plasticity diagram, based on the obtained values $LL_{\text{cup}}-PL_{\text{rolling}}$, $LL_{\text{cone}}-PL_{\text{cone}}$.

2.1. Determination of Liquid Limit

The Casagrande method uses a cup, within which a soil paste is placed, then the soil is split by cutting a groove and also the cup is drop on a base. The Liquid Limit, according to this method, is the water content of the soil determined for a number of 25 blows (Fig. 3).

The cone penetrometer technique uses a free falling cone (cone characteristics: apex angle 30° , weight 80 g) and is based on the relation between water content and cone penetration depth (Fig. 3). Considering this method, the Liquid Limit represents the water content equivalent to cone penetration depth of 20 mm.

2.2. Determination of Plastic Limit

The standard SRPS EN ISO 17892-12 for determining the plastic limit implies manual making of rollers on a glass plate (Fig. 3). The plastic limit represents the water content at which the roller with a thickness (diameter) of 3.0 mm is cracked. It has been shown that the values obtained by this method depend to a great extent on the assessment of the operator. Sherwood [4] came to the conclusion after a large number of tests that variations of the obtained results may be up to 12% for the same soil sample treated by several operators. The Modified Fall Cone method (cone characteristics: apex angle 60° , weight 240 g) can be considered as more reliable. Plastic Limit represents the water content equivalent to cone penetration depth of 20 mm. Although this method is not yet included in the standard, it has been proven to be very successful in numerous research [14–17]. By using this method, the influence of the laboratory technician on the obtained results is reduced, and thus, it is expected that the results will be much closer to each other than the results obtained by the thread-rolling method.

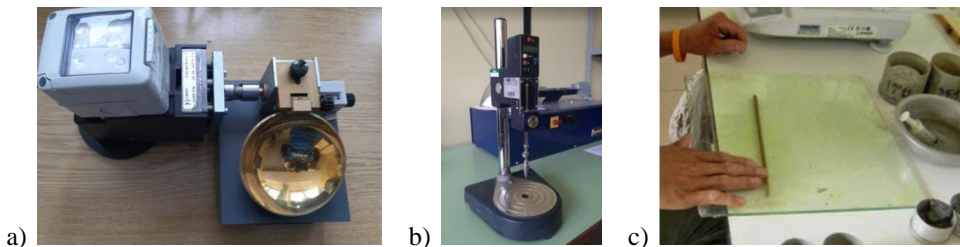


Fig. 3. Equipment for determination of Liquid Limit and Plastic Limit: a) Casagrande cup; b) Falling cone (penetrometer); c) thread-rolling method

3. RESULTS AND DISCUSSION

The correlations proposed by the authors based on the study of local fine-grained materials are numerous and different mathematical complexities, from simple linear equations to higher order equations. Some of the correlations can be seen in the Table 2. In the equations, LL_{cone} is Liquid Limit determined by Fall Cone method and LL_{cup} is Liquid Limit determined by Casagrande method.

Table 2 Equations correlating the LL values obtained by using the fall-cone apparatus and the Casagrande cup [18]

Author (Year)	Number of samples	LL range (%)	Correlation	R ²
Sherwood and Ryley (1970)	25	30–72	$LL_{\text{cone}} = 0.94 \cdot LL_{\text{cup}} + 0.97$	-
Leroueil and Le Bihan (1996)	43	30–74	$LL_{\text{cone}} = 0.86 \cdot LL_{\text{cup}} + 6.34$	-
Feng (2001)	66	25–76	$LL_{\text{cone}} = 0.94 \cdot LL_{\text{cup}} + 2.60$	-
Dragoni et al. (2008)	41	27–74	$LL_{\text{cone}} = 1.02 \cdot LL_{\text{cup}} + 2.87$	0.980
Fojtova et al. (2009)	52	20–51	$LL_{\text{cone}} = 1.00 \cdot LL_{\text{cup}} + 2.44$	0.978
Di Matteo (2011)	6	20–40	$LL_{\text{cone}} = 1.00 \cdot LL_{\text{cup}} + 2.20$	0.980
Spagnoli (2012)	50	20–61	$LL_{\text{cone}} = 0.99 \cdot LL_{\text{cup}} + 2.44$	0.990
Silva (2013)	10	38–45	$LL_{\text{cone}} = 1.05 \cdot LL_{\text{cup}} + 0.61$	0.978
El-Shinawi (2017)	40	28–70	$LL_{\text{cone}} = 0.91 \cdot LL_{\text{cup}} + 5.64$	0.949
Niazi et al. (2019)	65	11–65	$LL_{\text{cone}} = 0.89 \cdot LL_{\text{cup}} + 4.20$	0.985

The obtained values of LL and PL are shown in Table 3 and Table 4. Table 3 shows the values obtained by the Casagrande method (LL_{cup}) and by the Fall Cone method (LL_{cone}), and Table 4 shows the values obtained by the thread-rolling method (PL_{rolling}) and the Fall Cone method (PL_{cone}). Tables show the obtained results of the minimum and maximum values, their difference, as well as the mean value of LL and PL. For each tested sample, the standard deviation (S.D.) and the coefficient of variation (C.O.V.) of the obtained results were calculated. These statistical parameters better express the scattering of results and reproducibility. C.O.V. value is represented by default as a dimensionless quantity, but in the given tables, for the sake of a simpler comparison, the value is shown in percent.

It can be seen that LL values ranging from 16.56% to 49.74%, which is in accordance with the results of the tests performed so far on materials from this area (Table 3). For LL values less than 40%, a strong linear dependence and almost coincidence with the 45° line can be observed. Other authors have shown similar results in their research [5-10]. The obtained PL values are in the range from 11.37% to 30.50%. It is obvious that for all samples the scattering of the results is higher when the Casagrande cup and thread-rolling method were used. The differences in the liquid and plastic limits results obtained by Casagrande cup and thread-rolling, considering all samples, are greater than 2%. S.D. values for the Casagrande cup (0.84% to 1.74%) and thread-rolling method (0.78% to 1.35%) are significantly higher than for the Fall Cone method: LL (0.51% to 1.31%) and PL (0.62% to 1.24%). Similarly, C.O.V. values for thread-rolling method (3.74% to 6.31%) are significantly higher than for Fall Cone method (2.30% to 4.96%). Based on the fact that for all tested samples the values of S.D. and C.O.V. are significantly lower when using the Fall Cone method, it can be concluded that more reproducible results are obtained with this

method. In addition, it was shown that the mean value of the plastic limit for all samples is slightly higher when using the Fall Cone method.

Table 3 LL values determined by the Casagrande method and the Fall Cone method

Sample	LL (%)										
	S1	S2	S3	S4	S5	S6	S7	S8	S9	S10	
LL _{Cup}	LL _{max} (%)	17.97	28.42	32.45	34.09	36.86	38.16	41.23	44.56	46.72	49.56
	LL _{min} (%)	15.94	26.03	30.36	30.38	34.23	35.44	38.90	40.74	42.66	45.32
	ΔLL (%)	2.03	2.39	2.09	3.68	2.63	2.72	2.33	3.82	4.06	4.24
	LL _{mean} (%)	16.56	26.98	31.64	31.56	36.07	36.66	40.31	42.17	44.35	46.51
	S.D. (%)	0.84	1.23	0.98	1.25	1.16	1.22	1.42	1.37	1.63	1.74
	C.O.V. (%)	5.07	4.56	3.10	3.96	3.22	3.33	3.52	3.25	3.76	3.74
	LL _{Cone}	LL _{max} (%)	17.62	28.77	32.11	33.94	36.95	38.34	42.64	46.05	48.11
LL _{min} (%)		16.03	26.85	29.76	29.85	33.81	35.57	40.88	42.67	45.19	48.34
ΔLL (%)		1.59	1.92	2.35	4.09	3.14	2.77	1.76	3.38	2.92	4.01
LL _{mean} (%)		16.84	27.91	31.26	31.44	35.78	36.96	41.64	44.11	46.50	49.14
S.D. (%)		0.76	0.76	0.51	1.04	0.74	0.86	1.06	1.22	1.10	1.31
C.O.V. (%)		4.51	2.81	1.63	3.31	2.07	2.37	2.55	2.77	2.37	2.63

Table 4 PL values determined by the thread-rolling method and the Fall Cone method

Sample	PL (%)										
	S1	S2	S3	S4	S5	S6	S7	S8	S9	S10	
PL _{thread-rolling}	PL _{max} (%)	11.65	21.63	23.16	25.56	23.88	26.18	30.09	27.19	28.77	30.51
	PL _{min} (%)	9.24	18.21	20.68	21.71	20.14	23.41	26.19	24.10	26.14	27.16
	ΔPL (%)	2.41	3.42	2.48	3.85	3.74	2.77	3.90	3.09	2.64	3.35
	PL _{mean} (%)	11.37	19.55	21.93	23.66	22.03	24.81	27.59	25.75	27.97	28.73
	S.D. (%)	0.78	1.09	0.87	1.26	0.99	0.93	1.35	1.02	1.11	1.24
	C.O.V. (%)	6.31	5.56	3.97	5.33	4.49	3.75	4.81	3.96	3.97	5.33
	PL _{Cone}	PL _{max} (%)	12.90	22.29	23.84	26.14	25.11	27.42	28.34	28.89	29.62
PL _{min} (%)		10.92	19.86	21.98	22.87	23.37	25.06	26.59	26.66	27.03	28.14
ΔPL (%)		1.98	2.43	1.86	3.27	1.74	2.36	1.75	2.23	2.59	2.91
PL _{mean} (%)		11.56	20.74	22.79	23.59	24.06	26.18	27.45	27.24	28.16	30.50
S.D. (%)		0.62	0.70	0.62	1.24	0.58	0.77	1.12	0.63	0.96	1.06
C.O.V. (%)		4.96	3.35	2.71	5.18	2.41	2.94	4.08	2.31	3.41	3.59

The correlation factor (R^2) shows how close the calculated values are to the measured values. Theoretically, the maximum value of the correlation factor is $R^2 = 1$. In this case, the calculated values would be identical to the measured values. A higher correlation factor indicates a smaller difference between calculated and measured values (better regression line). Figure 4 shows the linear correlations for the values obtained when determining the liquid limit and plastic limit. The polynomial regression line has a higher correlation factor than the linear regression line (0.9891 vs. 0.9786), as well as a significantly smaller deviations of the calculated values from the measured ones ($\leq 0.88\%$ vs. $\leq 1.43\%$). Thus, the polynomial regression line $y = 0.009x^2 + 0.52x + 5.0972$ was chosen as adequate for the mathematical representation of the “LL_{Cone}–LL_{Cup}” correlation, whereas the polynomial regression line $y = -0.0048x^2 + 1.1685x - 0.1028$ was chosen as adequate for representation of the “PL_{Cone}–PL_{rolling}” correlation [19,20].

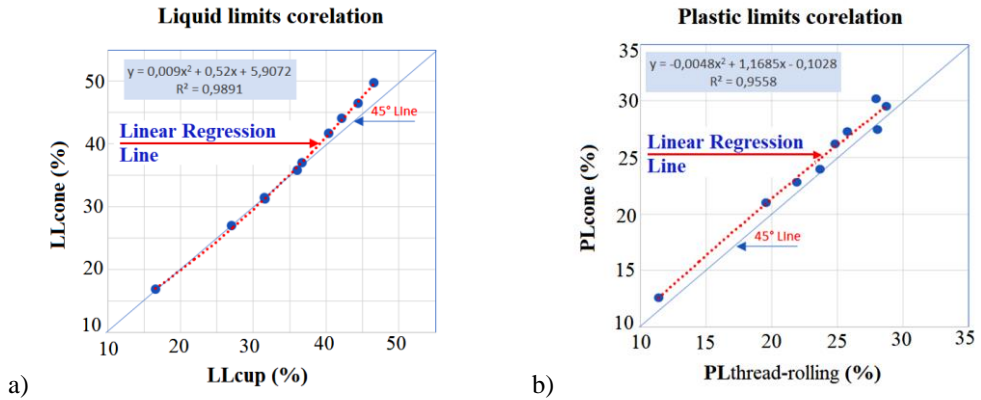


Fig. 4 Comparative analysis of the results obtained using two methods for: a) Liquid Limit; b) Plastic Limit

For the classification of soil, according to Unified Soil Classification System (USCS) (the method is prescribed by standard SRPS) it is necessary to determine LL, PL, and PI (Table 5).

Table 5 Values of LL, PL, and PI used in soil classification

Sample	Atterberg limits (%)									
	S1	S2	S3	S4	S5	S6	S7	S8	S9	S10
LL _{cup}	16.56	26.98	31.64	31.56	36.07	36.66	40.31	42.17	44.35	46.51
PL _{tr}	11.37	19.55	21.93	23.66	22.03	24.81	27.59	25.75	27.97	28.73
PI _{standard}	5.19	7.43	9.71	7.90	14.04	11.85	12.72	16.42	16.38	17.78
USCS	SC	CL	CL	ML	CI	MI	MI	CI	MI	MI
LL _{cone}	16.84	27.01	31.26	31.44	35.78	36.96	41.64	44.11	46.50	49.14
PL _{cone}	11.56	20.74	22.79	23.59	24.06	26.18	27.45	27.24	28.16	30.52
PI _{cone}	5.28	7.17	8.47	7.15	12.21	10.78	14.19	16.87	18.34	18.62
USCS	SC	CL	CL	ML	CI	MI	MI	MI	MI	MI

The plasticity index is the range of water contents where the soil exhibits plastic properties. Soils with a high PI are classified as clays and those with a lower PI are classified as silts. Table 5 shows the calculated PI values for each of the ten samples. The values of PI_{standard} are calculated based on values of LL_{cup} obtained by the Casagrande cup, and PL_{tr} obtained by thread-rolling method. Values of PI_{cone} are calculated based on values of LL_{cone} and PL_{cone} obtained by the Fall Cone test. The USCS classification is done using a diagram proposed by Atterberg (Fig. 5). A-line divides the diagram into two parts. Silty and organic soils are defined by fields below A-line, while clayey soils are defined by fields above A-line. It can be observed that only sample S8 was classified as medium plasticity clay (CI) using the Casagrande and thread-rolling methods, while using a fall cone method it was classified as medium plasticity silt (MI). The difference in classification can also occur by using alternative equations, as Di Matteo et al. [21] presented in their research.

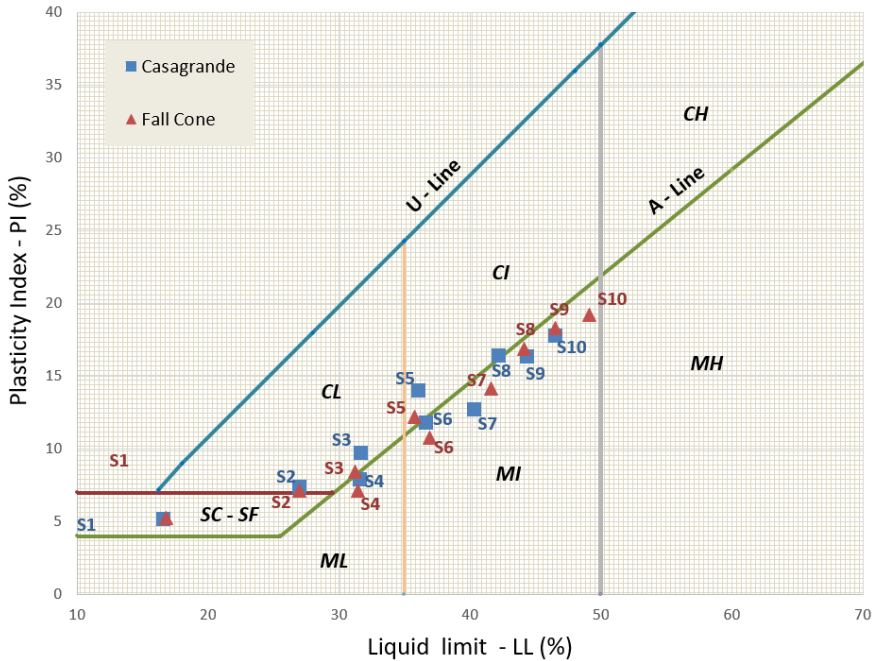


Fig. 5 Classification of tested soil samples on plasticity chart

4. CONCLUSION

The classification of fine-grained soils according to the standard SRPS EN ISO 17892-12 is based on the LL and PI values, using the plasticity chart. In order for the classification to be carried out correctly, it is necessary to first determine LL and PL as accurately as possible in laboratory tests. Based on the results of tests performed on each of the 10 fine-grained soil samples, the obtained results show that the Fall Cone method gives more reproducible results for a larger number of tests. LL values are very similar for $LL < 35\%$, while for higher values there is a difference up to a maximum of 4.24% (Casagrande cup) and 4.01% (Fall Cone). The results presented in this paper show the successful use of the modified Fall Cone method as an alternative method for PL determination. Obtained results show that the largest difference in PL values obtained by thread-rolling method is 3.74%, whereas the use of the Fall Cone method gives PL values with the largest difference of 2.91%. Based on the comparison of statistical parameters S.D. and C.O.V. it was observed that the dispersion of the results is significantly higher for the application of the thread rolling method. On the other hand, repeatability is higher when using the Fall Cone method. The fact that the C.O.V. for the obtained results is over 90% indicates that the Fall Cone method can be used very successfully as an alternative method for determining LL and PL of fine-grained soils. In addition, the obtained S.D. and C.O.V. values indicate that the Fall Cone method is adequate for more frequent use in practice. The results presented in this paper refer to local material and it is necessary to conduct tests with samples from a wider area.

Acknowledgement. *The authors gratefully acknowledge the support of the Science Fund of the Republic of Serbia in the scope of the scientific–research project “A New Concept in Improvement of Geotechnical Properties of Ground – Chemical Electrokinetic Treatment of Soils (ElectroSoil)”, Grant No. 7742530.*

REFERENCES

1. L. G. Crevelin and K. V. Bicalho, "Comparison of the Casagrande and Fall Cone methods for liquid limit determinations in different clay soils", *Revista Brasileira de Ciência do Solo* 43, article 0180105, 2019, pp. 1-12. doi:10.1590/18069657rbc20180105
2. ISO 17892-12:2018: Geotechnical investigation and testing - Laboratory testing of soil - Part 12: Determination of liquid and plastic limits, 2018.
3. E. Hrubesova, B. Lunackova and O. Brodzki, "Comparison of liquid limit of soils resulted from Casagrande test and modified cone penetrometer methodology", *Procedia Engineering* 142, 2016, pp. 364-370. doi:10.1016/j.proeng.2016.02.063
4. P. T. Sherwood and M. D. Ryley, "An investigation of a cone-penetrometer method for the determination of the liquid limit", *Geotechnique* 20(2), 1970, pp. 203-208. doi:10.1680/geot.1970.20.2.203
5. T. W. Feng, "A linear log $d - \log w$ model for the determination of consistency limits of soils", *Canadian Geotechnical Journal* 38, 2001, pp. 1335-1342. doi:10.1139/t01-061
6. L. Fojtova, M. Marschalko, R. Franekova, L. Kovar, "Study of compatibility of methods for liquid limit measurement according to Czech State Standard and newly adopted European standard", *GeoScience Engineering LV*, 2009, pp. 55-68.
7. L. Di Matteo, "Liquid limit of low-to medium-plasticity soils: comparison between Casagrande cup and cone penetrometer test", *Bulletin of Engineering Geology and the Environment* 71(1), 2012, pp. 79-85. doi:10.1007/s10064-011-0412-5
8. G. Spagnoli, "Comparison between Casagrande and drop-cone methods to calculate liquid limit for pure clay", *Canadian Journal of Soil Science* 92, 2012, pp. 859-864. doi:10.4141/cjss2012-011
9. A. El-Shinawi, "A comparison of liquid limit values for fine soils: a case study at the north Cairo-Suez district, Egypt", *Journal of the Geological Society of India* 89, 2017, pp. 339-343. doi:10.1007/s12594-017-0608-9
10. F. S. Niazi, A. Pinan-Llamas, C. Cholewa and C. Amstutz, "Liquid limit determination of low to medium plasticity Indiana soils by hard base Casagrande percussion cup vs. BS fall-cone methods", *Bulletin of Engineering Geology and the Environment* 79, 2020, pp. 2141-2158. doi:10.1007/s10064-019-01668-y
11. D. M. Wood and C. P. Wroth, "The use of the cone penetrometer to determine the plastic limit of soils", *Ground Engineering* 11(3), 1978, p. 37. <http://worldcat.org/issn/00174653>
12. I. L. Whyte, "Soil plasticity and strength: a new approach using extrusion", *Ground Engineering* 15(1), 1982, pp. 16-24. doi:10.1016/0148-9062(82)91670-9
13. A. D. Campbell and J. W. Blackford, *Fall Cone method used to determinate the liquid limit of soil*, Engineering and Research Center, Denver, 1984.
14. Y. Wasti and M. H. Bezirci, "Determination of consistency limits of soil by the Fall Cone test", *Canadian Geotechnical Journal* 23, 1986, pp. 241-246. doi:10.1139/t86-033
15. A. S. Muntohar and R. Hashim, "Determination of plastic limits of soils using cone penetration", *Journal Teknik Sivil (Civil Engineering Journal)* 11(2), 2005, pp. 87-98.
16. F. Ishaque, M. N. Hoque and M. A. Rashid, "Determination of plastic limit of some selected soils using rolling device", *Progressive Agriculture* 21(1-2), 2010, pp. 187-194.
17. B. Sharma and A. Sridharan, "Liquid and plastic limits of clays by cone method", *International Journal of Geo-Engineering* 9, 2018, pp. 1-10. doi:10.1186/s40703-018-0092-0
18. E. Diaz, J. L. Pastor, A. Rabat and A. Tomas, "Machine learning techniques for relating liquid limit obtained by Casagrande cup and Fall Cone test in low-medium plasticity fine grained soils", *Engineering Geology* 294, article 106381, 2021, pp. 1-10. doi:10.1016/j.enggeo.2021.106381
19. N. Marinković, N. Davidović, B. Stanković, E. Zlatanović, Z. Bonić and N. Romić, "Comparative analysis of plastic limit of fine-grained soil determined by various methods", *Proceedings of the International Scientific Conference “Earthquake Engineering and Geotechnical Aspects of Civil Engineering”*, Union of Engineers and Technicians of Serbia, Vrnjačka Banja, Serbia, November 03–05, 2021, pp. 354-361.

20. N. Marinković, N. Davidović, E. Zlatanović, B. Stanković, N. Romić and Z. Bonić, "Comparative analysis of liquid limit of clays from the Niš area determined by various methods", Proceedings of the 5th International Scientific Conference "MAG 2022", Macedonian Association for Geotechnics and ISRM Specialized Conference, Ohrid, Republic of North Macedonia, June 23–25, 2022, pp. 416-424.
21. L. Di Matteo, W. Dragoni, C. Cencetti, R. Ricco and A. Fucsina, "Effects of fall-cone test on classification of soils: some considerations from study of two engineering earthworks in Central Italy", Bulletin of Engineering Geology and the Environment 75, 2016, pp. 1629-1637. doi:10.1007/s10064-015-0808-8

KOMPARATIVNA ANALIZA ATERBERGOVIH GRANICA SITNOZRNOG TLA PRIMENOM RAZLIČITIH METODA

Određivanje Aterbergovih granica je veoma važno sa aspekta relevantne klasifikacije sitnozrnog tla. Ove granice se mogu odrediti prema važećem standardu SRPS EN ISO 17892-12. Standardom su propisane dve metode za određivanje granice tečenja: Kasagrandeova treskalica i metoda padajućeg konusa, i jedna metoda za određivanje granice plastičnosti: metoda ručnog valjanja valjčića vlažnog tla. U ovom radu je korišćena i metoda padajućeg konusa kao alternativna metoda za određivanje granice plastičnosti. Ispitivanja su sprovedena na deset uzoraka različitih sitnozrnih materijala, poreklom sa šireg područja grada Niša. U radu je data komparativna analiza rezultata dobijenih pri određivanju Aterbergovih granica primenom standardnih i alternativnih metoda. Takođe je izvršena i klasifikacija svih razmatranih vrsta sitnozrnog tla. Komparativna analiza pokazuje da su rezultati dobijeni primenom standardnih i alternativnih metoda bliski, ali i da je rasipanje rezultata dobijenih primenom metode padajućeg konusa značajno manje, dok je sa druge strane reproduktivnost veća.

Ključne reči: sitnozrno tlo, granica tečenja, granica plastičnosti, indeks plastičnosti, metoda padajućeg konusa

CIP - Каталогизacija y publikaciji
Narodna biblioteka Srbije, Beograd

71/72+62

FACTA Universitatis. Series, Architecture
and Civil Engineering / editor-in-chief Zoran Bonić
. - Vol. 1, no. 1 (1994)- . - Niš : University of Niš,
1994- (Niš : Atlantis). - 24 cm

Tri puta godišnje. - Drugo izdanje na drugom
medijumu: Facta Universitatis. Series: Architecture
and Civil Engineering (Online) = ISSN 2406-0860
ISSN 0354-4605 = Facta Universitatis. Series:
Architecture and Civil Engineering
COBISS.SR-ID 98807559

